Schweizerische Eidgenossenschaft
Confédération suisse
Confederazione Svizzera
Confederaziun svizra

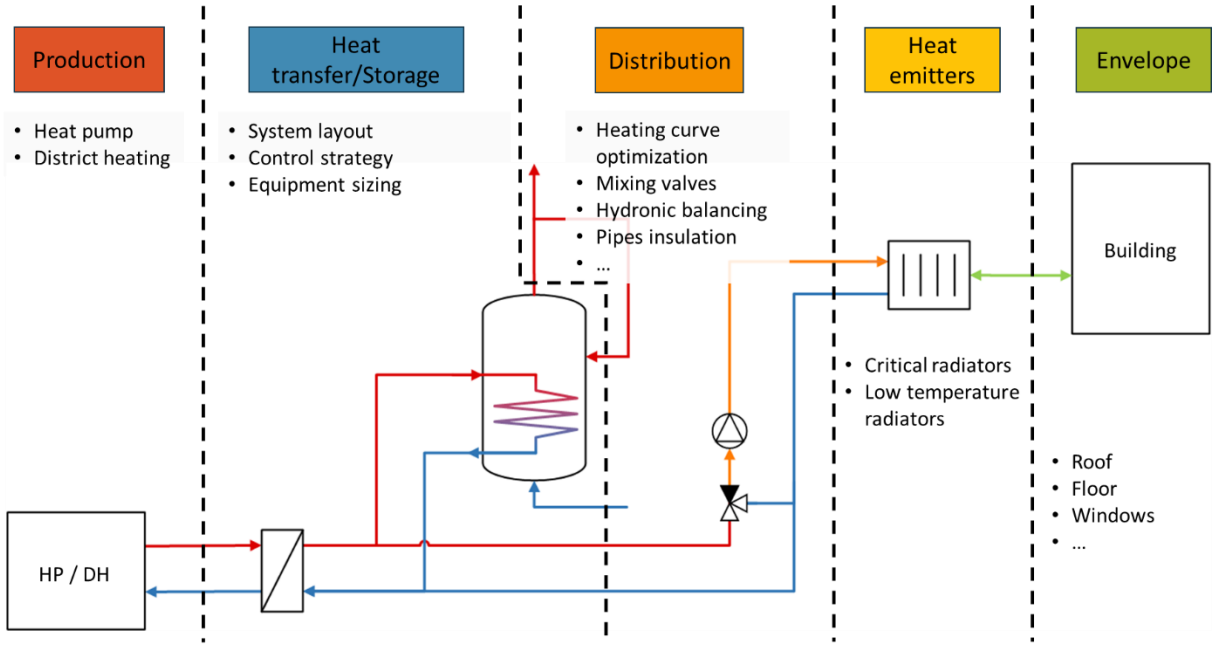
Federal Department of the Environment,
Transport, Energy and Communications DETEC

Swiss Federal Office of Energy
Energy Research and Cleantech

Final report from 25 September 2026

T-DROP

Lowering of heat distribution temperatures, for integration of renewables and decarbonization of multifamily buildings in dense districts



Publisher:
Swiss Federal Office of Energy SFOE
Energy Research and Cleantech
CH-3003 Berne
www.energy-research.ch

Co-financing:
Service Industriel de Genève (SIG)
CH-1219 Vernier
ww2.sig-ge.ch

Direction générale de l'environnement (DGE)
Direction de l'énergie
CH-1014 Lausanne
www.vd.ch/energie

Ville d'Yverdon-les-Bains
CH-1401 Yverdon-les-Bains
www.yverdon-energies.ch

Subsidy recipients:
Université de Genève (UNIGE)
CH-1205 Genève
www.unige.ch

Haute Ecole d'Ingénierie et de Gestion du canton de Vaud (HEIG-VD)
CH-1401 Yverdon-les-Bains
www.heig-vd.ch

Authors:
Pauline Brischoux, University of Geneva, pauline.brischoux@unige.ch
Rubén Novoa-Herzog, University of Geneva, ruben.novoa@unige.ch
Pierre Hollmuller, University of Geneva, pierre.hollmuller@unige.ch
Blaise Périsset, HEIG-VD, blaise.perisset@heig-vd.ch
Xavier Jobard, HEIG-VD, xavier.jobard@heig-vd.ch
Romain Guinouet, HEIG-VD
Alexis Duret, HEIG-VD, alexis.duret@heig-vd.ch

SFOE project coordinators:
Andreas Eckmanns, andreas.eckmanns@bfe.admin.ch
Nadège Vetterli, nadege.vetterli@anex.ch
Martin Ménard, menard@lowtechlab.ch

SFOE contract number: SI/502581-01

The authors bear the entire responsibility for the content of this report and for the conclusions drawn therefrom.

Summary

Buildings account for around 45% of Switzerland's final energy consumption and a third of its CO_2 emissions, most of it related to space heating (SH) and domestic hot water (DHW), and more than half are still heated by fossil fuel boilers. Replacing these boilers with heat pumps (HPs) or connecting buildings to district heating networks (DHNs) is central to decarbonizing the sector, particularly for multifamily buildings (MFBs) in dense urban areas, where few other renewable options are available. The performance of these renewable heat sources, however, is strongly penalized by the high distribution and production temperatures inherited from fossil fuel systems.

The T-DROP project investigates how existing MFBs can shift from high- to low-temperature heat distribution through combination of targeted envelope retrofitting and heat distribution optimization, and quantifies the resulting benefits for renewable heat integration and decarbonization. Focusing on decentralized HP systems, representative building and SH/DHW system typologies are defined from architectural fact sheets and case studies, then modeled and combined into an integrated TRNSYS model that captures the building-system interactions at each time step. The model is used to carry out a sensitivity analysis across building typologies, retrofitting depths and optimization measures.

The simulations show that the achievable reduction in SH supply temperature is primarily governed by the effective heat emitter oversizing, defined as the ratio between the installed emitter capacity and the actual heating load. Consequently, any measure that reduces the SH demand (e.g. envelope retrofitting, lower indoor temperature setpoints, optimized ventilation) increases the effective emitter oversizing and enables lower supply temperatures, provided that the heating curve is optimized and the distribution system is properly balanced. By contrast, DHW production remains the main limitation since the temperature required to limit the legionella risk keeps the overall system temperature high, increasingly so as retrofitting raises the DHW share of the heat demand, and the studied DHW optimization measures bring only modest gains.

Lower operating temperatures directly improve HP efficiency and reduce the associated CO_2 emissions, while demand reduction simultaneously lowers the total energy consumption and emissions per unit floor area. A central finding is that the role of system optimization depends on the indicator considered. For temperature levels and efficiency, system optimization measures can partly compensate for the absence of deeper envelope retrofitting (bringing a building to a performance otherwise reached only with further retrofitting), making it an effective short-term strategy for poorly performing buildings while waiting for deeper envelope retrofit. For the absolute emissions that ultimately drive decarbonization, however, envelope retrofit and system optimization are complementary: since optimization cannot substantially reduce the heat demand, envelope retrofitting remains fundamental, with optimization accelerating and reinforcing it rather than replacing it. The choice of the heat production unit also matters: a high-efficiency HP improves performance at unchanged temperatures, while a hybrid system can serve as a useful transitional solution as long as its control and hydraulics prevent the boiler from taking over.

Overall, lowering distribution temperatures can be considered as a co-benefit of reducing the heat demand, through measures prioritized according to the pre-existing characteristics and current state of each building. Future work should focus on DHW optimization, the extension to DHN substations, and the economic assessment of the studied measures.

Zusammenfassung

Gebäude verursachen rund 45% des Endenergieverbrauchs der Schweiz und ein Drittel ihrer CO_2-Emissionen. Der grösste Teil entfällt auf die Raumheizung und die Warmwasserbereitung, wobei mehr als die Hälfte des Gebäudebestands noch mit fossilen Heizkesseln beheizt wird. Der Ersatz dieser Heizkessel durch Wärmepumpen (WP) oder der Anschluss von Gebäuden an Fernwärmenetze (FWN) ist daher ein zentraler Baustein für die Dekarbonisierung des Gebäudesektors, insbesondere bei Mehrfamilienhäusern in dicht bebauten städtischen Gebieten, in denen nur wenige andere erneuerbare Wärmequellen zur Verfügung stehen. Die Leistungsfähigkeit dieser erneuerbaren Wärmesysteme wird jedoch durch die hohen Verteil- und Erzeugungstemperaturen bestehender fossiler Heizsysteme erheblich beeinträchtigt.

Das Projekt T-DROP untersucht, wie bestehende Mehrfamilienhäuser durch eine Kombination aus gezielter Gebäudehüllensanierung und Optimierung der Wärmeverteilung von einer Hoch- zu einer Niedertemperatur-Wärmeverteilung übergehen können, und quantifiziert die daraus resultierenden Vorteile für die Integration erneuerbarer Wärme und die Dekarbonisierung. Der Schwerpunkt liegt auf dezentralen Wärmepumpensystemen. Repräsentative Gebäude- sowie System-typologien werden auf Grundlage von Architektursteckbriefen und Fallstudien definiert, modelliert und anschliessend in einem integrierten TRNSYS-Modell zusammengeführt, das die Wechselwirkungen zwischen Gebäude und Heizsystem in jedem Zeitschritt abbildet. Mit diesem Modell wird eine Sensitivitätsanalyse für verschiedene Gebäudetypologien, Sanierungstiefen und Optimierungsmassnahmen durchgeführt.

Die Simulationen zeigen, dass die erreichbare Reduktion der Vorlauftemperatur der Raumheizung in erster Linie vom effektiven Überdimensionierungsgrad der Wärmeabgabesysteme abhängt, definiert als das Verhältnis zwischen der installierten Heizkörperleistung und der tatsächlichen Heizlast. Jede Massnahme, welche den Heizwärmebedarf reduziert (z. B. Gebäudehüllensanierung, tiefere Raumtemperatur-Sollwerte oder eine optimierte Lüftung), erhöht diesen effektiven Überdimensionierungsgrad und ermöglicht niedrigere Vorlauftemperaturen, sofern die Heizkurve optimiert und das Wärmeverteilungssystem hydraulisch abgeglichen ist. Demgegenüber stellt die Warmwasserbereitung weiterhin die wichtigste Einschränkung dar, da die zur Vermeidung des Legionellenrisikos erforderlichen Temperaturen das Temperaturniveau des Gesamtsystems hoch halten. Dieser Effekt nimmt mit zunehmender Sanierung zu, da der Anteil des Warmwasserbedarfs am gesamten Wärmebedarf steigt, während die untersuchten Optimierungsmassnahmen für die Warmwasserbereitung nur begrenzte Verbesserungen bewirken.

Niedrigere Betriebstemperaturen verbessern unmittelbar die Effizienz der WP und reduzieren die damit verbundenen CO_2-Emissionen, während die Verringerung des Wärmebedarfs gleichzeitig den Gesamtenergieverbrauch und die Emissionen pro Flächeneinheit senkt. Ein zentrales Ergebnis des Projekts ist, dass die Wirkung der Systemoptimierung vom betrachteten Indikator abhängt. Hinsichtlich Temperaturniveau und Effizienz können Optimierungsmassnahmen eine weitergehende Gebäudehüllensanierung teilweise kompensieren und stellen damit eine wirksame kurzfristige Strategie zur Verbesserung energetisch schlechter Gebäude dar. Für die absoluten Emissionen, die letztlich für die Dekarbonisierung entscheidend sind, ergänzen sich Gebäudehüllensanierung und Systemoptimierung jedoch: Da Optimierungsmassnahmen den Wärmebedarf nicht wesentlich reduzieren können, bleibt die Gebäudehüllensanierung unverzichtbar, während die Systemoptimierung deren Wirkung beschleunigt und verstärkt, sie jedoch nicht ersetzen kann. Auch die Wahl des Wärmeerzeugers spielt eine wichtige Rolle: Hocheffiziente WP verbessern die Systemleistung bei unveränderten Betriebstemperaturen, während Hybridanlagen eine sinnvolle Übergangslösung darstellen können, sofern Regelung und Hydraulik den Einsatz des Heizkessels auf ein Minimum begrenzen.

Insgesamt zeigt das Projekt, dass die Senkung der Verteilungstemperaturen als Folge einer Verringerung des Wärmebedarfs betrachtet werden kann, die durch auf die Eigenschaften und den aktuellen Zustand jedes einzelnen Gebäudes abgestimmte Massnahmen erreicht wird. Zukünftige Arbeiten sollten sich auf die Optimierung der Warmwasserbereitung, die Ausweitung der Analyse auf Fernwärme-Übergabestationen sowie auf die wirtschaftliche Bewertung der untersuchten Massnahmen konzentrieren.

Résumé

Les bâtiments représentent environ 45% de la consommation finale d'énergie en Suisse et un tiers de ses émissions de CO_2, dont la majeure partie est liée au chauffage et à la production d'eau chaude sanitaire (ECS). Plus de la moitié du parc immobilier est encore chauffée par des chaudières à combustibles fossiles. Le remplacement de ces chaudières par des pompes à chaleur (PAC) ou le raccordement des bâtiments à des réseaux de chauffage à distance (CAD) constitue donc un levier essentiel pour décarboner le secteur, en particulier pour les immeubles résidentiels collectifs situés en zone urbaine dense, où les autres solutions renouvelables sont limitées. Les performances de ces systèmes de production de chaleur renouvelable restent toutefois fortement pénalisées par les températures élevées de distribution et de production héritées des installations fonctionnant aux énergies fossiles.

Le projet T-DROP étudie comment les immeubles résidentiels collectifs existants peuvent passer d'une distribution de chaleur à haute température à une distribution à basse température grâce à des combinaisons de rénovations ciblées de l'enveloppe et de mesures d'optimisation du système de distribution de chaleur, et quantifie les bénéfices qui en résultent pour l'intégration des énergies renouvelables et la décarbonisation. En se concentrant sur les systèmes de PAC décentralisées, des typologies représentatives de bâtiments et de systèmes de chauffage/ECS sont définies à partir de fiches architecturales et d'études de cas, modélisées puis couplées dans un modèle TRNSYS permettant de représenter les interactions entre le bâtiment et le système à chaque pas de temps. Ce modèle est utilisé pour réaliser une analyse de sensibilité couvrant différentes typologies de bâtiments, niveaux de rénovation de l'enveloppe et mesures d'optimisation.

Les simulations montrent que la réduction atteignable de la température de départ du chauffage est principalement gouvernée par le surdimensionnement effectif des émetteurs de chaleur, défini comme le rapport entre leur puissance installée et la charge réelle de chauffage. Toute mesure réduisant les besoins de chauffage (par exemple la rénovation de l'enveloppe, l'abaissement de la température de consigne intérieure ou l'optimisation de la ventilation) augmente ce surdimensionnement effectif et permet d'abaisser les températures de départ, à condition que la courbe de chauffe soit optimisée et que le réseau de distribution soit correctement équilibré. À l'inverse, la production d'ECS demeure la principale limitation, la température requise pour prévenir le risque de légionellose maintenant la température globale du système à un niveau élevé, d'autant plus que la rénovation augmente la part de l'ECS dans les besoins thermiques, tandis que les mesures d'optimisation de l'ECS étudiées n'apportent que des gains modestes.

La réduction des températures de production améliore directement le rendement des PAC et réduit les émissions de CO_2 associées, tandis que la diminution de la demande de chaleur réduit simultanément la consommation totale d'énergie et les émissions par unité de surface. Un résultat majeur du projet est que le rôle de l'optimisation dépend de l'indicateur considéré. En termes de températures de production et de rendement, les mesures d'optimisation peuvent compenser en partie l'absence d'une rénovation plus poussée de l'enveloppe, constituant ainsi une stratégie efficace à court terme pour améliorer les bâtiments les moins performants dans l'attente d'une rénovation complète. En revanche, pour les émissions absolues qui conditionnent la décarbonisation, rénovation de l'enveloppe et optimisation sont complémentaires : l'optimisation ne pouvant réduire significativement les besoins de chauffage, la rénovation de l'enveloppe reste indispensable, tandis que l'optimisation permet d'en accélérer et d'en renforcer les bénéfices sans pouvoir s'y substituer. Le choix du système de production de chaleur est également déterminant : une PAC à haut rendement améliore les performances sans modifier les températures de fonctionnement, tandis qu'un système bivalent peut constituer une solution transitoire pertinente, à condition que sa régulation et sa configuration hydraulique limitent le recours à la chaudière.

Dans l'ensemble, l'abaissement des températures de distribution peut être considéré comme un cobénéfice de la réduction des besoins de chaleur, obtenu grâce à des mesures adaptées aux caractéristiques et à l'état de chaque bâtiment. Les travaux futurs devraient notamment porter sur l'optimisation de la production d'ECS, l'extension de l'analyse aux sous-stations de CAD et l'évaluation économique des mesures étudiées.

Main findings («Take-Home Messages»)

- **Lowering space heating distribution temperatures is mainly a matter of reducing the heat demand.** The minimum achievable space heating supply temperature is governed by the effective oversizing of the heat emitters, so any measure that reduces the space heating demand enables lower supply temperatures and thus improved heat pump efficiency, provided the heating curve is optimized accordingly and the system is hydraulically balanced.
- **System optimization is an effective short-term strategy to accelerate decarbonization and renewable integration.** Although system optimization cannot replace envelope retrofitting for reducing the absolute CO_2 emissions, it can substantially lower operating temperatures and improve heat pump efficiency, allowing existing buildings to accommodate renewable heat sources before deep renovation is carried out. This supports policies that promote system optimization alongside, rather than as an alternative to, envelope retrofitting.
- **Domestic hot water is the main barrier to further reducing operating temperatures.** Besides the high temperatures required to control the legionella risk, many promising DHW optimization measures remain insufficiently documented under real operating conditions for large MFBs. This limits stakeholders' confidence in implementing them and highlights the need for further research and pilot and demonstration (P&D) projects.
- **Transition to low-temperature renewable heat production and decarbonization requires building-specific retrofit pathways.** The most effective strategy combines targeted envelope retrofitting, system optimization and an appropriate heat production system, with measures prioritized according to the pre-existing characteristics and current state of each building. Coordinated planning of these measures would maximize their contribution to building decarbonization while facilitating their practical implementation.

Acknowledgements

We would like to thank the Swiss Federal Office of Energy (SFOE), the *Services Industriels de Genève* (SIG), the *Direction de l'énergie du canton de Vaud* (DGE-DIREN) and the City of Yverdon-les-Bains for funding this project.

We also warmly thank the members of the advisory board for their constructive input, namely:

- Nadège Vetterli, Martin Ménard (SFOE)
- Loïc Quiquerez, Carolina Fraga, Gautier Falize, Hadia Khimda-Ouendi (SIG)
- Cédric Blondel (SIL)
- Jean-François Mino (MBG)
- François Baud (François Baud & Thomas Früh Atelier d'architecture SA)
- Anne-Valérie Narath, Charles Thoumyre (DGE-DIREN)
- Fabien Poumadère (Service des énergies de la ville d'Yverdon-les-Bains)

Finally, we also thank the other people who provided us with data and insights on various issues, in particular Stefanie Schwab (HEIA-FR), Lionel Rinquet (HEPIA) and Thomas Ravier.

Executive summary

Buildings account for around 45% of Switzerland's final energy consumption and a third of its CO_2 emissions, most of it related to space heating (SH) and domestic hot water (DHW), and more than half are still heated by fossil fuel boilers. Replacing these boilers with heat pumps (HPs) or connecting buildings to district heating networks (DHNs) is central to decarbonizing the sector, particularly for multifamily buildings (MFBs) in dense urban areas, where few other renewable options are available. The performance of these renewable heat sources, however, is strongly penalized by the high distribution and production temperatures inherited from fossil fuel systems.

The T-DROP project investigates how existing MFBs can shift from high- to low-temperature heat distribution through combination of targeted envelope retrofitting and heat distribution optimization, and quantifies the resulting benefits for renewable heat integration and decarbonization. The project focuses on decentralized air-source heat pump (HP) systems, although several of the optimizations investigated are also applicable to district heating substations.

The project is organized into three main parts. The first part consists in defining and modeling building typologies of interest, as well as establishing a list of retrofitting scenarios. The second selects and models optimization or replacement measures for the SH/DHW system. Finally, the building and SH/DHW system models are combined into a single integrated model. This model is used to quantify the benefits of these measures for renewable heat integration and the decarbonization of existing MFBs, through a sensitivity analysis across building typologies, retrofitting depths and SH/DHW optimization measures.

Building typologies and envelope retrofitting measures (Chapter 3)

The first part of the study defines the building typologies of interest, establishes a list of targeted envelope retrofit measures to reduce the SH demand and distribution temperatures, and develops building models suitable for coupling with detailed SH/DHW system models.

Building typologies (section 3.1)

The MFB typologies considered are selected from the literature, in particular the architectural fact sheets developed in the eREN project and its follow-up projects, Solution Rénovation and TypoRENO, mainly focusing on MFBs built during the 20th century. To keep the number of cases manageable, the study focuses on the predominant MFB typologies representative of the building stock in need of retrofitting, identified through discussions with architects and an analysis of Geneva's MFB stock. For the relevant typologies identified, the corresponding LESOSAI models and architectural fact sheets are updated and made mutually consistent in terms of weather station, SIA standard version and costs.

Envelope retrofitting measures (section 3.2)

For each selected typology, a set of targeted envelope retrofit scenarios (e.g. window replacement, roof and façade insulation) is established from the available fact sheets, and the associated retrofitting costs are analyzed in detail and compared across the typologies. The cost analysis allows to rank the measures from most to least cost-effective, both per unit of energy saved (CHF/kWh) and per unit of floor area (CHF/m²), in the following order: floor insulation, attic and roof insulation, windows replacement and façade insulation (Figure A). A wide range of cost values is observed, reflecting the variability in renovation approaches, architectural constraints, existing building conditions and contractor estimates. A comparison with the cost analysis from the Effiwag project shows similarly large variability, at generally lower cost, though the small sample size in our project and the different perimeters of these analysis limits firm conclusions. These results are used to define the retrofitting sequence for each typology, and three typologies are ultimately selected for the rest of the study, spanning small-scale (1'500 m²) to very large-scale (8'000 m²) MFBs.

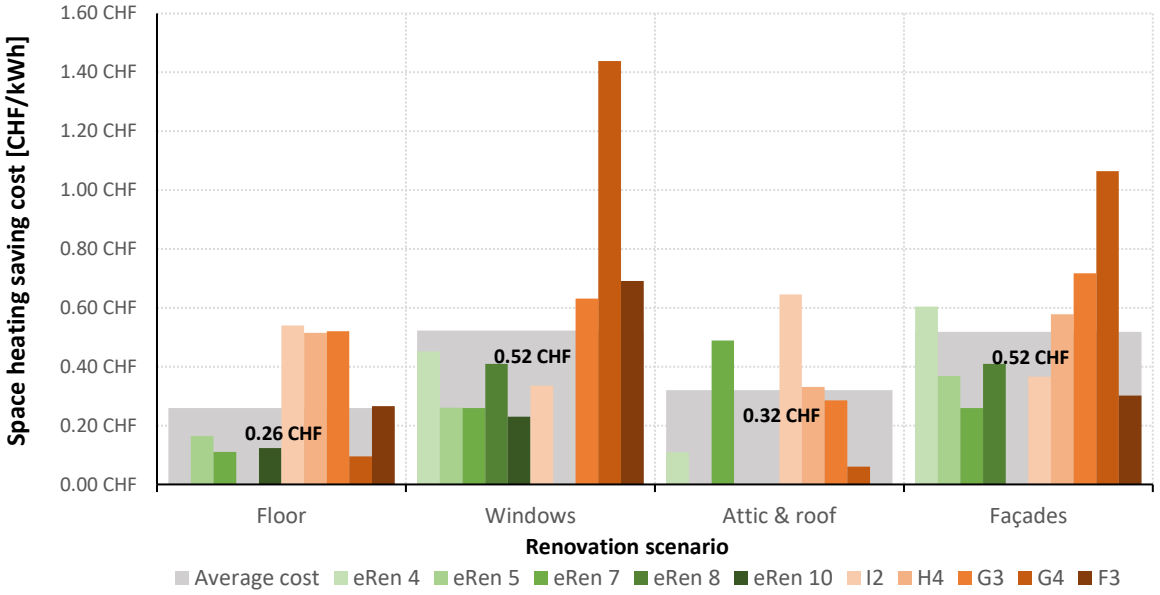


Figure A: Cost of each envelope retrofitting measure per kWh of SH saved over its service life

Building modeling (section 3.4)

To capture the interactions between the building and the SH/DHW system, the LESOSAI building models are transposed into simplified TRNSYS building models, based on a resistance-capacitance (RC) model. Compared with detailed building models, this approach is faster to configure and, most importantly, allows the building model to be coupled with the SH/DHW system model in TRNSYS, capturing at each time step the interactions between the indoor temperature and the SH/DHW system (an integration not possible with the LESOSAI models). The model is validated against a case study by comparing simulated results with both measurements and LESOSAI results: the differences in SH demand are small in winter and grow in mid-season, but cancel out over the year, giving an annual deviation of only 0.2% against measurements and below 1.5% against LESOSAI results.

SH/DHW systems and optimization and replacement measures (Chapter 4)

The second part identifies and models representative SH/DHW system typologies, reviews and selects replacement and optimization measures, and develops the corresponding numerical models.

SH/DHW typologies (section 4.1)

Representative systems are first identified and modeled, with particular attention to their hydraulic configuration and control strategy. The systems considered represent properly functioning installations, excluding faulty components and configurations inherited from fossil fuel boilers that would need to be modified before renewable heat production could be implemented. The study focuses on decentralized air-source HP systems, with or without a backup gas boiler, which corresponds to the systems most commonly installed in existing MFBs in dense urban areas as a replacement for fossil fuel boilers where DH is unavailable.

Optimization and replacement measures (section 4.2)

A literature review of replacement and optimization measures is then carried out, while their feasibility and temperature reduction potential discussed with professionals, drawing on practical experience and implementation feedback. This review shows that SH-related measures are well documented, well known and commonly implemented, whereas DHW-related measures are less well known: they are mainly studied through simulation, with little feedback from real operating conditions for large MFBs.

Given the sensitivity of DHW to legionella risk, professionals remain reluctant to test optimization measures on the DHW system, even though high DHW temperatures are what most limits the reduction of the overall system temperature and typically cause more operational issues than SH.

Focus on heat emitters and heating curves (section 4.4)

The review is complemented by a specific focus on heat emitters and heating curves, since they play a central role in the transition from high- to low-temperature SH distribution. Several case studies are analyzed to estimate the current level of heat emitter oversizing in existing Swiss MFBs and how it evolves after envelope retrofitting. Despite conservative assumptions, the four case studies analyzed are generally well sized in their current state (oversizing factor of 0.83-1.12), although a room-by-room analysis reveals some heterogeneity, with living rooms typically showing a higher oversizing factor than bedrooms. After envelope retrofitting, the oversizing factor rises to 1.75-2.60, revealing significant potential for reducing the SH supply temperature.

Two main heating curve optimization methods are identified from the literature: the "low-flow" method, better suited to DHN-supplied buildings, which minimizes the return temperature at the cost of a higher supply temperature; and the "high-flow" method, preferable for HP-supplied buildings, which minimizes the supply temperature but requires a higher distribution flow rate (example in Figure B).

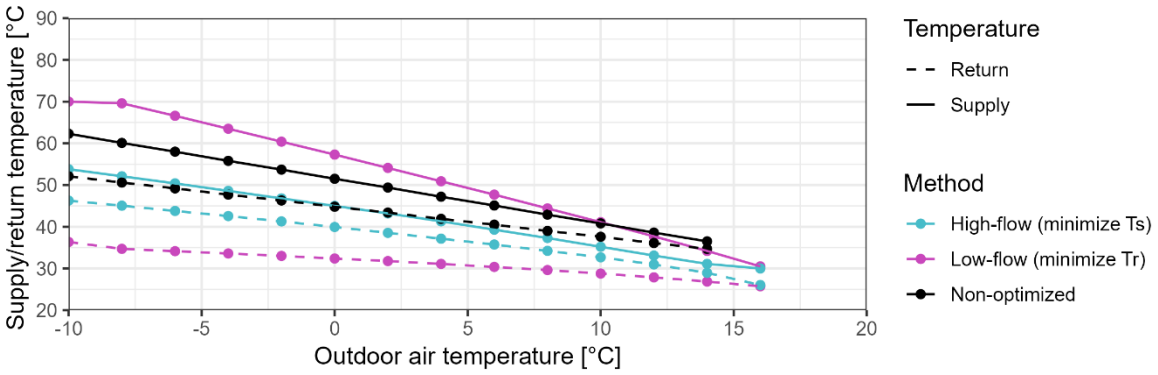


Figure B: Non-optimized heating curve (baseline) and optimized heating curves using the "low-flow" and "high-flow" methods for building typology eREN 4 partially retrofitted, for an indoor temperature setpoint of 22°C and a ventilation flow rate of 1.0 m³/h.m², without initial oversizing of the heat emitters

System modeling (section 4.5)

Finally, the selected replacement and optimization measures are integrated into the SH/DHW system models, using either a simplified rule-of-thumb approach (where detailed modeling would be too complex or time-consuming) or more detailed energy models in TRNSYS.

Integrated simulation and decarbonization potential (Chapter 5)

In the last part of the study, the building and SH/DHW system models are combined into a single TRNSYS model that captures, at each time step, the interactions between the SH load, the indoor temperature, the heat emitters and the rest of the system, providing more realistic temperature levels than uncoupled models would.

Baseline scenario and sensitivity analysis (sections 5.2, 5.3 and 5.4)

Relevant energy and environmental performance indicators are first defined, including the HP seasonal performance factor (SPF), or overall system efficiency for hybrid systems, and the CO_2 emissions per unit of heat produced and per unit of floor area. The integrated model is then used to simulate a baseline scenario (a non-retrofitted building with an air-source HP). The identified measures are then combined

into various scenarios representing different levels of system optimization and retrofitting depth, across different building and system typologies (Figure C).

A table (Table 14) summarizes the results of the sensitivity analysis for the baseline scenarios and for each sensitivity parameter. It quantifies the impact of each parameter on the energy and environmental performance indicators and highlights the key takeaways.

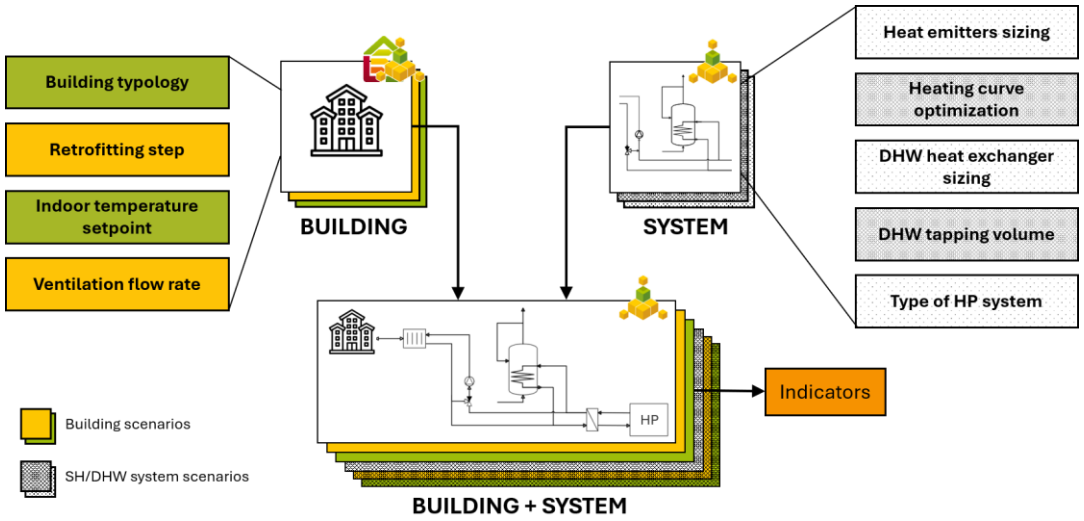


Figure C: Illustration of the sensitivity analysis parameters and scenarios

SH optimization measures (section 5.4.2, 5.4.3, 5.4.4 and 5.4.5)

On the SH side, the sensitivity analysis identifies heating curve optimization as the key enabling measure. Without it, retrofitting alone barely lowers production temperatures or improves the HP SPF, and only the CO_2 emissions per floor area decrease, driven by the lower demand (Figure D). With heating curve optimization, supply temperatures are significantly reduced through building retrofit and the SPF rises substantially, which is why it is treated as a prerequisite for all other measures examined.

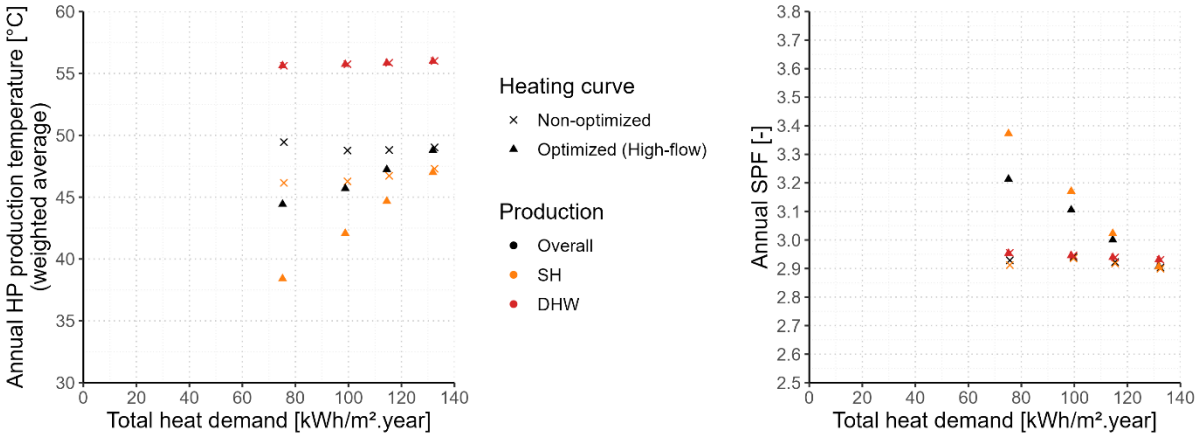


Figure D: Annual average HP production temperature and HP SPF for each service, with and without heating curve optimization

The supply temperature reduction is itself governed by the effective heat emitter oversizing, i.e. the ratio between the installed emitter capacity and the actual SH load (Figure E). This ratio can be raised either by replacing existing radiators or by reducing the SH demand. The ventilation flow rate and the indoor temperature setpoint both act on the indicators indirectly, through there influence on the SH demand and therefore effective emitter oversizing. Through these optimizations, a well-optimized building at a

given retrofitting step can reach a performance comparable to that of the next retrofit step (e.g. a non-retrofitted building approaching a partially retrofitted one, and a partially retrofitted building approaching a fully retrofitted one). The building typology itself has no direct effect: typologies differ only through their initial SH demand, which in turn sets the installed capacity, the effective oversizing and the resulting indicators.

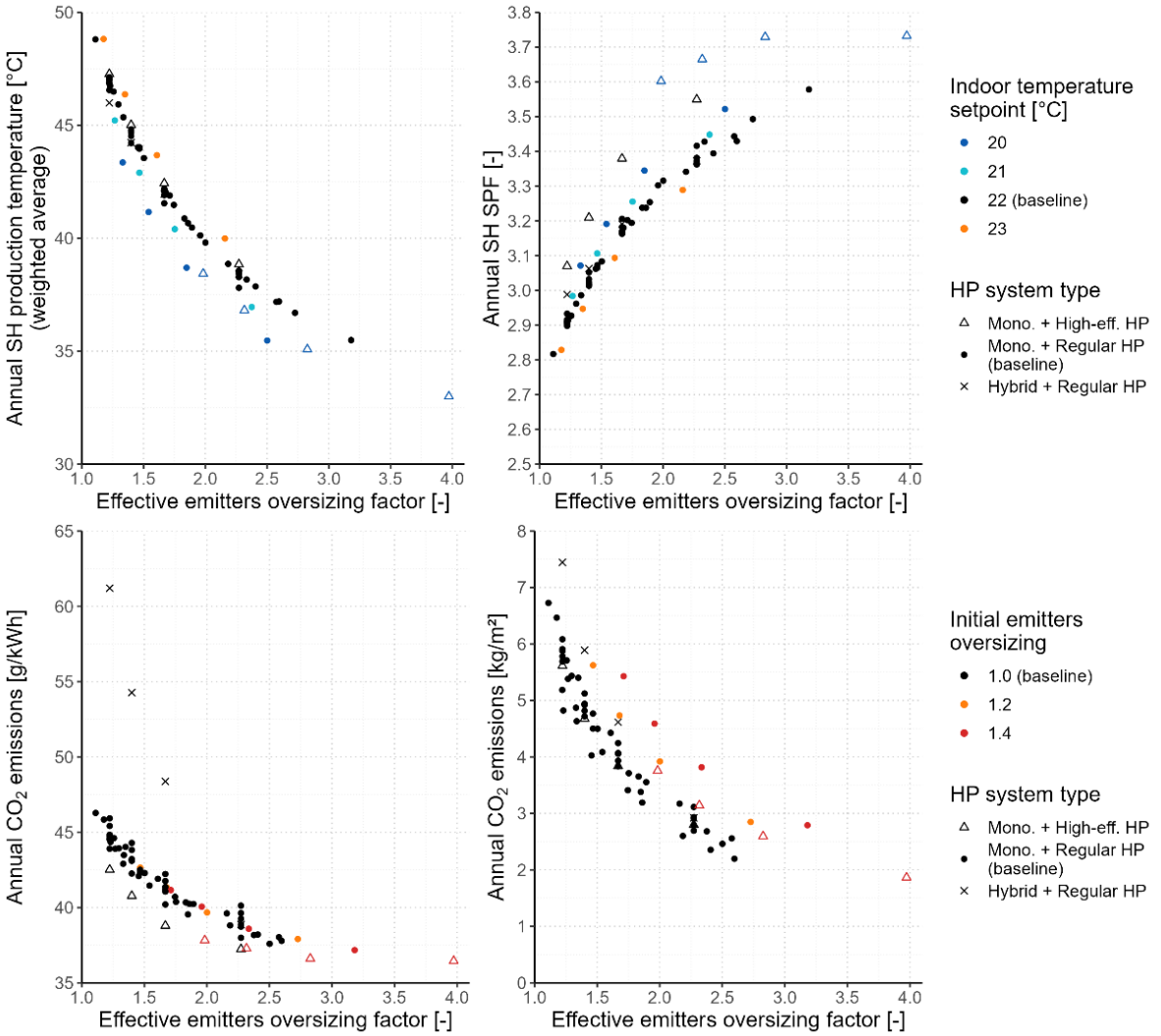


Figure E: Annual average HP production temperature for SH, HP SPF in SH, and CO_2 emissions in g/kWh and kg/m². All results from the sensitivity are included, except for scenarios without heating curve optimization.

Importantly, the results clearly show that DHW production constitutes the main temperature constraint within the SH/DHW system. While SH supply temperatures can be substantially reduced through retrofitting and optimization measures, DHW production still requires significantly higher temperature levels to prevent legionella proliferation. Consequently, the average production temperature of the overall system decreases only about half as fast as the SH production temperature. This limitation becomes increasingly important as buildings are retrofitted, since the DHW share of the total heat demand rises as the SH demand decreases.

DHW optimization measures (section 5.4.6)

On the DHW side, increasing the heat exchanger transfer area affects mainly the DHW production temperature and DHW SPF, but only marginally the rest of the system. This is due to several factors: i) the

relatively low DHW fraction of the total heat demand, and ii) the low carbon content of the summer electricity mix. DHW is produced throughout the year, including summer periods (about one third of the heat produced for DHW) when the carbon intensity of the Swiss electricity mix is relatively low. As a result, improving DHW production efficiency has a smaller effect on annual CO_2 emissions than improving SH production. Despite this relatively modest impact on performance indicators, a small heat exchanger area is nonetheless detrimental for the system and should be avoided.

Counter-intuitively, reducing the DHW demand (through a lower DHW tapping volume) does not necessarily improve production efficiency. This effect is linked to tank stratification. With higher DHW tapping volumes, more cold water enters the bottom of the tank, reducing the average tank temperature, improving stratification and lowering the average return temperature to the HP. Since the HP operates at a roughly constant condenser temperature difference (about 5 K), the average DHW production temperature decreases accordingly. Lower DHW tapping volumes have the opposite effect, raising the average DHW production temperature and thus lowering the DHW SPF and increasing the CO_2 emissions per unit of heat produced. Reducing the DHW demand does, however, still lower the absolute CO_2 emissions per unit of floor area. These opposing effects limit the overall impact of DHW demand reduction on the annual performance indicators.

HP system type (section 5.4.7)

Regarding the choice of HP system, the use of a high-efficiency HP unit improves performance at unchanged temperatures (+0.18 on the SPF on average, and a reduction of 4-6% of emissions). A hybrid system, despite its boiler covering only a small share of the demand (9% at most), can noticeably increase emissions in poorly retrofitted buildings. Hybrid HP systems yet remain an attractive transitional solution to accelerate decarbonization of MFBs, allowing HPs to be deployed early rather than after full retrofit, provided the control and hydraulics prevent the boiler from taking over.

Best-case scenario (section 5.4.8)

When combining all optimization measures (best-case scenario, Figure F), the indicators depend little on the retrofitting status, except for the CO_2 emissions per floor area, which remain strongly influenced by the reduction of the heat demand. The improvement over other scenarios is more pronounced for non-retrofitted buildings. For fully retrofitted ones, it is much smaller, since some scenarios with only one optimization measure come close to the same performance. This shows that applying the full set of optimization measures to an already fully-retrofitted building may not prove cost-effective, and that optimization measures can therefore partly compensate for the absence of deeper envelope retrofitting.

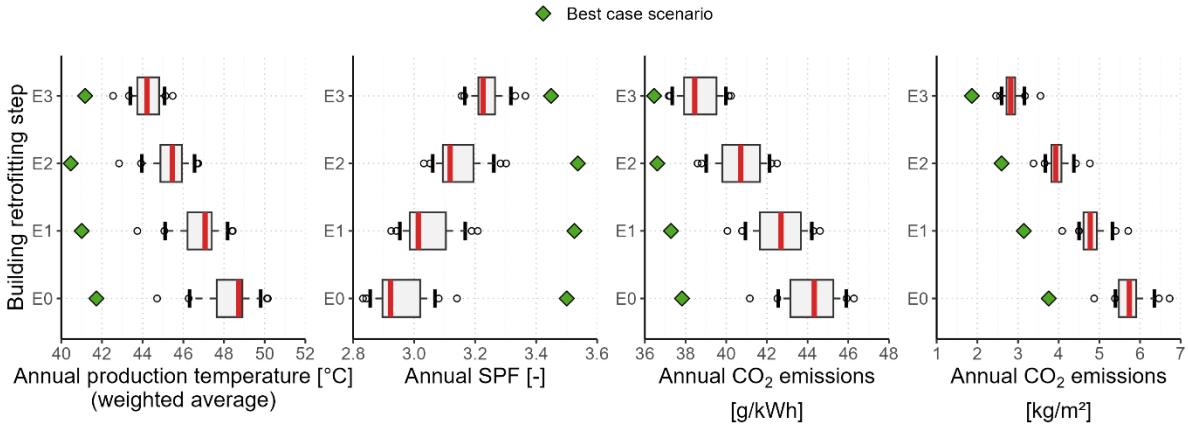


Figure F: Comparison of the annual average HP production temperature and performance indicators at each building retrofitting step (Ei), between the best-case scenario and all other scenarios. Results are shown for the eREN 4 building typology (baseline) heated by a monovalent HP system. Scenarios with hybrid HP systems or without heating curve optimization are excluded. The whiskers represent the 1st and 9th deciles (10% and 90% of values), and the box the 1st and 3rd quartiles (25% and 75% of values).

Conclusions

Overall, the project shows that lowering distribution temperatures is best pursued not as an isolated objective but as a co-benefit of reducing the heat demand. The most effective decarbonization pathways combine targeted envelope retrofitting, heat distribution optimization and a well-chosen heat production system. The selection and implementation of these measures should be prioritized on a case-by-case basis according to the pre-existing characteristics and current state of each building, rather than applied uniformly across the building stock. Optimization measures offer a fast, low-cost way to improve the performance of poorly performing buildings while deeper retrofitting is planned, but they cannot substitute for it where absolute decarbonization is the goal. DHW remains the main barrier to further temperature reduction, and the measures most likely to overcome this barrier are still insufficiently documented under real operating conditions for MFBs, highlighting the need for future pilot and demonstration projects, alongside the extension of this analysis to DH substations and the economic assessment of the system optimization measures.

Authorship contribution statement

Section	Contributors
Chapter 1: Introduction	P. Brischoux, P. Hollmuller, X. Jobard, A. Duret
Chapter 2: Approach and method	P. Brischoux, P. Hollmuller, X. Jobard, A. Duret
Chapter 3: Buildings typologies and envelope retrofitting measures	B. Périsset, R. Guinouet, X. Jobard, A. Duret, P. Brischoux
Chapter 4: SH/DHW systems and optimization and replacement measures	P. Brischoux, P. Hollmuller, R. Guinouet, A. Duret
Chapter 5: Integrated building and SH/DHW system simulations	P. Brischoux, R. Novoa-Herzog, P. Hollmuller
Chapter 6: Discussion	P. Brischoux, P. Hollmuller

Contents

Summary ... **3**
Zusammenfassung ... **4**
Résumé ... **5**
Main findings («Take-Home Messages») ... **6**
Acknowledgements ... **7**
Executive summary ... **8**
Building typologies and envelope retrofitting measures (Chapter 3) ... 8
SH/DHW systems and optimization and replacement measures (Chapter 4) ... 9
Integrated simulation and decarbonization potential (Chapter 5) ... 10
Conclusions ... 14
Authorship contribution statement ... **15**
Contents ... **16**
List of abbreviations ... **18**
1 Introduction ... **19**
1.1 Context and motivation ... 19
1.2 Project objectives ... 20
2 Approach and method ... **21**
2.1 Building typologies and envelope retrofitting measures ... 21
2.2 SH/DHW systems and optimization and replacement measures ... 22
2.3 Integrated simulation and decarbonization potential ... 22
3 Buildings typologies and envelope retrofitting measures ... **23**
3.1 Buildings typologies ... 23
3.2 Envelope retrofitting measures ... 25
3.3 Selected building typologies and retrofitting measures ... 30
3.4 Building modeling ... 31
4 SH/DHW systems and optimization and replacement measures ... **38**
4.1 SH/DHW systems typologies ... 38
4.2 Optimization and replacement measures ... 40
4.3 Selected optimization measures ... 45
4.4 Focus on heat emitters and heating curves ... 46
4.5 System modeling ... 53
5 Integrated building and SH/DHW system simulations ... **56**
5.1 Integrated building and SH/DHW system model ... 56
5.2 Performance indicators ... 56
5.3 Baseline scenario ... 58
5.4 Sensitivity analysis ... 64

6 Discussion 80
6.1 Insights from simulation results 80
6.2 Limitations and possible future work 82
7 Conclusions and outlook 87
8 National and international cooperation 89
9 Publications and other communications 90
10 References 91
11 Appendix 98
11.1 Application of the methodology to eREN No5 building typology 98
11.2 Updated building retrofit sheets for predominant eREN typologies 100
11.3 Parameters and inputs of heat emitter model (TRNSYS Type 5897) 105
11.4 Installed heat emitters capacity and optimized heating curves 106
11.5 Modeling of DHW optimization measures 108
11.6 Heat pump performance maps 111
11.7 Hydraulic balancing 112
11.8 Carbon emissions and renewable energy fraction of the Swiss electricity mix 116

List of abbreviations

ASHP	Air-source heat pump
DHN	District heating network
DHW	Domestic hot water
ERA	Energy reference area
HX	Heat exchanger
HP	Heat pump
MFB	Multifamily building
P&D	Pilot and demonstration
SH	Space heating
SFOE	Swiss Federal Office of Energy
SST	Substation

1 Introduction

1.1 Context and motivation

Buildings account for around 45% of Switzerland's final energy consumption and 33% of its CO_2 emissions [1], representing one of the most important sectors for massive decarbonization. Approximately 87% of their final energy consumption is related to space heating (SH) and domestic hot water (DHW), and 55% of all buildings are still heated with individual fossil fuel boilers [2,3]. Finally, 80% of them have an area-specific heating demand which exceeds the current minimum energy performance value for new constructions, 40% of them reaching more than twice this threshold. This points out to the need of massive and efficient retrofit of the existing building stock, with combined switch from fossil fueled boilers to renewable energy systems [4].

A specific issue concerns multifamily buildings (MFBs) which represent about 55% of the residential heated floor area at national level, but up to 80% in urban Cantons like Basel or Geneva [4,5]. Especially in dense urban areas, district heating networks (DHNs) or air-source heat pumps (HPs) often turn out to be the only available option for replacing fossil fuel boilers, since other renewable energy sources are frequently limited [6]: prohibition of wood boilers in areas with excessive emissions; limitation of solar energy resource due to roof size and patrimonial constraints; low availability of adapted ground for boreholes; no groundwater or in water protection areas; too long distance to lake or river. In terms of retrofit, MFBs further face specific issues (technical, financial, organizational), namely lack of robust, standardized retrofit solutions, as well as landlord/tenant dilemma in relation to investment and repayment.

In existing MFBs, even without retrofit of the building envelope and when considering the hourly Swiss electricity mix (taking into account imports/exports), transition from fossil fuel boilers to HPs can in principle bring substantial CO_2 savings of 60-80% [7]. However, as highlighted in several recent P&D projects [8–10], high distribution temperatures penalize or impede proper operation of renewable heat production via HPs at building and DH level.

In this regard, building envelope retrofit, while primarily aiming at reducing the SH demand, can also contribute to lower SH distribution temperatures, by way of simple optimization measures on heating curves, flowrates, hydraulic circuit configuration [11–14], or possibly with selective replacement of heat emitters [15]. While the demand for DHW is independent of the building envelope and is subject to specific temperature regulation (related to the legionella issue). Several temperature reduction techniques can in principle also be implemented [16], namely direct DHW production (without storage), or cascading of SH and DHW production to lower the return temperature to the heat production system. At district level, lowering the DHN temperature has also been identified as a key measure for decarbonization of the heat supply [17] and reduce DHN operating costs [18,19].

In this context, combination of targeted envelope and system retrofit, along with optimization and/or replacement measures of SH/DHW distribution, appear as the most appropriate solution to lower the system temperatures and accelerate the integration of renewables and related decarbonization. However, combinations of such measures have so far not been investigated in a systematic way, in particular in terms of lowering SH and DHW distribution/production temperatures.

T-DROP explores optimal combinations of targeted envelope retrofit and technical optimization of heat distribution systems in buildings, to lower heat distribution temperatures and decarbonize heat production. It focuses on decentralized HP systems, but some of the investigated optimizations are also applicable to DH substations. Specific objectives are:

- For various building typologies, identify key technical measures for temperature reduction of heat distribution (SH and DHW), transition to renewable heat production, with or without targeted envelope renovation.
- Evaluate the impacts of such measures in terms of energy mix, CO_2 reduction (direct and indirect), accounting for architectural and technical constraints.

1.2 Project objectives

Based on the context and motivations presented above, this project aims to tackle the following research questions:

1) How to transition from high to low temperature heat distribution (SH and DHW) through the combination of envelope retrofitting measures and heat distribution optimizations, to facilitate HP integration in existing buildings?
2) What are the benefits of such measures on energy and environmental performance indicators?

The following specific objectives will be achieved within the project:

1) Quantify the temperature reduction potential for various typologies of MFBs following optimization of heat distribution systems and different combinations of envelope retrofit measures.
2) Evaluate the impact of temperature reduction on heat production efficiency for different heat production systems, in particular HP.
3) Quantify the decarbonization potential for various typologies of building following temperature reduction through a combination of targeted envelope retrofits, heat distribution systems optimization and fuel switch.

2 Approach and method

The project is divided into three main parts. The first part consists in defining and modeling building typologies of interest, as well as establishing a list of retrofitting scenarios. The second part consists in selecting and modeling optimization or replacement measures for the SH/DHW system. Finally, those numerical models of both building and SH/DHW system are combined to quantify the benefits on renewable heat integration and decarbonization of existing MFBs.

Throughout the study, an extensive set of case studies from past and ongoing projects, with diverse and mixed building typologies, are used to: i) characterize the building and system typologies; ii) provide inputs for the energy models and iii) test strategies for the reduction of SH and DHW production temperatures and integration of renewables.

Modeling of the building and SH/DHW system is first carried out separately. These models are later on combined into an integrated building and SH/DHW system model to be able to accurately evaluate the temperature levels. Finally, a sensitivity analysis is conducted for different retrofit and optimization scenarios to quantify the impact of the implemented measures on renewable heat integration and building decarbonization.

2.1 Building typologies and envelope retrofitting measures

The first part of the study focuses on building typologies and envelope retrofitting measures, with three main objectives: i) to define building typologies of interest and their characteristics, ii) to establish a list of targeted envelope retrofit measures to reduce SH demand and distribution temperature levels, and iii) to develop building models of the selected building typologies and targeted retrofitting measures suitable for coupling with detailed SH/DHW system simulations.

The MFB typologies considered in this project are selected based on the literature, in particular architectural fact sheets developed in the eREN project [20] and its follow-up projects (TypoRENO [21] and Solution Rénovation [22]). To keep the number of cases manageable, the study focuses only on predominant MFB typologies representing the building stock in need of retrofitting. These typologies are identified through discussions with architects from the RENOWAVE project [23], together with the Solution Rénovation project database [24], which assigns a building typology to a significant share of Geneva's MFB stock. Each considered typology is defined by a set of parameters (envelope characteristics, SH demand …) characterizing the initial situation, before envelope retrofitting measures are applied.

For each selected typology, a set of targeted building envelope retrofit scenarios (e.g. window replacement, roof/façade insulation…) is established from the available architectural fact sheets. Since these typologies originate from different projects carried out at a different time and under different assumptions, the fact sheets and corresponding LESOSAI models are first made consistent with each other. This includes updating the calculations to the latest SIA 380/1 standard, adopting a common weather station and updating the retrofitting cost assessment. The retrofitting costs are then analyzed in more details and compared with results from other projects. Results from this analysis are used to establish the sequence in which the retrofitting measures are applied for each building typology.

To account for the interactions between the building and the SH/DHW system, the LESOSAI building models are transposed into simplified TRNSYS building models. The latter are based on a resistance-capacitance (RC) model developed for TRNSYS [25], based on the ISO13790:2008 standard (hourly method) [26]. Compared to detailed building models, it is less time-consuming to configure. It also allows the building model to be coupled with the SH/DHW system model in TRNSYS, thereby accounting at each time step for the interactions between the building's indoor temperature and the SH/DHW system (an integration that would not be possible with LESOSAI building models). The TRNSYS building model is validated using a case study by comparing simulated results with both measurements and LESOSAI modeling results. The resulting building models allow to quantify annual and hourly SH demand, peak load and the impact of envelope retrofitting measures.

For more detailed information, see Chapter 3.

2.2 SH/DHW systems and optimization and replacement measures

The second part of the study focuses on the SH/DHW system with three main objectives: i) to identify and model representative SH/DHW system typologies, ii) to review and select replacement and optimization measures for SH/DHW distribution and production; iii) to develop the corresponding numerical models.

The first step consists in identifying and modeling representative SH/DHW systems, with particular attention to their hydraulic configuration and control strategy. The systems considered represent properly functioning installations, and therefore exclude faulty components, malfunctions and hydraulic configurations inherited from fossil-fuel boilers that must be modified prior to implementing renewable heat production.

A review of replacement and optimization measures is then carried out based on the literature. Their feasibility and potential for lowering temperature levels are discussed with professionals, drawing on their practical experience and feedback from implementation projects. A final selection of measures is made based on the expected impact on temperature levels and modeling feasibility.

This review is complemented by a specific focus on heat emitters, since they directly determine the minimum SH temperature required to maintain indoor thermal comfort. Several case studies are analyzed to assess heat emitter oversizing for existing buildings in Switzerland, providing a range for this parameter in the present study. The modeled heat emitter capacity is then determined from the design SH load of each building typology in its initial state, taken from the results of the building model. On this basis, the corresponding supply and return temperature requirements (and therefore the achievable reduction in temperature levels) can be calculated for each building typology and envelope retrofitting scenario, for a given installed emitter capacity.

Finally, the selected replacement and optimization measures are integrated into the SH/DHW system models, using either a simplified rule-of-thumb approach (where detailed modeling would be too complex or time-consuming) or more detailed energy models in TRNSYS [27].

For more detailed information, see Chapter 4.

2.3 Integrated simulation and decarbonization potential

In the last part of the study, the building and SH/DHW system models developed in the previous parts are combined into a single TRNSYS model. This integrated model accounts, at each time step, for the interactions between the building's indoor temperature, the heat emitters, and the rest of the SH/DHW system, thereby providing more realistic system temperature levels than uncoupled models would.

Relevant energy and environmental performance indicators are first defined. The integrated model is then used to simulate a baseline scenario, consisting of a non-retrofitted building supplied by an air-source HP system. The identified retrofitting and optimization measures are then implemented into the model and combined into various scenarios, representing different levels of system optimizations and retrofitting depth (from partial to full). Their impact on the defined temperature levels and performance indicators is assessed to identify the most favorable scenarios. The aim is to support decision-making by highlighting the impact of each measure for enabling decarbonization and integration of renewable energy sources.

For more detailed information, see Chapter 5.

3 Buildings typologies and envelope retrofitting measures

This chapter focuses on building typologies and envelope retrofitting measures, with three main objectives: i) to define building typologies of interest and their characteristics, ii) to establish a list of targeted envelope retrofit measures to reduce SH demand and distribution temperature levels, and iii) to model the selected building typologies and targeted retrofitting measures.

The chapter first reviews existing building typology fact sheets to identify the predominant MFB typologies representative of the multifamily building stock in need of retrofitting, then analyses the proposed envelope retrofitting measures and their costs, using existing LESOSAI energy models updated for the current study. Based on this analysis, a set of representative typologies is selected. Finally, the TRNSYS-based building modeling approach is described, including model parameterization and validation against both measured data and LESOSAI simulation results.

3.1 Buildings typologies

3.1.1. Existing fact sheets

The building typologies considered in this work are drawn from architectural and constructive fact sheets developed in three successive projects on the residential building stock in the French-speaking part of Switzerland, summarized in Table 1. eREN and Solution Rénovation focus on multifamily buildings (MFBs), while TypoRENO-VD covers residential buildings more broadly. Each project identifies representative typologies in need of retrofitting and, for a reference building per typology, defines detailed envelope retrofit scenarios with the estimated SH demand before and after retrofitting and the associated investment costs. The aim is to facilitate and accelerate the renovation process for building owners.

- eREN [20] proposes a global, interdisciplinary approach to the envelope renovation of MFBs, balancing energy efficiency, heritage and architectural value, occupant comfort and cost. It covers 10 typologies representative of the building stock in the French-speaking part of Switzerland, spread across five construction periods (pre-war to post-oil-crisis, 1900–1990).
- Solution Rénovation [22] revisits the post-war eREN fact sheets for the Geneva context, and adds three locally specific typologies, for a total of 9 fact sheets. It also maps the occurrence of the selected typologies across a large portion of the existing building stock [24].
- TypoRENO-VD [21] focuses on the energy retrofit of heritage residential buildings (not only MFBs) in the canton of Vaud, with 20 fact sheets covering buildings selected by location, size, period, construction type and architectural features. It also favors sustainable materials, leading to higher retrofitting costs than the eREN buildings. Unlike the other two projects, it proposes a step-by-step retrofitting sequence rather than full-retrofitting scenarios, ordered by ease of implementation in occupied buildings and by the condition and remaining lifetime of each element.

Table 1: Characteristics of the available building retrofitting fact sheets for MFBs

Fact sheets/Project	Project date	Region	Construction period	Type of retrofitting scenarios	Number of fact sheets
eREN [20]	2015-2017	French-speaking Switzerland	1900-1990	2 or 3 full-retrofitting scenarios	10
Solution Rénovation [22]	2018-2022	Canton of Geneva	1946-1990	2 full-retrofitting scenarios	9
TypoRENO-VD [21]	2021-2026	Canton of Vaud	All (16th to 20th cent.)	1 step-by-step retrofitting scenario	20 (as of Sept. 2025)

3.1.2. Predominant typologies

To limit the number of cases, the current project focuses on predominant MFB typologies representing the Swiss building stock in need of retrofitting. Predominant typologies are identified based on discussions with architects from the Renowave project [23], as well as the Solution Rénovation project database [24]. The latter assigns a building typology to a significant portion of Geneva's MFB stock built after 1945. With a statistical analysis, it is then possible to determine the predominant building typologies in terms of number of buildings, energy reference area (ERA) and heat demand (see Figure 1 and Table 2 from [28]). It should be noted that this analysis was carried out on the portion of the multifamily building stock in Geneva that has both an assigned typology and available heat demand data. It is also limited to MFB built between 1945 and 1990 (about 53% of the MFB ERA in GE), because the Solution Rénovation project focused only on that construction period. Ultimately, this subset represents approximately 40% of Geneva's total MFB stock ERA.

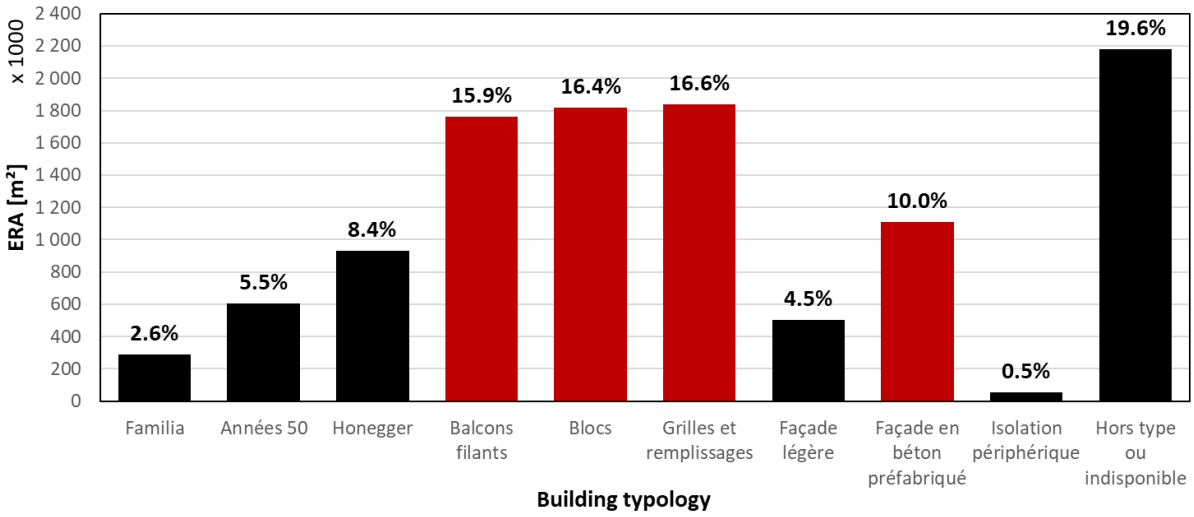


Figure 1: Distribution of the ERA of MFB in Geneva by building typology according to the "Solution Rénovation" project (MFB buildings built between 1945 and 1990, with an ERA > 500 m²)

Table 2: Predominant building typologies in Geneva's multifamily building stock [28]

Typology name	eREN fact sheet No.	% ERA in GE MFB stock	% buildings in GE MFB stock	% heat demand in GE MFB stock
Balcons filants	5	15.9%	13.9%	16.1%
Blocs	7	16.4%	15.9%	15.9%
Grilles et remplissage	8	16.6%	14.7%	17.3%
Préfabriqué	10	10.0%	9.0%	9.4%

This analysis was complemented by discussions with architects, which led to the addition of eREN typology No. 4, common in the German-speaking part of Switzerland, but not predominant in the canton of Geneva. The resulting predominant typologies are illustrated in Figure 2. They correspond to the construction period 1950-1990.



eREN 4
1950-1970

eREN 5
“Balcons filants”
1960-1975

eREN 7
“Blocs”
1960-1975

eREN 8
“Grilles et remplissage”
1960-1975

eREN 10
“Préfabriqué”
1975-1990

Figure 2: Selected predominant multifamily building typologies (pictures from eREN project sheets [20] and typology names from Solution Rénovation project [22])

3.2 Envelope retrofitting measures

3.2.1. Method for adapting retrofitting scenarios

The eREN and TypoRENO projects have demonstrated that a global approach to energy renovation, involving a complete renovation of the thermal envelope to comply with the SH demand limit (Qh,li) defined respectively by the SIA 380/1:2009 [29] and SIA 380/1:2016 standards [30], is economically difficult to promote compared to the potential energy savings. The approach for the T-DROP project is to decompose the retrofitting process into several steps (as done in the TypoRENO fact sheets), i.e. to apply each measure one after the other and to assess the influence on SH demand (Qh) and retrofitting investment costs. Using the typologies from the eREN and TypoRENO projects requires reworking the base building thermal model for each building so they are consistent with each other. For the eREN project, the cost data from 2015 is adjusted using a coefficient to update it for the T-DROP study.

In the eREN and TypoRENO projects, the normalized SH demand for each building typology were calculated using LESOSAI software, in accordance with the respective calculation methods of the SIA 380/1:2009 and SIA 380/1:2016 standards. As the building typologies were based on case studies of existing MFBs located in the cantons of Vaud, Fribourg and Geneva, the reference weather stations for each of these cantons were used to calculate the SH requirements according to each building location.

Table 3 gives a comparison between the three projects in terms of building modeling.

Table 3: Comparison of the building modeling between the eREN, TypoRENO, and T-DROP projects

Parameter	eREN project	TypoRENO project	T-DROP project
SIA standard for calculation of SH demand (Qh)	SIA 380/1:2009	SIA 380/1:2016	SIA 380/1:2016
Reference weather station	Depends on the actual building location (VD, GE or FR)		Geneva (GE)
Year of completion	2015-2017	2022-2025	2023-2025
Building reference state	According to the state observed during the visits (including past retrofitting actions)		

The LESOSAI files produced for the eREN and TypoRENO projects were retrieved by the T-DROP project team. These were modified/adapted in order to be able to apply the phased approach to renovation measures. The modifications described below were made to the LESOSAI files:

1) **Adaptation of the calculation method:** Geneva's energy legislation requires the application of the SIA 380/1 standard, 2016 edition. The canton of Vaud is also planning to apply this standard as part of its energy law update. It was decided to apply this calculation method instead of the one used in the eREN project (SIA 380/1:2009 standard). The SIA standard update impacts only slightly the building SH needs.

2) **Modification of the reference weather station:** As the eREN and TypoRENO case studies are divided between the cantons of Vaud, Fribourg and Geneva, the reference weather stations for each of these cantons were used to calculate SH requirements. To be able to compare the typologies with each other, a common weather station must be used for all buildings. Since the predominant typologies were identified from an analysis of Geneva's building stock, the reference station for the canton of Geneva (Geneva-Cointrin) was chosen.

3) **Update of renovation investment costs:** The eREN project was published in 2015. The investment costs have been updated by applying the Swiss construction price index for renovation/conversion in the Lake Geneva region, using October 2015 as the base value and April 2024 as the correction value [31] (the latest index published at the time of this work). The index used is 110.3 (base 100 October 2015). Building renovation costs in the Lake Geneva region therefore increased by an average of 10% between October 2015 and April 2024. For the TypoRENO project, the costs do not need to be updated. As they are more recent, they are representative of current renovation prices.
   A step-by-step approach requires a long-term vision of the work to be carried out and thus a renovation that can be described as comprehensive. In this context, the overhead costs defined in the eREN project have been allocated pro rata to each renovation measure.
   The investment cost per renovation measure is expressed per square meter of ERA.

4) **Assessment of existing condition without taking into account renovations carried out between the year of construction and the present:** Some of the buildings analyzed in the eREN and TypoRENO projects had already undergone renovations (e.g., window replacement, roof renovation, attic insulation) at the time of the assessment. For the T-DROP project, it was decided not to take these renovations into account and to return the existing condition analyzed in eREN and TypoRENO to the initial condition of the building (building envelope). This adaptation of the building thermal balance, in terms of heat loss coefficients, is based on values taken from the literature [32].

Note that the adaptation of the calculation method and the modification of the weather station for the five buildings may lead to different results for the SH demand (Qh) than those obtained in the eREN and TypoRENO projects.

A detailed example of application of this methodology is presented in Appendix 11.1, and updated fact sheets for predominant eREN typologies (from section 3.1.2) are available in Appendix 11.2.

3.2.2. Retrofitting cost analysis

The retrofitting costs and SH demand for each building typology and retrofitting scenario, obtained with the method described in the previous section, are analyzed and compared across the predominant eREN typologies and the relevant TypoRENO typologies. The aim is: i) to refine the selection of typologies for the present project, and ii) to propose a renovation phasing strategy (i.e. a sequence for implementing the retrofitting measures) for the eREN typologies, whose fact sheets provide only full-retrofitting scenarios rather than step-by-step ones.

To this end, the LESOSAI software was used to perform the thermal assessment of each building typology, in accordance with the SIA 380/1:2016 standard. By combining these results with the cost estimates associated with each renovation step, a theoretical planning approach can be derived. These

data, originating from the aforementioned projects, are based on contractor quotes, the experience of architectural offices, as well as catalogues and price lists. The cost assessment of the renovation scenarios was carried out using the Building Construction Cost Code (eCCC-Bât), established by the CRB (Swiss Construction Standards Centre) and compliant with the SN 506 511 standard. It should be noted that the calculations incorporate the service life specific to each measure, according to data from the DUREE project (October 2019) [33]. The median service lives of renovation measures in Switzerland are shown in Table 4.

Table 4: Median service life of renovation measures in Switzerland [33].

Renovation measure	Service life [years]
Floor insulation	26
Window replacement	29
Façade insulation	30
Attic insulation	40
Roof insulation and renovation	30

Figure 3 shows the renovation costs associated with saving one kilowatt-hour over the entire service life of each measure. It allows comparison between different renovation options and establishes a prioritization order for the implementation of the works. These costs are defined as follows:

$$Space\ heating\ saving\ cost = \frac{Renovation\ measure\ cost}{Space\ heating\ savings\ \times\ Service\ Life} \quad (1)$$

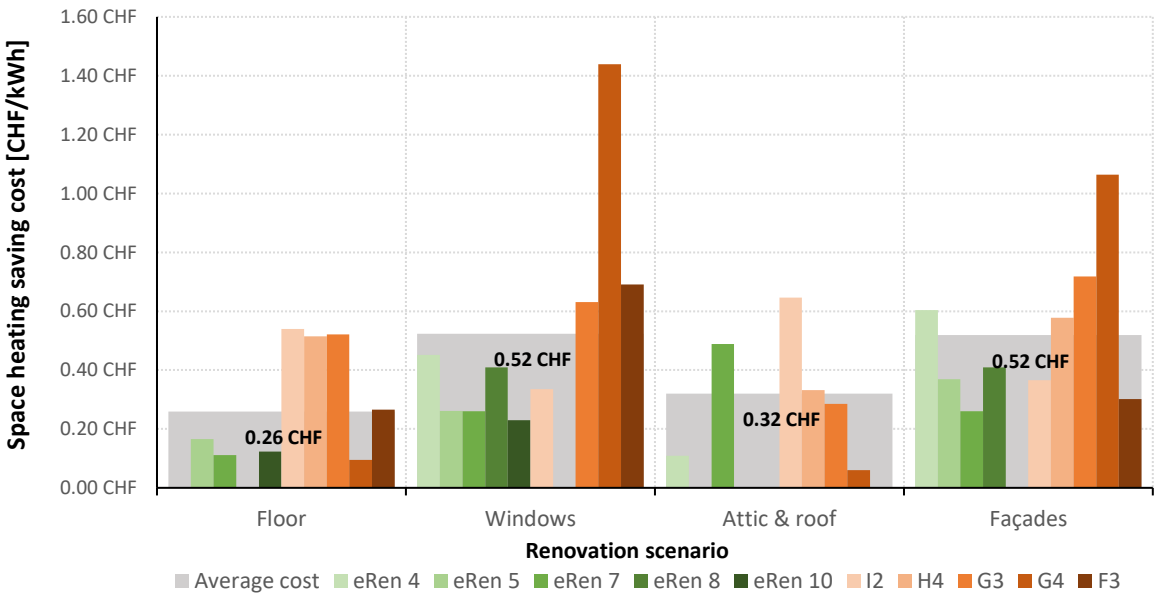


Figure 3: Cost of the measure for saving 1 kWh over the service life

Nevertheless, it is important to discuss each proposed scenario. Indeed, the case studies are very different and each project has its own specificities, which may temper a direct comparison. Some variants could not be studied because, in some cases, the renovation works were not feasible. This is particularly the case for eREN 5 and eREN 8, where the roof had been recently renovated and therefore does not require further work. The same applies to the original roof of eREN 10, which, thanks to its good

condition and still-satisfactory performance (notably due to its relatively recent construction), does not require renovation.

Floor insulation

Floor insulation appears to be the most cost-effective solution for improving the building's energy performance at a low cost. The cost of this measure is competitive because its implementation is straightforward. In most cases, the works are carried out from an unheated ground floor or basement. No direct access to the apartments is required, and preparatory work remains limited. This is the case for eREN 5, eREN 7, eREN 10 and for all TypoRENO projects.

However, this solution cannot be considered in all configurations, particularly when the floor is in direct contact with the ground or rests on a crawl space. Furthermore, if hydraulic and electrical networks are located in the upper part of the basement or within suspended ceilings, installing insulation would require relocating these installations, resulting in additional costs.

It is also important to note that the thermal assessments are obtained according to the SIA 380/1 calculation standard. This standard uses a reduction factor b to correct thermal losses through walls adjacent to unheated spaces. This factor tends to be conservative, as it underestimates the actual temperatures of these spaces. As a result, the thermal gains from floor insulation are often overestimated in the LEOSAI calculations. In reality, the effective gain from the measure would therefore be lower.

Attic or roof insulation

First, it is important to differentiate between insulation works carried out in unheated or unfinished attics with pitched roofs, and those carried out on flat roofs requiring waterproofing renewal.

To assess the relevance of these works, we can consider the following situations:

- **First case:** If access to unheated, unfinished attics allows for the installation of mineral wool insulation, the competitiveness of this scenario is remarkable. This applies in particular to eREN 4 and TypoRENO G4. Installation costs are low and the impact on occupants is minimal.
- **Second case:** For flat roofs, installing insulation often implies renewing the waterproofing layer, which leads to additional costs, as observed in eREN 8, TypoRENO I2 and TypoRENO H4.

Windows replacement

Window replacement emerges as a versatile solution. All case studies are already equipped with double glazing; therefore, the measure consists of replacing them either with triple glazing or selective double glazing, and replacing the frames.

The significantly higher costs for TypoRENO G4 are due to the integration of an insulation return along the entire interior wall to reduce thermal bridges.

It is important to examine the investment costs to ensure the viability of the works. This is particularly relevant for TypoRENO G4. While the median cost per m² of ERA is 220 CHF/m² for the other projects, TypoRENO G4 exceeds 720 CHF/m² ERA due to the treatment of thermal bridges at shutter boxes and insulated window reveals. This may discourage renovation works.

The actual gains obtained from window replacement may be more modest. In buildings without controlled ventilation systems, replacing windows may lead to more frequent window opening, reducing the expected energy savings.

Façade insulation

Finally, when the objective is to improve the thermal envelope to reduce heating demand, façade and balcony insulation are the least advantageous measures in relation to their cost. They require extensive preparatory work, long execution times, and significant material quantities.

Furthermore, there is substantial variability in how façade insulation can be conceived. Depending on building architectural characteristics, such as the concrete façade of eREN 8, the presence or absence of balconies, or the strategy adopted to avoid creating thermal bridges, façade renovation works must be adapted to each building.

For eREN 7, eREN 8, TypoRENO H4, and TypoRENO G3, implementing internal insulation raises feasibility issues. Indeed, occupants would need to be temporarily relocated. In cities like Geneva or Lausanne, this would be extremely challenging and generate major additional costs.

Comparative analysis

To consider potential renovation works, it is useful to look at the investment cost required from owners and indirectly from tenants. Since these results are expressed per m² of ERA, floor, attic, or roof insulation is generally more feasible and easier to promote.

The wide range of cost values (see Figure 4), particularly for windows and façades, reflects the significant variability in renovation approaches, architectural constraints, existing building characteristics, initial condition, renovation materials used, and, ultimately, the variability in contractor quotes and cost estimates.

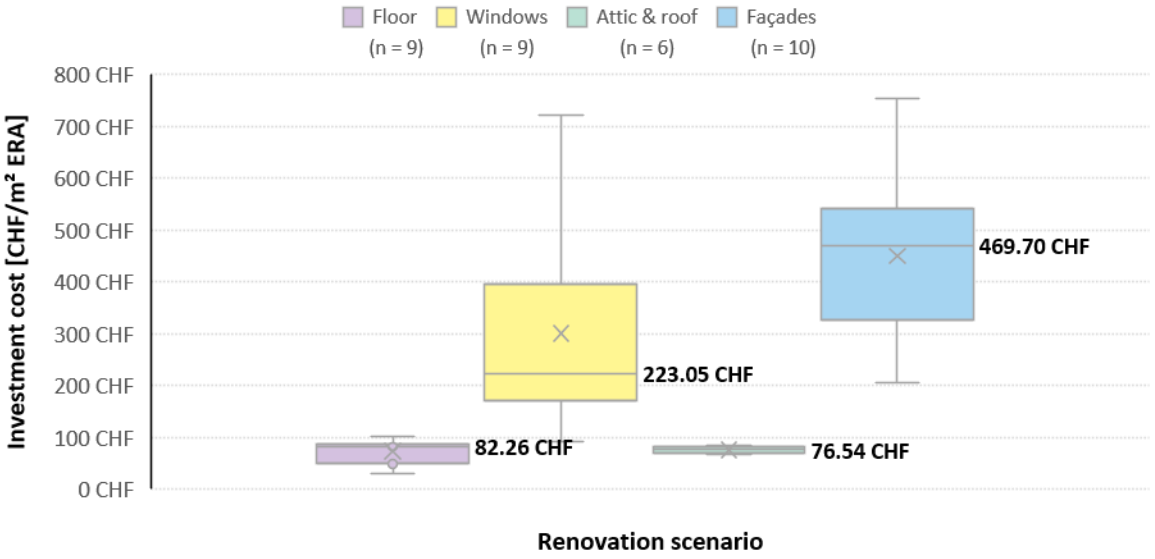


Figure 4: Specific costs in CHF per m² of ERA

In this context, cost analysis can be challenging. The subject may be sensitive given the financial burden for owners and tenants. Nevertheless, we were able to obtain and compare our data with those from the Effiwag project, carried out by the engineering and consulting firm Lemon Consult [34]. The latter reports the costs of thermal insulation measures from subsidy applications submitted to the cantons of Basel-Stadt (BS), Schaffhausen (SH), and Thurgau (TG), within the “Gebäudeprogramm”. The comparison is shown in Figure 5.

Overall, the specific costs associated with the T-DROP project are higher. While consistency is observed for windows, attics, and roofs, a threefold difference appears for façade and floor-related data. This can be explained by the small number of data points available from T-DROP (fewer than 10), as well as the different nature of the projects: multi-family residential buildings for T-DROP versus both apartment buildings and single-family houses for Effiwag. Without a more detailed cost breakdown in the Effiwag report, it is not possible to analyze these discrepancies in depth or undertake a comprehensive critical assessment.

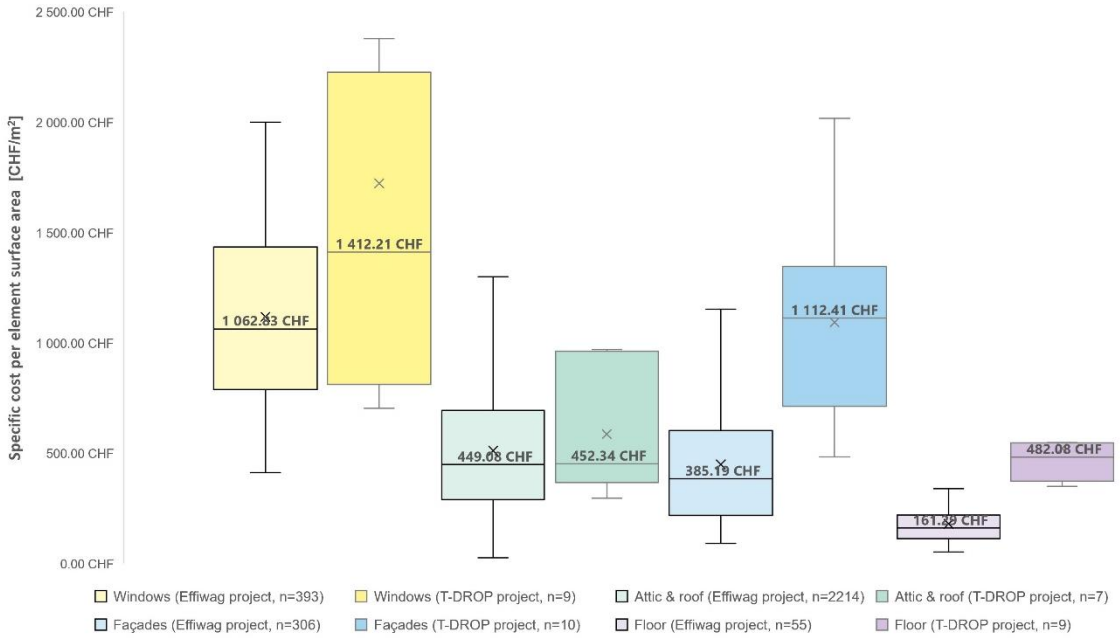


Figure 5: Comparison of specific costs (CHF/m² of building element) in the T-DROP and Effiwag projects [34]

3.3 Selected building typologies and retrofitting measures

Given the results presented in the previous sections, three building typologies are selected for the sensitivity analysis (Table 5). They are chosen to represent buildings of different sizes, while still offering a large number of retrofitting measures to implement. As explained earlier, some of the case studies from the eREN and TypoRENO fact sheets have already been partially retrofitted, so that only a few measures remain to be applied in these cases, which make them less relevant for the current project.

The selected typologies are as follows:

- **eREN 4:** small-scale building (ERA of approximately 1'500 m²), representative of multifamily buildings in German-speaking Switzerland
- **eREN 7:** large-scale building (ERA of approximately 5'000 m²), among the predominant building typologies in the Canton of Geneva
- **TypoRENO I2:** very large-scale building (ERA of approximately 8'000 m²), relatively cost-effective compared to other TypoRENO typologies (which focus on buildings with patrimonial values and retrofitting using sustainable materials, leading to higher retrofitting costs than for eREN)

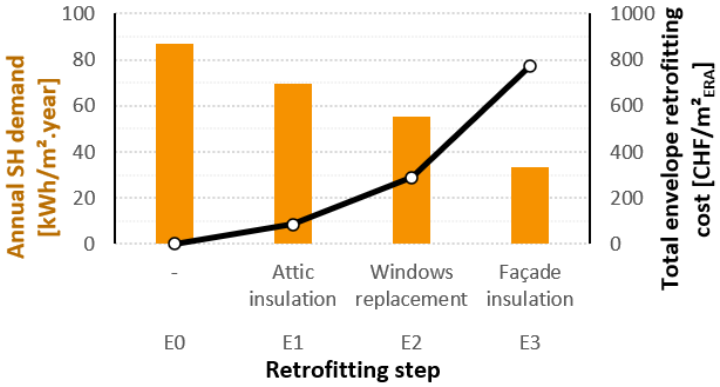
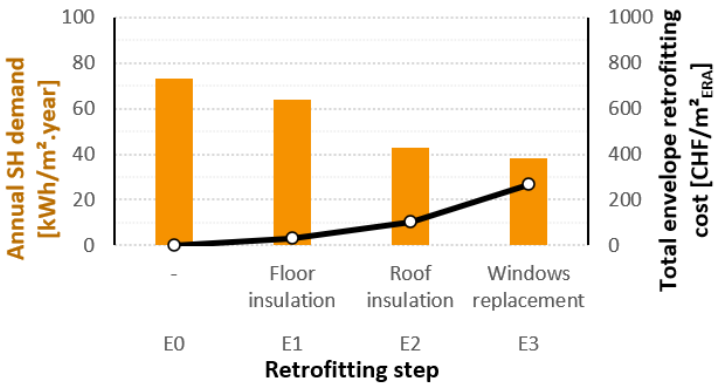
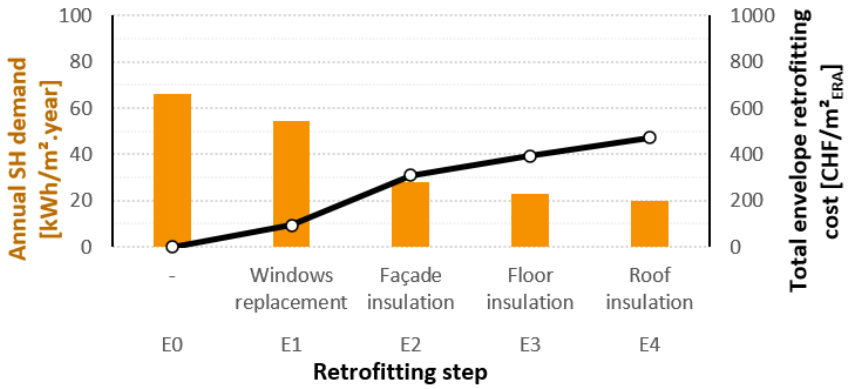
For the two selected eREN typologies, the order in which retrofit measures are applied is based on the average cost analysis presented in Figure 3. Measures are implemented in the following order, from the most cost-effective to the least cost-effective according to their average annualized cost per unit of energy saved (CHF/kWh):

1) Floor insulation
2) Attic or roof insulation
3) Windows replacement
4) Façade insulation

For the selected TypoRENO typology (I2), the retrofit sequence defined in the fact sheet, established based on the condition of the building elements and the feasibility of implementation, is retained.

SH demand and total envelope retrofitting costs for each of these typologies and renovation step are presented in Table 5.

Table 5: SH demand under SIA standard operating conditions and total envelope retrofitting costs for each envelope retrofitting step (Ei) for the selected building typologies (pictures from eREN [20] and TypoRENO [21] project sheets and typology names from Solution Rénovation project [22])

eREN 4		
eREN 7 “ Blocs”		
TypoRENO I2 “ Tour locative 2ème moitié XXe”		

3.4 Building modeling

To be able to account for the interactions between the building and the SH/DHW system, the LESOSAI building models are transposed into simplified TRNSYS building models. The latter are done with Type 5897, a resistance-capacitance (RC) model developed for TRNSYS [25], based on the ISO13790:2008 standard (hourly method) [26]. This model offers several advantages, including a relatively small number of parameters and inputs, as well as a very short computation time. In contrast to

detailed multizone models such as EnergyPlus, IDA-ICE, TRNSYS Type 56 and Pléiade-Comfie, Type 5897 is easy to parametrize, enabling efficient analysis of a large number of scenarios at an hourly time step. It also allows the building model to be coupled with the SH/DHW system model in TRNSYS, thereby accounting at each time step for the interactions between the building's indoor temperature and the SH/DHW system (an integration that would not be possible with LESOSAI building models).

This section first describes the RC building model, then explains how its parameters are obtained from the LESOSAI models described in the previous sections, for each selected building typology and retrofitting scenario. Finaly, it presents a validation of the TRNSYS building model against a case study, comparing the simulated results with both measurements and LESOSAI modeling results.

3.4.1. Description of Type 5897 from ISO13790:2008

The ISO13790:2008 standard uses the electrical-thermal analogy to model heat flows in a building. Thermal resistances and capacities, as well as heat loads, are modelled using an analogous electrical circuit consisting of 5 resistors, 1 capacitor and 4 generators (see Figure 6). These models are commonly referred to as the 'RC model' (R: resistance, C: capacitance) and are more precisely identified by the number of each element, in this case 'R5C1'. The resolution at hourly (and sub-hourly) time steps is performed with the TRNSYS software in Type 5987 using the method described in Annex C of the ISO13790 standard.

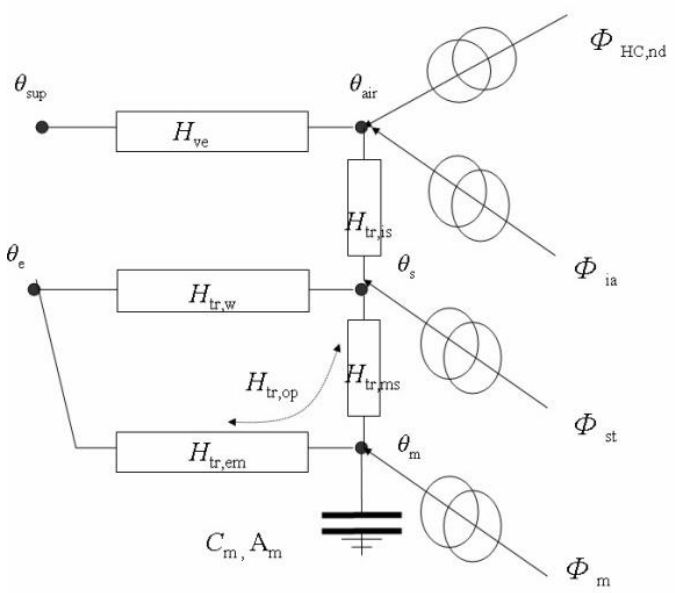


Figure 6: R5C1 thermal model diagram [26]

The R5C1 model takes into account heat loss due to ventilation (H_{ve}) and transmission through opaque ($H_{tr,op}$) and glazed ($H_{tr,w}$) walls. The ventilation heat transfer coefficient H_{ve} is directly related to the temperature of the indoor air θ_{air} and the temperature of the air supplied by the ventilation θ_{sup} ($\theta_{sup} = \theta_e$ is used for the calculations). The heat transfer coefficients through the glazed walls $H_{tr,w}$ and through the opaque walls $H_{tr,op}$ are defined between the external temperature θ_e and that of the central node (on the inside of the wall) θ_s, which represents the temperature of the internal surfaces of the building. This node is then coupled to the air node of the building by the coupling heat transfer coefficient $H_{tr,is}$, which characterises the convective heat transfers between the walls and the air. In this model, the opaque walls have an effective thermal mass that allows them to store part of the heat. This phenomenon is modelled as an electrical capacitor and is characterised by C_m (thermal capacity of the building), A_m (surface area of the effective thermal mass) and θ_m (internal temperature of the walls). In the case of glazed windows, their thermal capacity is neglected, i.e. they do not store heat and the heat transfer coefficient is not coupled to the thermal mass of the building.

The model considers four energy inputs, represented by generators:

- $\Phi_{HC,nd}$: heat flow produced by the space heating or air conditioning system,
- Φ_{ia}, Φ_{st} and Φ_m are calculated to correctly distribute the internal Φ_{int} and solar gains Φ_{sol} to the different nodes according to the ISO13790 standard.

The full list of parameters and inputs of TRNSYS Type 5897 is presented in Appendix 11.3.

3.4.2. Procedure for model parametrization and inputs definition in T-DROP

As described in the previous sections, buildings studied in the T-DROP project are based on building typologies and renovation scenarios defined and analyzed in related projects (eREN, TypoRENO-VD) using the LESOSAI software. In the T-DROP project, several procedures for the parameterization of Type 5897 have been developed to allow a more or less automated transfer of data from LESOSAI building model to the TRNSYS model presented above (Type 5897).

Figure 7 illustrates the methodology for parameterizing the TRNSYS model and the results it generates. First, the characteristics and properties of the building envelope are automatically extracted from the LESOSAI building model. Next, the parameters and inputs required for the TRNSYS model are calculated. Using these inputs, the TRNSYS model simulates the building's thermal losses and gains.

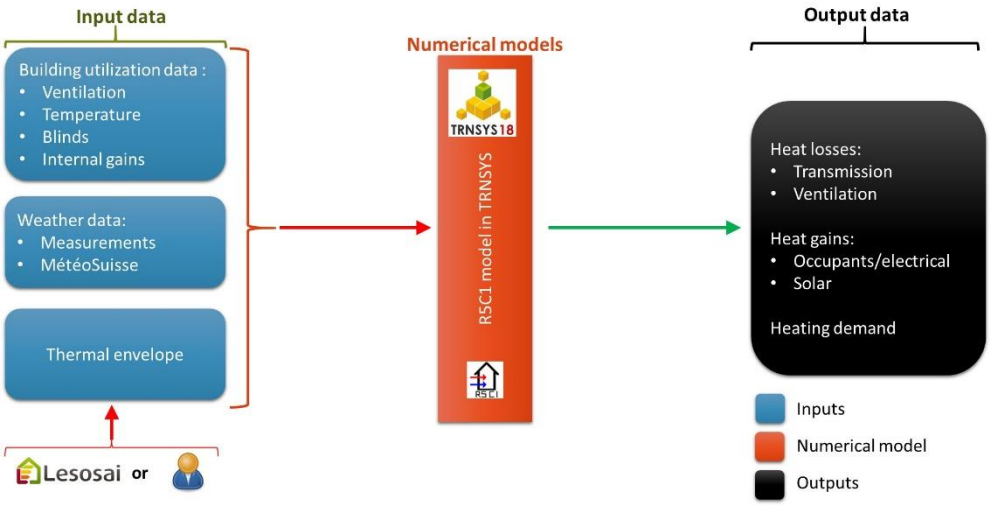


Figure 7: Procedure to define TRNSYS Type 5897 model inputs and parameters and to compute the building space heating needs

For each selected building typology and envelope retrofitting scenario, the building envelope parameters are taken from the LESOSAI model and implemented into Type 5897 (RC building model) in TRNSYS. Each case is then simulated with an ideal SH system to produce the daily SH demand and generate the building energy signature. This is done not only for various building typologies and envelope retrofitting measures, but also different indoor temperature setpoints or ventilation fresh air flow rates, parameters that are analyzed as optimization measures in the sensitivity analysis (section 5.4). The resulting building energy signature is then used for each scenario for two purposes: i) sizing the system components (heat pump, circulation pumps, etc.), based on the SH load at the design outdoor air temperature, and ii) calculating the optimized heating curves using one of the methods described in section 4.4.

3.4.3. Building model validation

In order to validate the TRNSYS building model presented above based on Type 5897, measured SH needs collected from an existing non-renovated multifamily building have been used. This building is located in the heart of the Cité Nouvelle d'Onex, overlooking the Avenue du Gros-Chêne (see Figure 8). It is part of an apartment block, built in the early 1960s (1963). This rental complex consists of two blocks of semi-detached buildings, 36-38 and 40-42, facing south-west and north-east. This building has 8

stories and an energy reference area of 5'357 m² for each block. The building typology corresponds to eREN No5 typology ("Balcons filants") (see section 3.1). In 2008, the 40-42 block has been retrofitted to the Minergie standard. The other block (36-38) has not been retrofitted. In order to quantify the real SH needs reduction following the retrofitting, the thermal energy needs of both blocks have been monitored in 2008-2010. A complete description of the building, the retrofitting project and an analysis of the thermal energy needs is available in a scientific report published by the University of Geneva [35]. The model validation is based on the SH needs of the non-retrofitted block.

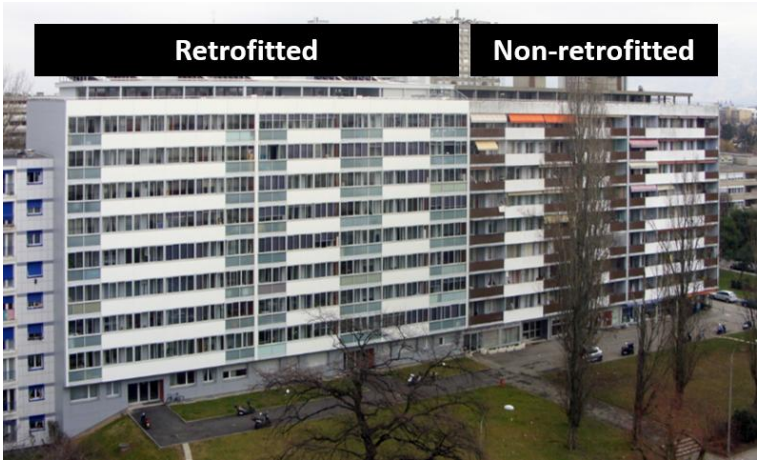


Figure 8: Picture of the "Gros-Chêne" building with the retrofitted block (left) and non-retrofitted block (right) [35]

The TRNSYS outputs of the Gros-Chêne building model were validated using two approaches:

1) A comparison with the daily and monthly monitored space heating demands
2) A comparison with the monthly outputs from the LESOSAI model

The results of these comparisons are detailed below.

Comparison with the daily and monthly monitored SH demands

The monitoring data are first compared to the results of the TRNSYS building model on a monthly and daily basis. To compare the TRNSYS model with the monitoring data, the following assumptions are made:

- Indoor temperature setpoint = 22.5°C (as per monitored indoor air temperature)
- Average internal heat gains = 16.58 kW (or 59'685 kJ/h and annual heat gain = 27.1 kWh/m²), calculated based on standard SIA values
- Weather: on-site measurements (outdoor temperature, horizontal solar radiation)
- Constant shading of glazed surfaces (taken from the LESOSAI model of the building)

Figure 9 shows the monthly SH consumption (in MJ/m²) for two sets of data: data from consumption measurements (monitoring) and a simulation carried out with TRNSYS18. The hatched bars represent the monitoring data, while the dotted bars represent the simulation results. The differences between the measurements and the simulation are quite small (< 5%) in winter, when SH consumption is highest, and increase in the low season (spring and autumn) as SH demand decreases. The errors cancel each other out on an annual basis, resulting in a relative deviation of only 0.2% for the annual SH needs. Table 6 shows the relative monthly and annual differences.

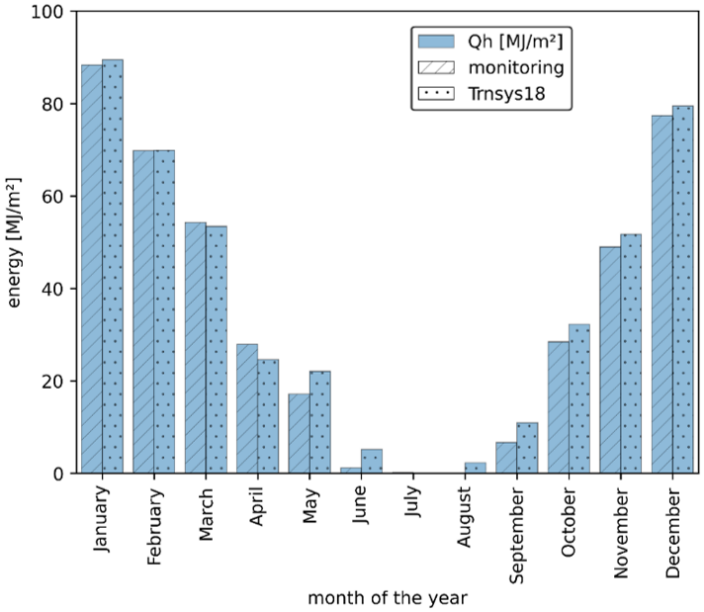


Figure 9: Monthly comparison of SH needs (Qh) in MJ/m² between monitored data for the Gros-Chêne building and TRNSYS18 simulation results for a whole year. The hatched bars represent measured values, while the dotted bars represent simulated values.

Table 6: Relative differences between SH needs monitored and simulated in TRNSYS. Relative differences are not taken into account for the summer months (June, July, August), but are included in the annual total SH needs.

Month	δQh [%]
Jan	-1.2
Feb	-2.8
Mar	-5.7
Apr	-18.4
May	17.4
Jun	-
Jul	-
Aug	-
Sep	37.2
Oct	5.9
Nov	1.3
Dec	-0.2
Year	**0.2**

At the daily level, Figure 10 compares the daily SH demand from the monitoring data and the TRNSYS simulation, shown both as a time profile over the year (left) and as a scatter plot (right).

The temperature setpoint of 22.5°C results in high SH consumption in summer. Defining a heating period would eliminate this phenomenon. The cvRMSE is acceptable (12.6%) for this granularity and the level of detail of the input data (in particular given the constant internal gain and constant shading).

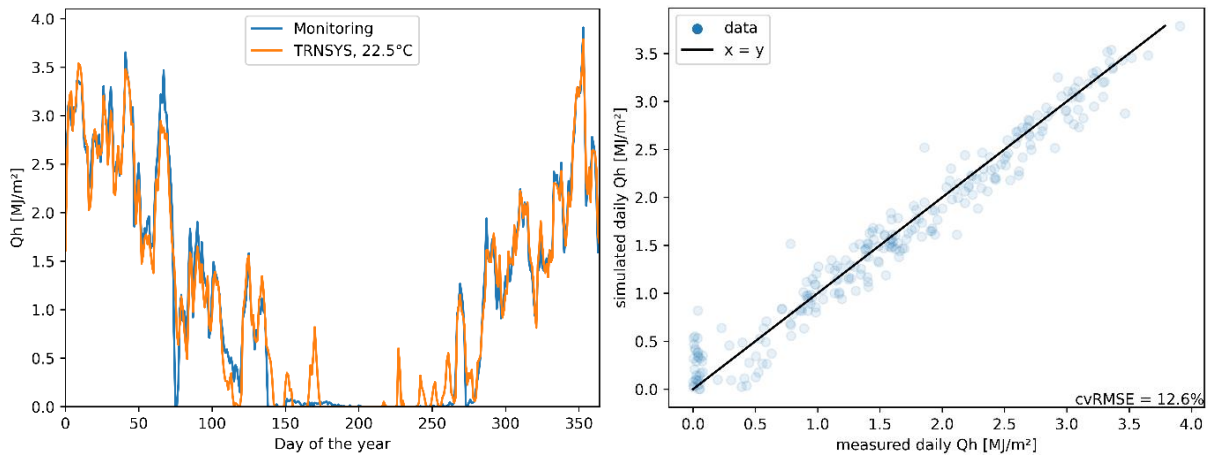


Figure 10: Comparison of the daily SH consumption (Qh) in MJ/m² from the monitoring data and the TRNSYS simulation with an indoor temperature setpoint of 22.5°C. Left: time profile over a whole year; right: scatter plot around the bisector.

Note that various studies (e.g. [36,37]) point to substantial and systematic differences between theoretical and actual SH consumption, particularly in the case of energy-efficiency retrofits of large residential

buildings. In a previous study on these buildings [35], the modeled SH consumption of the retrofitted building turned out to be 12% lower than the monitored SH demand on an annual basis. It would therefore also have been interesting to compare the monitored and simulated SH consumption of the retrofitted building obtained with the RC building model.

Comparison with the monthly outputs from the LESOSAI model

In order to complete the validation of the TRNSYS model, and in particular to ensure that the various heat losses and gains are correctly accounted for and distributed, a comparison was made between the TRNSYS model and the SIA 380/1 thermal balance produced by the LESOSAI software. The following assumptions were made for this study:

- Temperature setpoint = 20°C
- Average internal heat gain = 16.58 kW (59'685 kJ/h and annual heat gain = 27.1 kWh/m²)
- Weather: on-site measurements (outdoor temperature, horizontal solar radiation)

Note that the weather used in the LESOSAI model was adapted to the monitored weather. The irradiation on the south, east, north and west orientations used in LESOSAI were calculated from the monitored global horizontal irradiation using the TRNSYS Type 16 model.

Figure 11 shows the monthly transmission losses (QT) and infiltration losses (QV) as well as the solar (Qs), internal (Qi) and space heating (Qh) gains for the LESOSAI simulation (hatched bar) and TRNSYS 18 (dotted bar). The relative differences between these models are shown in Table 7. Since the input data were identical in both cases, there were no significant errors in the internal contributions (only rounding errors). On the other hand, there are more or less significant differences for the other components of the heat balance. The largest relative difference is for air exchange losses (QV) with -12% per year. On the other hand, losses and gains during the main winter months are sufficiently well modelled. The errors for SH consumption are less than 10% from October to March and -1.5% annually.

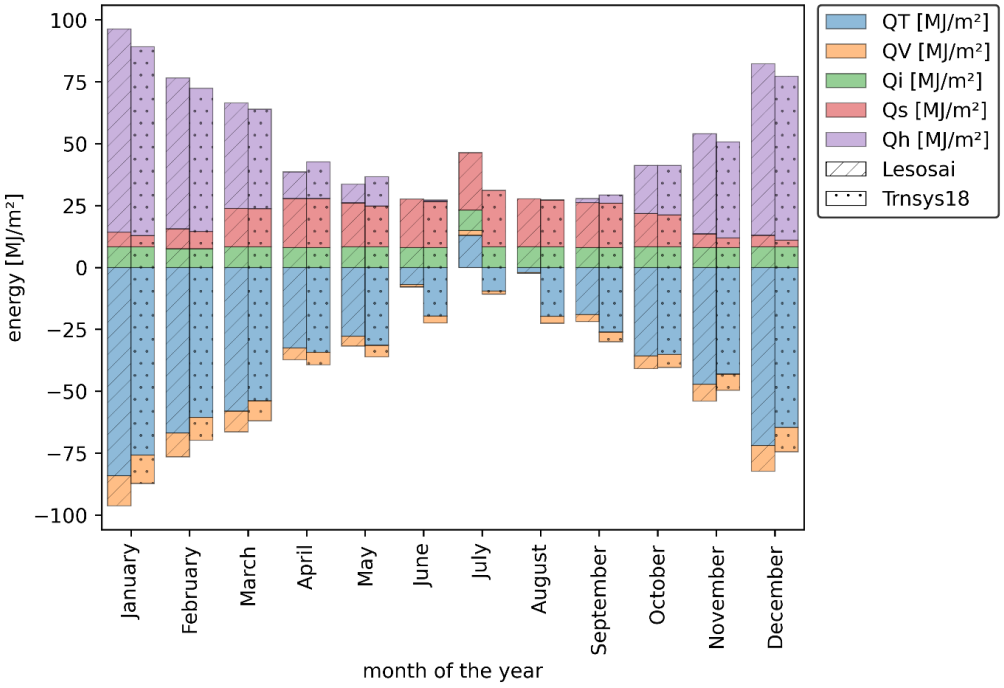


Figure 11: Monthly comparison of heat losses (QT, QV) and gains (Qi, Qs, Qh) in MJ/m² for the 'Gros-Chêne' building between the LESOSAI monthly balance and the TRNSYS18 simulation results over a whole year. Hatched bars represent the TRNSYS18 results, while dotted bars represent the LESOSAI results.

Table 7: Monthly and annual relative differences in heat losses (QT, QV) and gains (Qi, Qs, Qh) for the 'Gros-Chêne' building between the LESOSAI monthly balance and the TRNSYS18 simulation results.

Period	Transmission losses δQ_T	Ventilation δQ_V	Internal gains δQ_i	Solar gains δQ_s	Space heating δQ_h
January	10.0%	5.2%	-0.1%	-22.6%	-7.1%
February	9.4%	4.6%	-0.2%	-12.6%	-5.1%
March	7.2%	2.6%	-0.1%	-0.5%	-5.9%
April	-5.2%	-8.4%	0.3%	-0.1%	37.7%
May	-13.1%	-16.4%	-0.1%	-7.3%	57.6%
June	-	-	-	-	-
July	-	-	-	-	-
August	-	-	-	-	-
September	-36.9%	-37.1%	0.3%	-1.4%	105.6%
October	1.9%	-2.8%	-0.1%	-4.0%	3.0%
November	8.6%	4.3%	0.3%	-30.4%	-3.9%
December	10.2%	4.9%	-0.1%	-41.2%	-4.6%
Year	**-7.8%**	**-12.3%**	**-0.0%**	**-5.9%**	**-1.5%**

4 SH/DHW systems and optimization and replacement measures

This chapter focuses on SH/DHW systems and optimization and replacement measures, with three main objectives: i) to identify representative SH/DHW system typologies and their characteristics, ii) to review and select targeted replacement and optimization measures for SH/DHW distribution and production, and iii) to develop the corresponding numerical models.

The chapter first presents the selected SH/DHW system typologies, then reviews the optimization and replacement measures identified from the literature and discussions with professionals, leading to the selection of the measures investigated in this study. It then focuses on heat emitters and heating curves, assessing heat emitter oversizing in existing Swiss multifamily buildings from case studies and defining the methodology used to determine the corresponding SH supply and return temperatures for each building typology and retrofitting scenario. Finally, it describes the SH/DHW system modeling approach.

4.1 SH/DHW systems typologies

Figure 12 shows two categories of SH/DHW systems: systems for buildings connected to a DHN, i.e. DHN substations (SST), and systems for buildings equipped with their own heat generator. Since the main renewable energy source in dense urban areas is the air, we only illustrate air-source heat pump systems (ASHP), but other type of systems could be implemented in some cases, depending on the resource availability and local restrictions (e.g. ground-source HP system, PV/T collectors,…). These systems correspond to the most common configurations found in existing systems, and the most promising architectures regarding temperature levels.

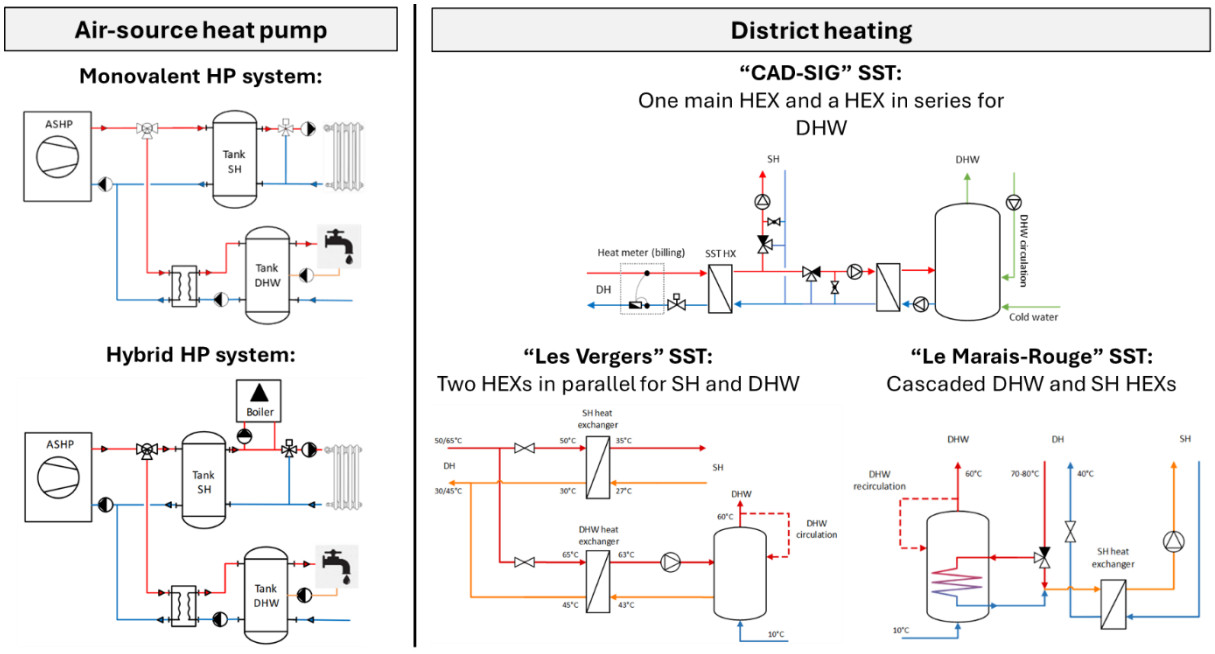


Figure 12: Most common or most promising SH/DHW systems in terms of temperature levels

Air-source heat pump systems

Common SH/DHW systems installed in existing MFBs in dense urban areas as replacement for fossil-fuel boilers are ASHP systems, with or without backup heater. Indeed, hybrid HP systems with gas boilers can significantly reduce CO_2 emissions of the heat production compared to existing systems [8], which for the most part rely entirely on fossil-fuel boilers. Therefore, hybrid HP systems constitute an

interesting option as a temporary solution before building envelope retrofitting or when it is not possible to implement a monovalent system (noise emissions, structural constraints of the roof, insufficient capacity of the electrical grid,…). It can also limit peak power usage in winter.

Case studies on several ASHP systems installed in large existing buildings have been analyzed [8] and are available as comparison for system sizing, control strategies, as well as energy model inputs and validation.

District heating substations

Several SST architectures (Figure 12) are identified based on existing district heating networks located in Switzerland. Some of these networks are old DHN in need of lowering their temperature levels in the upcoming years/decades, and others are new low temperature DHN, namely:

- **"CAD-SIG" SST** [38]**:** It consists in one main heat exchanger, followed by another heat exchanger in series for DHW preparation and direct SH. Due to the two heat exchangers in series for DHW, this architecture tends to result in high return temperatures from the DHW system to the DHN. Moreover, it requires higher supply temperatures from the DHN than architectures with one heat exchanger between the DHN and the DHW storage tank. It is commonly found in existing old DHN in Switzerland, such as Geneva's main DHN "CAD-SIG" and Lausanne's main DHN. Operators of both DHN are planning to reduce the supply and return temperatures of the network in the upcoming years/decades.
- **"Les Vergers" SST** [39]**:** It consists in two heat exchangers in parallel, one for SH and one for DHW preparation. In principle, it is easier to control and optimize than the "CAD-SIG" SST architecture, in particular because both heat exchangers can be sized separately based on their respective constraints.
- **"Le Marais-Rouge" SST** [38]**:** It consists in cascaded DHW and SH heat exchangers. It is an innovative substation architecture, designed to minimize the impact of the DHW preparation on the SST return temperatures.

It should be noted that such SST architectures can also represent different system layouts in case of decentralized heat production with a HP (without DH), in particular for DHW preparation.

Case studies on each one of these SST architectures installed in large existing buildings have been analyzed [38,39] and are available as comparison for system sizing, control strategies, as well as energy model inputs and validation.

Focus and other considerations for this study

This study focuses on decentralized heat pumps, but it is expected that impact of optimization and retrofitting measures would be different for DH substations as the temperature levels are different. For example, ASHP usually operate with a supply/return temperature difference (ΔT) of 5 K on the condenser side, while DH systems operate with large ΔT between supply and return (e.g. 15 K for Les Vergers [39], 20-45 K for CADSIG [38], 15-40 K for Marais-Rouge [38]).

The systems considered represent properly functioning installations and therefore exclude faulty components, malfunctions, and hydraulic configurations inherited from fossil-fuel boilers that must be modified prior to implementing renewable heat production. In addition, in terms of SH distribution, we assume that all heat emitters are equipped with thermostatic radiator valves, as it is the case for most buildings. Single-pipe distribution systems are excluded from the scope of this project since they are relatively rare and complex to optimize.

4.2 Optimization and replacement measures

4.2.1. Literature review

The following literature review relates to lowering temperature production levels for SH and DHW, as well as more general considerations.

Space heating

1) **Thermostatic radiator valves:** Optimizing the control system (heating curve, emitter regulation) is the least capital-intensive lever. Cholewa et al. [40] evaluated, over the long term and under real conditions, the energy savings actually achieved by installing thermostatic radiator valves (TRVs), highlighting a marked gap between theoretical potential and observed gains. Benakopoulos et al. [41] proposed an improved control strategy for TRVs without a pre-setting function, explicitly targeting the reduction of return temperatures. At the building scale, Fine and Touchie [42] developed a grouped control strategy for retrofitting the hydronic SH systems of post-war MFBs, illustrating the benefit of coordinated rather than purely local regulation, a finding consistent with field feedback favoring centralized intelligence.

2) **Hydraulic balancing:** Hydraulic balancing is regularly presented as a prerequisite for lowering temperatures, as it removes excess flows and allows both the supply temperature and the pumping electricity consumption to be reduced. The literature nonetheless underlines its variable nature: the gain depends strongly on the initial state of the installation and on the order in which measures are carried out. This echoes the practitioner debate between an “engineering” approach (systematic prior balancing) and an “investor” approach (monitoring first, targeted balancing afterwards). Some publications report potential energy savings from hydraulic balancing ranging from 4% to 24% [79,80], depending on the measures implemented and the initial conditions of the system and building.

3) **Resizing and replacement of heat emitters:** Where control alone is insufficient, action turns to the emitters themselves. Østergaard and Svendsen [43] showed, on four Danish houses from the 1930s, that the targeted replacement of the critical (undersized) radiators alone is enough to make an installation compatible with a low-temperature network, at a cost far lower than wholesale replacement. Tunzi et al. [44] proposed a systematic method to investigate and plan the application of low temperature to existing radiator systems, identifying the limiting emitters room by room. These approaches are more cost-efficient than the wholesale implementation of low-temperature radiators, whose cost and scope of work remain prohibitive in the existing stock. In Switzerland, the EFFIWAG project [34] specifically investigated the efficiency potential of replacing the heat emission system of buildings, and identified key obstacles to the widespread use of low-temperature heat emission systems in existing buildings.

4) **Integrating HPs into existing radiator systems:** Several studies directly address the performance of HPs connected to unmodified radiator systems. Lämmle et al. [15] analyzed the performance of air-source and ground-source HPs retrofitted to radiator heating systems and reviewed the measures available to reduce SH temperatures in existing buildings, explicitly linking temperature reduction and HP performance. Primas et al. [14] proposed a system-level evaluation of HP use in the context of building refurbishment, providing a methodological framework for the Swiss context. It includes essential modifications to the existing system to meet temperature level requirements of HP systems.

5) **Less-documented measures (ventilation, indoor temperature sensors):** Some measures, such as replacement of the distribution pumps, ventilation optimization (e.g. humidity-controlled ventilation), deployment of indoor temperature sensors, and distribution optimization systems of the “E-Gain”/”E-NNO”/”EVO SPE” type, remain sparsely covered by the recent peer-reviewed academic literature, although they reflect well-established operational know-how in Switzerland. They fall within the broader rationale of monitoring as a precondition for targeting interventions.

Domestic hot water

1) **The temperature / legionella dilemma:** DHW constitutes the most binding constraint, as controlling the risk of legionella proliferation traditionally requires high temperatures. The bacterium grows preferentially between 25 and 45°C, and most countries impose a DHW operating temperature above 55°C to prevent its proliferation. In Switzerland, the SIA 385/1:2020 standard [45] requires that, in most system configurations, DHW be maintained above 55°C at all points of the distribution network.

2) **Instantaneous and decentralized production:** Reducing the volume of circulating hot water is the most frequently cited design strategy. Kropp et al. [46] analyzed instantaneous water heater concepts to optimize DHW production with heat pumps, with centralized and decentralized configurations. Brand et al. [47] modelled and measured a low-temperature district heating substation providing instantaneous DHW preparation, demonstrating the feasibility of storage-free production at reduced network temperatures. At the dwelling scale, the decentralized substation, equipped with an instantaneous heat exchanger sized to cover both SH and DHW, produces hot water locally and thereby minimizes the total DHW volume while reducing losses [48,49]. This principle is compliant with standards that prohibit storage, but its actual deployment remains limited by the cost of contracted capacity on district heating networks. In addition, the feasibility of implementation of such systems in existing MFBs in Switzerland is yet to be evaluated, in particular regarding the configuration of the existing DHW distribution network.

3) **Storage optimization and stratification:** Where storage is retained, its control becomes decisive. Tahiri et al. [50] and Huang et al. [51] proposed staged control methods of DHW storage tanks to reduce return temperatures without compromising comfort and hygiene requirements. The quality of tank stratification is a key factor: the Swiss DHWStrat project [52] analyzes the stratification efficiency of various types of DHW tank, assessing the effect of baffles and connection-point positions. The study however focuses on small buildings as it uses a heat generator with a capacity of approximately 10 kW, therefore results might not be applicable to larger buildings such as MFBs.

4) **Non-thermal disinfection:** To free the system from the temperature constraint, several studies review alternative disinfection solutions to thermal treatments, such as chemical treatments or filtration [53,54]. Benakopoulos et al. [53] demonstrated, on a case study, the achievement of low return temperatures from a DHW system based on an instantaneous heat exchanger coupled with a chemical-based disinfection solution.

5) **Heat recovery from greywater:** Heat recovery from domestic wastewater directly implemented in each shower/bath (“Joulia”-type systems) is another possible measure to optimize DHW production. However, it relates more to reducing DHW demand than to directly lowering temperatures.

6) **Other measures:** More broadly, the international literature catalogues the range of alternative approaches intended to reconcile low temperatures with sanitary control, such as micro HPs for temperature boosting, electric heating elements, electric trace heating, pipes insulation, optimized circulation pump [48].

System-level approach and case studies

Beyond individual measures, several studies address system-wide optimization to reduce temperature levels through secondary-side (building-side) measures, mainly for buildings connected to DHN. The Austrian T2LowEx project [55] investigates the transformation of conventional DHN into low-temperature networks by means of secondary-side measures, drawing on several case studies where such measures were applied in practice. At the international level, the low-temperature implementation guidebook produced under IEA DHC Annex TS2 [48] consolidates the state of the art and the lessons learned from practice.

4.2.2. Workshop

In complement to this literature review, a workshop with professionals was organized to discuss the feasibility and temperature-reduction potential of the identified measures, drawing on practical experience and implementation feedback. Participants represented a broad range of expertise, including DH operators, contracting providers, engineers, researchers and public authorities (UNIGE, HEIG-VD, SIG, MBG, SFOE, Müller Energie).

Cross-cutting observations

Beyond the technical aspects, the discussion highlighted that the main obstacles to implementing optimization measures are often organizational rather than technical. For instance, in case of multiple ownership, it is difficult to convince every owner to act, which postpones or even prevents the implementation of optimization measures. Measures requiring extensive administrative steps or significant time on-site in occupied apartments are more costly and complex to implement. As a result, they are less likely to be pursued, unless they were already identified as key measures for the building in question. The phasing between building retrofitting and system optimization also raises the question of how to avoid duplicating work, as some optimization measures (e.g. hydraulic balancing) have to be implemented after envelope retrofitting, even if already carried out before.

A recurring difficulty is that the party implementing a measure is not always the one who benefits from it, which strongly shapes which measures actually get implemented. For instance, an optimization that lowers operating costs benefits the tenants rather than the owner who pays for it. Similarly, in buildings supplied by DH, it is primarily the network operator who benefits from a lower return temperature (through lower operating costs, easier integration of renewables,…), while the building owner bears the cost of the optimization. Under most current DH supply contracts, the building owner sees no corresponding benefit (no discount or bonus for the temperature reduction), yet legal constraints make it difficult for the DH operator to invest in secondary-side optimization himself. In addition, on the owner's side, connecting to the DHN is sometimes seen as marking the end of further investment.

For HP systems, energy contracting offers an easier lever, as contract terms can be used to incentivize the owner to implement optimizations. It was also noted that energy optimization contracts (COE, “Contrat d’Optimisation Energétique”) and HP system management under contracting pursue different objectives: the former target energy savings, while the latter increasingly aim at lowering temperatures to improve HP performance.

In Geneva, the heat demand index (IDC, “Indice de dépense de chaleur”) is a useful incentive for owners to optimize their SH/DHW installations, but it lacks clear incentive for buildings whose IDC is already below the 450 MJ/m² threshold, below which there is no legal obligation for energy retrofitting or optimization.

More broadly, the implications of high production/distribution temperatures remain poorly understood or taken into account, particularly regarding return temperatures, and many stakeholders are not fully aware of them. Further outreach and awareness-raising within the sector is still needed.

Space heating

Space heating optimization measures are generally well known and commonly implemented by heating engineers, though they typically target a reduction in space heating demand rather than a reduction in distribution temperatures as such. The so-called "basic" measures were broadly agreed upon as a starting point: optimizing the heating curve, checking the correct operation of three-way valves, and removing inappropriate bypasses. A recurring issue is the presence of injection circuits rather than mixing circuits (not necessarily inherited from fossil fuel boilers) which should be converted to mixing circuits.

Several points generated debate. Regarding hydraulic balancing, two approaches emerged: some stakeholders carry it out first, considering that it establishes a sound basis for subsequent optimizations and reduces pumping electricity consumption. One documented case reported a reduction of the space heating supply temperature of around 6 to 7 K. Others favor prior monitoring and only undertake

balancing if it proves to be a bottleneck, as the operation is administratively demanding and its benefit often limited on an already well-tuned installation. Installing indoor temperature sensors in a few apartments helps identify imbalances and understand the system's actual behavior. Hydraulic balancing is nonetheless recognized as necessary to minimize pump electricity consumption. Motorized, dynamically controlled valves were also mentioned as a practical way of maintaining network balance over time.

Targeted replacement of critical radiators often proves simpler and less costly than overheating the rest of the building and oversupplying the entire system (though this trade-off may apply mainly in the context of HP contracting). The critical radiators are relatively easy to identify through discussions with tenants and the use of indoor temperature sensors.

Optimization algorithm systems such as "E-Gain"/"E-NNO"/"Système GE" were also mentioned as tools to optimize system control based on measurements taken in the boiler room and/or in individual apartments. Finally, optimizing the building's ventilation was raised as an effective way to reduce the space heating demand by about 8-10%.

Domestic hot water

DHW production and distribution optimization is less familiar to professionals in the field, partly because its importance has only recently increased with the reduction in space heating demand and the integration of renewables. It is therefore more challenging to address, especially as lowering DHW production and distribution temperatures also raises concerns about compliance with sanitary standards (SIA and SVGW [45,56,57]) and the risk of legionellosis. These standards require high-temperature operation, which limits the effective integration of renewables. In particular, keeping the DHW circulation loop above 55°C pushes DHW return temperatures upward. It is important to note, however, that in some cases, raising the DHW temperature is not always sufficient to prevent legionella proliferation, owing to dead legs in the distribution network.

The main issues identified were: i) undersized heat exchangers, including internal coil heat exchangers (found in about 80% of cases for existing MFBs), typically showing a pinch of 7-8 K where 1-2 K would be necessary; ii) oversized charging pumps, or pumps operated at excessive flow rates; iii) undersized DHW storage tanks, with up to around thirty charging cycles per day observed in some buildings; iv) poorly positioned circulation loop returns (to the bottom of the tank or to the cold water inlet); and v) a need for hydraulic balancing of the DHW network. On DHW circulation specifically, it was noted that optimizing the circulation pump alone is not enough, the DHW distribution/circulation network itself also needs to be balanced.

Several optimization measures were discussed. DHW tank charging optimization involves adjusting the hysteresis (widening it to avoid re-heating a tank that is not yet discharged) and correcting the charging pump flow rate, which is often set too high. Heat exchanger replacement, tank replacement and modifying the connection points are often addressed together, though it is sometimes possible to modify only the connection points if the existing tank allows it (an option that is generally easier to justify to owners, especially since some older tanks are very robust and still in good condition). Distribution pipe insulation is easier to implement in some buildings than others, depending on pipe accessibility, and can sometimes be carried out during other planned renovation work. Instantaneous DHW production (i.e. without drinkable water storage) is an attractive solution in theory for reducing DHW production temperatures, but still lacks real-world feedback. In particular, it raises questions about compliance with the sanitary standards and the capacity required for DHW charging. In addition, for buildings supplied by DH, the cost of the contracted capacity can be a barrier to implementing such storage-free systems.

Survey results

As a complement to the above discussions, two surveys gathered participants' priorities regarding the first measures to implement to lower the temperature levels in existing MFBs. The survey results are presented in Table 8 for SH and Table 9 for DHW.

Table 8: Results of the survey on measures to reduce SH temperature levels (9 respondents)

Measure	Votes
Heating curve optimization	9
Hydraulic balancing	5
"Système GE" / E-Gain type system	4
Ventilation optimization	4
Circulator replacement	4
Critical radiator replacement	4
Indoor temperature sensors in apartments	2
Low-temperature radiators	0

Table 9: Results of the survey on measures to reduce DHW temperature levels (8 respondents)

Measure	Votes
Charging optimization (sensors, variable-speed circulator, etc.)	6
Hydraulic modification (tank connections, etc.)	6
Heat-exchanger replacement	5
Tank replacement (larger volume, baffles, etc.)	4
Pipe insulation	4
Recirculation optimization (flow rate/schedule)	3
Direct DHW production	2
Non-thermal anti-legionella treatment	1
Heat recovery ("Joulia" type)	0

On the SH side, the consensus is very clear on heating curve optimization (unanimous), reflecting its simple and inexpensive nature, whereas low-temperature radiators attract no priority as a first step. On the DHW side, votes are more dispersed, with priority shared between charging optimization and hydraulic modifications to the tank.

Summary

Lowering production and distribution temperatures is generally treated as a co-benefit of demand-reduction measures rather than a goal in itself, since current DHN heat supply contracts create little pressure to do so. The issue is nonetheless sometimes addressed for HP systems, particularly under energy contracting. Financial considerations and the workload required are the primary drivers in selecting which measures to implement, and no general rule applies: each building differs both technically (e.g. the current condition of the installation) and organizationally (e.g. ownership structure, other planned renovation work that could create synergies), which requires a case-by-case approach. Monitoring is therefore key to understanding the dynamics of each system and better targeting the measures needed to reduce heat demand and lower production and distribution temperatures.

DHW remains a particularly delicate topic, gaining importance as heating demand decreases and renewables are integrated, all the more so as the SIA and SVGW standards' requirements diverge considerably from the reality of the existing building stock and are difficult to meet in practice. Finally, dedicated incentives are needed to encourage the wider adoption of optimization measures, even though some are already supported by existing subsidy programs.

4.3 Selected optimization measures

Based on the above literature review and discussions with professionals, the following optimization measures are selected for this study. The selection is guided by their expected impact on temperature levels and their modeling feasibility.

Space heating

- **Heating curve optimization:** Optimization of the heating curve to lower the supply/return temperature levels while keeping the same indoor temperature setpoint (same service). It implicitly includes the replacement of the SH distribution pump, as the existing distribution pumps might not match the new operating conditions (especially after a retrofit). As a co-benefit, it also reduces the electricity consumption as new pumps are more efficient than old ones and allow a better modulation of the flow rate (so it prevents operation at high speed when low speed only is necessary).

  More information on the heating curve optimization in section 4.4.2.

- **Heat emitters sizing/critical radiator replacement:** This optimization measure reflects both the possible heterogeneity in heat emitter oversizing from one building to another (sensitivity analysis), and the replacement of critical radiators which increases the overall emitter oversizing of the building and therefore allows to lower the distribution temperatures.

  More information on heat emitter oversizing factor in section 4.4.1.

- **Indoor air temperature reduction:** Reducing the indoor temperature of the building is a measure relatively cost-effective to implement. It can be done by solely adjusting the heating curve progressively to reduce the amount of heat supplied, or it can be associated with the implementation of temperature sensors in a few representative apartments to control that the indoor temperature is close to the targeted value.

- **Ventilation optimization:** MFBs are often ventilated in excess, with a ventilation flow rate higher than the normative fresh air flow rate of 0.7 $m^3/h.m^2$ (SIA 380/1 standard value [30]). Khoury et al. [58] highlighted that operating conditions frequently observed in existing non-renovated MFB in Switzerland have a ventilation flow rate of about 1.0 to 1.5 $m^3/h.m^2$ (with and without air change due to window opening). They point out that reducing the flow rate can significantly reduce the SH demand of the building (reduction of 17.5 MJ/m^2 for a reduction of 0.2 $m^3/h.m^2$). Among other methods, reducing the excessive air change can be done by controlling the ventilation flow rate based on the humidity of the exhaust air [59].

Domestic hot water

- **Increased DHW heat exchanger transfer area:** DHW heat exchangers are often sized for high return temperatures from the tank on the secondary side (e.g. 52/60°C inlet/outlet heat exchanger temperatures). There are therefore not designed to meet large temperature differences on the DHW tank side and cannot reach low outlet temperatures on the primary side. To improve the efficiency of the heat transfer and increase DHW tank stratification, an optimization measure consists in choosing heat exchangers with larger heat transfer area. The improved heat transfer efficiency allows for lower inlet temperatures and a higher outlet temperature on the secondary side (e.g. 15-45°C/63-64°C inlet/outlet temperatures).

- **DHW heat recovery system implementation:** A “Joulia” DHW heat recovery system can reach heat recovery efficiencies of up to 60% (depending on the model implemented and flow rate, see Figure 44), and therefore reduce by 60% the DHW tapping volume from the central system. This measure is selected despite receiving no votes in the workshop survey because it is very easy to incorporate in the system model and include in a sensitivity analysis on the DHW demand.

Heat pump type

- **High-efficiency HP:** Use of high-efficiency R290 HP with inverter instead of regular R410A HP without inverter to reach higher COP and reduce the CO_2 emissions associated with the heat production.

Several other optimization measures were identified as promising through the literature and discussions with professionals. However, they were not retained as they are difficult or highly time-consuming to implement in TRNSYS, or require detailed Computational Fluid Dynamics (CFD) to be accurate in terms of temperature levels (for example improving DHW tank connections and hydraulic layout, as done in [60]). This is particularly true for DHW optimization measures.

Furthermore, other promising measures are considered indirectly in the analysis through the implementation of other measures. For example, hydraulic balancing is indirectly included in the heating curve optimization since it is not possible to fully optimize the heating curve down the considered temperature levels if the SH distribution system is not balanced (more info on hydraulic balancing in Appendix 11.6). Depending on the degree of imbalance of the current SH distribution system or the constraints imposed by critical thermal zones (e.g. with undersized heat emitter), the heating curve optimization would be less efficient than described in this study.

4.4 Focus on heat emitters and heating curves

The heat emitters and their associated heating curve play a central role in the transition from high- to low-temperature heat distribution. Low-temperature operation is only possible if the heat emitters are capable of delivering the required heat at lower temperatures. This capability is determined by the effective heat emitter oversizing, defined as the ratio between the installed emitter capacity and the actual SH load. Since envelope retrofitting reduces the SH demand without changing the installed emitters, it increases the effective oversizing and thereby enables lower supply temperatures.

Heating systems installed during the last century and supplied by fossil-fuel boilers were generally designed for supply temperatures between 70 and 90°C, depending on the geographic area and the design practices of the time. Combined with potentially conservative design assumptions and the subsequent improvement of building envelopes over time, this can result in heat emitters being oversized with respect to the current SH demand.

Several studies conducted in Denmark, the United Kingdom and Germany [15,61–63] have shown that heat emitters in existing buildings are often oversized relative to the current SH demand. This suggests that supply temperatures could be reduced compared to the heating curves typically observed in practice. However, no similar assessment has been carried out for existing MFBs in Switzerland. Because historical sizing practices are unknown, the present study analyses several Swiss case studies to estimate the current level of heat emitter oversizing and how it evolves after envelope retrofitting.

This section first presents the analysis of heat emitter oversizing based on several Swiss case studies, considering both the current state of the buildings and different envelope retrofitting scenarios. It then describes the simplified heat emitter model adopted in TRNSYS and the assumptions used to determine the installed emitter capacity for the simulations. Finally, it presents the heating curves commonly observed in existing buildings (used as baseline in this study), as well as different heating curve optimization methods, together with an illustrative example showing the influence of heat emitter oversizing on the achievable temperature reduction.

4.4.1. Heat emitters

Analysis of existing heat emitter oversizing on case studies

This analysis aims to determine whether heat emitters in Switzerland also show signs of oversizing. Because historical sizing methods are unknown, it is necessary to analyze real case studies in order to identify potential trends.

We analyzed the sizing of heat emitters, room by room, in four apartments located in French-speaking Switzerland (Lausanne): two on intermediate floors, one on the ground floor, and one under the roof. The case studies examined presented in Figure 13.



Building A
1950

Building B
1963

Building C
1964

Figure 13: Case studies used for the heat emitter sizing analysis

The objective was to determine the oversizing factor based on the current characteristics of the thermal envelope (surface heat-loss coefficients measured during site visits in 2023, see TypoRENO-VD fact sheets [21]), and then to evaluate how this factor evolves if renovation measures are implemented, such as window replacement, façade insulation, roof insulation, or floor insulation.

To do this, a room-by-room heat-loss calculation was carried out following the SIA 384/2 standard. A minimum outdoor temperature, corrected for altitude, is taken into account. This temperature is determined based on the reference weather station, in accordance with SIA2028. Total heat losses correspond to the sum of transmission losses and ventilation losses.

It is important to note that the assumptions in SIA 384/2 are conservative. In addition to imposing a minimum reference temperature (conditions typically encountered only a few hours per year and therefore not representative of the actual climate to which the building is exposed), the standard does not account for solar gains or internal gains from occupants. As a result, transmission heat losses are overestimated, which leads to an underestimation of the oversizing factor.

The heating power of the emitters is determined in accordance with the EN 442 standard, as follows:

$$P_{\Delta T} = P_{\Delta T_{Norm}} \times \left(\frac{\Delta T}{\Delta T_{Norm}}\right)^{n} \quad (2)$$

where

- $P_{\Delta T}$ and $P_{\Delta T_{Norm}}$ are the thermal power of the heat emitters under real conditions and standard conditions respectively
- ΔT and ΔT_{Norm} is the effective and standard temperature difference between the heat emitter and the room.
- n is the radiator exponent which depends on the type of radiator used

To best reflect the operating regimes commonly observed [64], a 60/50 °C supply/return regime was selected, with an indoor temperature of 20°C. This corresponds to the most frequently observed regime in a city such as Geneva, and more generally in French-speaking Switzerland. Radiator characteristics are defined by the number of elements, the number of columns, and their length. The oversizing factor is defined as follows:

$$Oversizing\ factor = \frac{Heat\ emitter\ power}{Heat\ losses} \quad (3)$$

Note that this oversizing factor refers to the effective heat emitter oversizing, which is defined with respect to the actual SH load. It differs from the initial oversizing factor, which is defined with respect to

the SH load of the building in its current state (before any additional envelope retrofitting). Consequently, in the current state of the building, the effective and initial oversizing factors are identical.

It is relevant to analyze the oversizing not only at the apartment level but also room by room, in order to identify potential disparities in sizing practices from the design stage. The renovation scenarios studied follow the same logic as in Section 3.3: first the current state of the building, followed by various renovation variants—façade insulation, window replacement, roof works, or basement insulation, depending on the apartment.

All results are presented in Table 10.

Table 10: Results of the sizing analysis of heat emitters

Case study	Building envelop variant	Effective oversizing factor (at 60/50/20°C)	Installed power per ERA [W/m²]
Building A	Existing state	1.12	47.35
	Windows	1.52	
	Façade	1.59	
	Façade + Windows	2.60	
Building C 6th floor	Existing state	0.83	33.81
	Windows	1.02	
	Façade	1.26	
	Façade + Windows	1.75	
Building C 13th floor (under roof)	Existing state	0.96	61.06
	Windows	1.09	
	Façade	1.22	
	Roof	1.36	
	Façade + Windows	1.44	
	Façade + Windows + Roof	2.50	
Building B	Existing state	0.99	51.17
	Windows	1.23	
	Floor	1.63	
	Windows + Roof	2.34	

Despite the conservative assumptions used, the four case studies appear to be generally well-sized in their current state. However, the room-by-room analysis reveals some heterogeneity within the apartments. In particular, living rooms tend to be better sized than bedrooms, reflecting a prioritization of thermal comfort at the time.

Retrofitting measures contribute to increasing the oversizing factor of heat emitters. This confirms the benefit of improving the thermal envelope to enable lower distribution temperatures. However, the presence of critical radiators (particularly in bedrooms) may require their replacement to ensure optimal low-temperature operation. This also raises the issue of hydraulic balancing, for which more details are available in Appendix 11.6.

Simulated heat emitters

The heat emitters are represented in TRNSYS by a single equivalent heat emitter (representing the total installed emitter capacity of the building) using Type 362 [65], a dynamic radiator model that accounts for the thermal capacitance of the emitter. Based on the installed emitter capacity, the inlet fluid temperature and flow rate, as well as the building indoor temperature at each simulation time step, the model calculates the resulting outlet fluid temperature. This emitter model allows to couple the SH system with the single-zone RC building model described in section 3.4, and therefore capture the interactions between them.

This modeling approach is a compromise between a simplified building model based on an energy signature, which does not take into account interactions between the building and the distribution system in terms of temperature levels, and a detailed multizone building model (e.g. EnergyPlus, TRNSYS Type56, etc.), which explicitly simulates one heat emitter per zone but is more time-consuming to configure and simulate.

For each building typology, the installed heat emitters capacity is assumed to remain unchanged after envelope retrofitting, corresponding to the capacity installed when the building was initially built (non-retrofitted building, i.e. step E0 in Table 5). Heat emitters are sized based on the design SH load (Q_{SH}, see Appendix 11.3) of the non-retrofitted building under the operating conditions 62/52/22°C (supply/return/indoor), representative of the baseline heating curves considered in this study (Figure 14). The design SH load is calculated for an outdoor air temperature of -10°C, corresponding to the design outdoor air temperature commonly used for the Swiss Plateau at the time the studied buildings were built, and assuming the baseline ventilation fresh air flow rate of 1.0 m³/h.m².

In scenarios where an initial emitter oversizing is considered (i.e. effective oversizing for the non-retrofitted state), the installed emitter capacity is multiplied by the selected oversizing factor. Consequently, for a given building typology and initial oversizing factor, the installed emitter capacity remains identical across all envelope retrofitting and system optimization scenarios.

The detailed methodology for calculating the installed heat emitters capacity is detailed in Appendix 11.3.

4.4.2. Heating curves

Several supply/return temperature scenarios are considered for this project: i) a baseline scenario, representing the most common conditions observed in existing buildings, referred to as the “non-optimized heating curve” throughout the next sections of this report, and ii) optimized heating curves, used to evaluate the potential for lowering the SH distribution temperatures after implementation of retrofitting and/or optimization measures.

Baseline heating curves (“non-optimized heating curves”)

The baseline heating curves (Figure 14) are derived from a study of SH distribution temperatures in 68 buildings in Geneva [64], encompassing various typologies, construction periods and SH demands. The study showed that the measured supply/return temperatures for buildings equipped with radiators are remarkably consistent from one building to another, with minimal dependence to the building’s SH load or construction period. The median values obtained from this benchmark are therefore adopted as the baseline scenario for the present study.

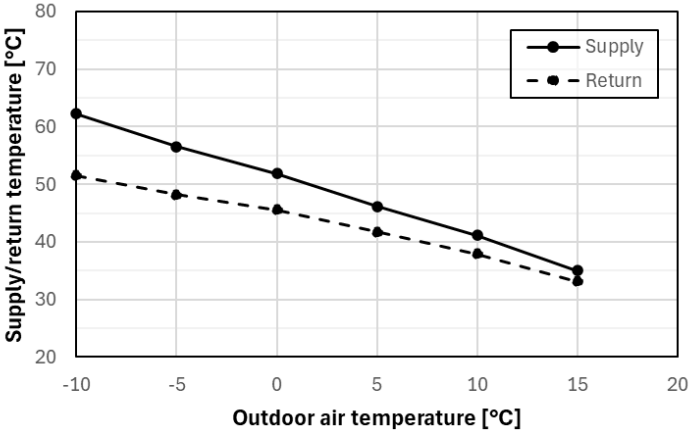


Figure 14: Heating curves for the baseline scenario (“non-optimized heating curves”), derived from median values measured in radiators systems in [64]

Optimized heating curves

Heating curve optimization aims to reduce the temperature levels of the SH distribution system while maintaining the required heat supply. Two main optimization approaches can be distinguished depending on the heat production system.

The most common heating curve optimization approach consists in minimizing the supply temperature, thereby improving HP efficiency for buildings supplied by HPs. Since the same SH output must still be delivered, the distribution flow rate is increased. This reduces the temperature drop across the heat emitters, allowing the same average emitter temperature (and therefore the same heat output) to be maintained with a lower supply temperature and a correspondingly higher return temperature.

However, studies [66–68] suggest that for buildings supplied by DHNs, it is more beneficial to minimize the SH return temperature rather than the supply temperature. This approach, known as the "low-flow" method, reduces the SH distribution flow rate while increasing the supply temperature to meet the SH demand. Consequently, it lowers the SH return temperature, which in turn reduces the DHN substation return temperature. This method is particularly interesting when the DHN supply temperature is relatively high and cannot be further reduced, such as Geneva's main DHN (CADSIG-CADIOM) which supply temperature will be reduced to 90°C by 2035. By lowering the return temperature of the DHN, renewable energy integration in the DHN mix is maximized, and the DHN distribution capacity is increased. Conversely, this approach is not suitable for HP systems, as the higher supply temperatures reduce HP efficiency.

The applicability and effectiveness of each method in terms of achievable temperature reduction depend on the characteristics of the existing distribution system. For the “high-flow” method, the required increase in distribution flow rate is limited by the existing pipe size and the maximum flow rate that can be reached while complying with standards regarding flow noise. For the “low-flow” method, the achievable reduction in return temperature depends on the maximum allowable supply temperature. In this study, the supply temperature is limited to 70°C to reduce the risk of burns to occupants, particularly children.

The two heating curve optimization approaches can therefore be summarized as follows:

1) **The "low-flow" method**, which minimizes the return temperature at the expense of higher supply temperatures. This approach is better suited to buildings connected to DHNs.
2) **The "high-flow" method**, which minimizes the supply temperature but requires a higher flow rate in the distribution system. This approach is preferable for buildings supplied by HPs.

Since this project focuses on decentralized HP systems, all optimized heating curves are calculated using the “high-flow” method.

For the chosen baseline conditions (non-retrofitted building, indoor temperature setpoint of 22°C and ventilation fresh air flow rate of 1.0 m³/h·m²; see section 5.3), it is assumed that the "non-optimized" heating curves already correspond to the optimized heating curve obtained with the high-flow method. We therefore consider that the heating curves observed in existing buildings are optimum for the current state of the building. The high-flow method is therefore calibrated to match the heating curves in Figure 18, by sizing the heat emitters for design operating conditions of 62/52/22°C (supply/return/indoor).

Figure 15 summarizes the procedure used to determine of the optimized heating curves for each building typology, retrofitting/optimization scenario and initial heat emitter oversizing factor. The optimized heating curves are calculated from the installed heat emitter capacity and the building SH load resulting from the selected retrofitting and/or optimization measures. The detailed methodology is presented in Appendix 11.3.

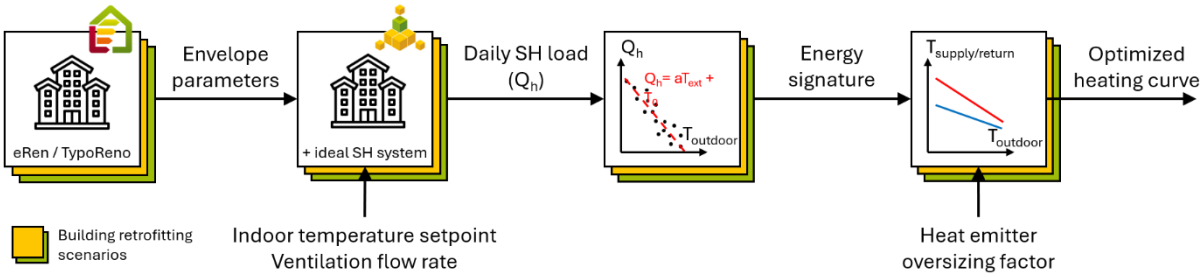


Figure 15: Procedure to determine the optimized heating curve for each building typology, envelope retrofitting/SH optimization scenario and initial heat emitter oversizing factor.

The following figures illustrate the optimized heating curves, and corresponding distribution flow rates, for the eREN 4 building typology at retrofitting step 2, without initial heat emitter oversizing (Figure 16) and with +40% initial heat emitter oversizing (Figure 17). Without initial oversizing, the reduction in SH demand achieved through envelope retrofitting allows the supply temperature to be reduced by approximately 8 K at -10°C outdoor air temperature compared to the non-optimized heating curve (from 62°C to 54°C), and by about 6 K at 10°C outdoor temperature (from 41°C to 35°C). This reduction is achieved by increasing the flow rate from approximately 5.0 m³/h to 6.5 m³/h. With an initial oversizing of +40%, the achievable reduction is substantially greater, reaching approximately 16 K at -10°C (to 46°C) and 9 K at 10°C (to 32°C), with a design flow rate of 9 m³/h. The higher flow rate reflects the larger installed emitter capacity: oversized emitters are designed to meet a greater SH load with a same supply temperature, and therefore require a higher design flow rate.

It should be noted that the achievable temperature reduction strongly depends on the pre-existing characteristics and condition of the heat distribution system. The simulations assume a properly balanced hydraulic network, free of faulty components, radiators all equipped with thermostatic valves, etc. A poorly balanced system cannot reach the performance reported here, as the hydraulically disadvantaged zones limit the temperature reduction. Likewise, undersized emitters in specific zones will limit the extent to which supply temperatures can be reduced, even in a well-balanced system. This can be addressed by selectively replacing certain radiators with larger or more efficient units, as proposed in [15,34].

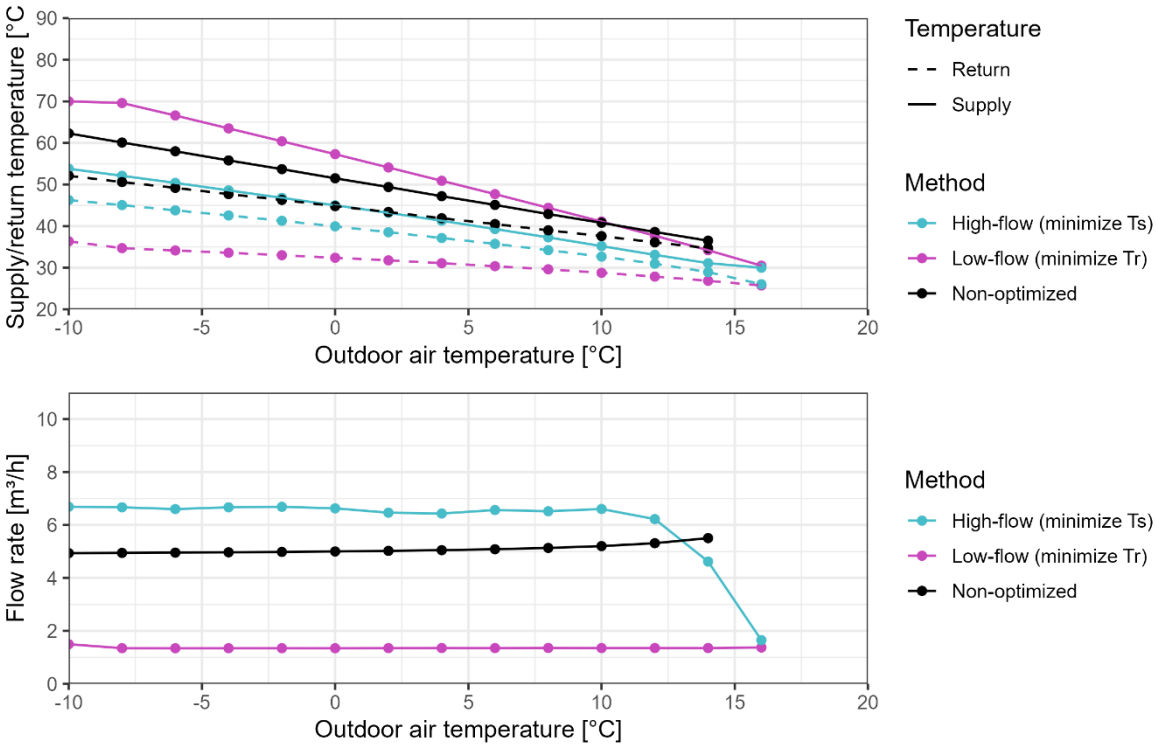


Figure 16: Non-optimized heating curve (baseline) and optimized heating curves using the "low-flow" and "high-flow" methods for building typology eREN 4 [20] partially retrofitted (step 2) for an indoor temperature setpoint of 22°C and a ventilation flow rate of 1.0 m³/h.m², without initial oversizing of the heat emitters

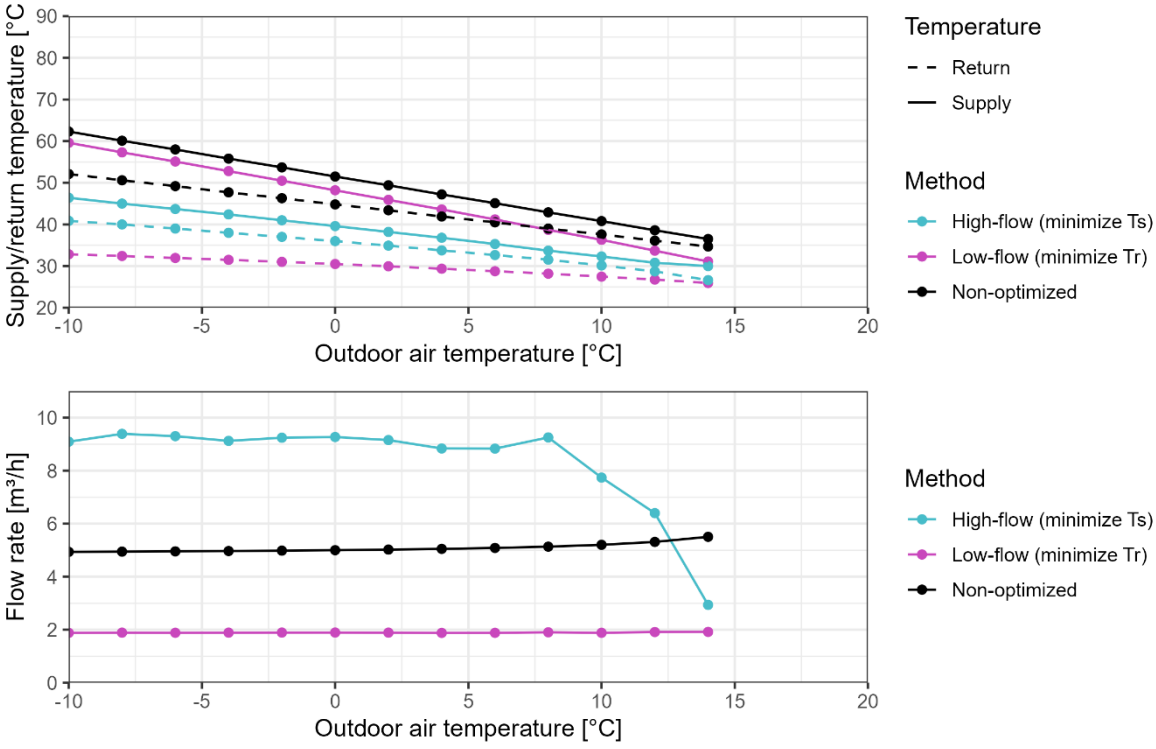


Figure 17: Non-optimized heating curve (baseline) and optimized heating curves using the "low-flow" and "high-flow" methods for building typology eREN 4 [20] partially retrofitted (step 2) for an indoor temperature setpoint of 22°C and a ventilation flow rate of 1.0 m³/h.m², with an initial oversizing of the heat emitters of +40%

4.5 System modeling

The modeled air-source HP system with/without backup heater (Figure 18) is partially based on the TRNSYS model developed in the AirBiVal project [69], which was validated on a monitored SH/DHW system. It is simulated with a timestep of 1 minute. Key information on the system components, sizing and control strategy are described below.

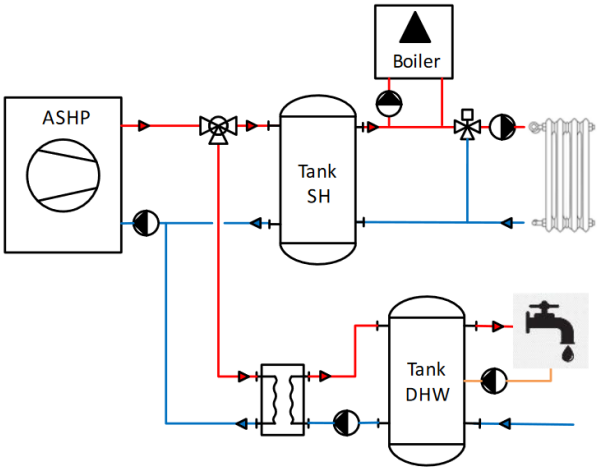


Figure 18: Schematic diagram of the air-source heat pump system with backup boiler for SH [70]

Weather

Weather conditions, including outdoor air temperature and solar irradiation, are based on hourly values from 2035 weather projections [71] for an average year in Geneva (2'546 HDD_{18}; global horizontal radiation: 1'234 kWh/m²/year), representative of the Swiss Plateau.

Building

The building is simulated using the RC building model (TRNSYS Type 5897) [25] described in section 3.4.1. Building envelope parameters are derived from the updated LESOSAI energy models for the desired building typology and retrofitting state as explained in section 3.4.2. Optimization scenarios regarding the ventilation fresh air flow rate are modeled by changing coefficient H_{ve} in type RC, which represents heat losses due to ventilation.

For all cases simulated in this project, as an indicator that the indoor temperature setpoint is met and kept within a reasonable range, the indoor temperature is verified not to fall more than 1 K below the setpoint for more than 300 hours per year. This indicator is inspired by the definition of unmet load hours in ASHRAE Standard 90.1-2019 [72].

Space heating

- **Load:** Space heating is supplied to the building via radiators (TRNSYS Type 362 [65]) that calculate heat output and fluid outlet temperature based on heat emitters capacity, inlet fluid temperature, flow rate, and building indoor temperature.
- **Control strategy:** Heat is supplied to the distribution loop by the HP, via a buffer tank maintained at a temperature range defined by the heating curve (+ 5 K). In hybrid systems, when the outdoor air temperature falls below the bivalence temperature, the backup boiler ensures that the SH loop supply temperature does not fall below the setpoint defined by the heating curve. Return flow from the distribution is mixed with buffer tank output to match the supply temperature setpoint if needed. The SH pump modulates the distribution flow rate to maintain the chosen indoor temperature setpoint. If the indoor temperature reaches the setpoint temperature but the SH pump is already operating at its minimum flow rate (20% of its maximum flow rate), it will

maintain this flow rate and only switch off if the indoor temperature exceeds the setpoint by 1.5 K. Additionally, SH is switched off entirely from June 1 to October 1, as it is now common practice in Geneva to delay the start of the heating season until October in order to save energy [73].

- **Heating curve:** Defined as described in section 4.4.2 and Appendix 11.3. The optimized heating curves are calculated based on the installed heat emitter capacity and SH load using the "high-flow" method, which minimizes the SH supply temperature but requires a higher flow rate in the distribution system. The SH return temperature is a result of the modulation of the SH pump, SH load and indoor temperature at each time step.
- **Sizing:**
    - **SH buffer tank:** The SH buffer tank is sized at 10 L/kW_{th} of HP capacity (as observed on several case studies, e.g. [69]).
    - **SH pump:** The distribution pump is sized to meet the setpoint supply/return temperature difference for the SH load (Q_{SH}^{+}, see Appendix 11.3) at an outdoor temperature of -4°C.
    - **Heat emitters:** Heat emitters are sized based on the design SH load (Q_{SH}, see Appendix 11.3) of the non-retrofitted building under the operating conditions 62/52/22°C (supply/return/indoor). The design SH load is calculated for an outdoor air temperature of -10°C, corresponding to the design outdoor air temperature commonly used for the Swiss Plateau at the time the studied buildings were built, and assuming the baseline ventilation fresh air flow rate of 1.0 m³/h.m². In scenarios where an initial emitter oversizing is considered (which can also correspond to critical radiator replacement), the installed emitter capacity is set equal to that design SH load multiplied by the selected oversizing factor. For more details on heat emitters modeling, see section 4.4.1 and Appendix 11.3.

Domestic hot water

- **Load:** DHW demand is modeled using the hourly tapping schedule from the SIA 385/2 standard [74] for multifamily buildings, combined with a daily DHW tapping volume per occupant. A constant cold-water inlet temperature of 10°C is assumed throughout the year. The occupancy density is set to 40 m²/occ., which roughly corresponds to the average for MFBs of the considered construction period in Switzerland [75] (note that the occupant density is usually higher for more recent buildings, around 44-48 m²/occ.). To model the use of "Joulia" heat recovery systems, it is considered that the DHW tapping volume is divided by 2, i.e. a heat recovery of 50% thanks to the Joulia heat recovery system (more details in Appendix 11.5).
- **Control strategy:** Heat is supplied to the DHW tank by the HP via an external heat exchanger. The tank is maintained at 50–60°C, controlled by a sensor placed in the upper third of the tank. The load-side pump is activated whenever tank charging is required. If charging exceeds one hour, it is temporarily interrupted and the HP switches back to SH production to avoid comfort issues. The circulation pump operates continuously at a constant flow rate.
- **Sizing:**
    - **DHW buffer tank:** Tank sizing follows the SIA 385/2 standard [45], assuming six 45-minute DHW charging cycles per day, 45 L/day per occupant, 40 m²/occupant, and 30% storage and distribution heat losses. The tank geometry is characterized by a diameter-to-height ratio of 0.5, an average value derived from manufacturer data for DHW tank up to 2 m³.
    - **DHW heat exchanger:** The heat exchanger is sized to meet the design DHW load calculated according to SIA 385/2 standard [45], assuming the same conditions used for DHW tank sizing.

- **Pipes:** Distribution and circulation pipes characteristics are defined to result in approximately 35% storage and distribution losses in the baseline case (i.e. with 35 L/occ.day).
- **Charging pump:** The pump between the heat exchanger and the tank is sized to achieve a temperature difference of 7.5 K between supply and return at the design DHW load, calculated as per SIA 385/2 standard.
- **Circulation pump:** The circulation pump flow rate is set to 0.0002 $m^3/h.m^2_{ERA}$, based on values observed in several case studies.

- **Energy performance:** The DHW heat exchanger efficiency is modeled using a performance map derived from manufacturer data (see Appendix 11.5). At each time step, the performance map provides the overall heat transfer coefficient of the heat exchanger (UA) as a function of the inlet primary and secondary flow rates. This approach simulates more realistic operating conditions and resulting temperature levels compared to a constant-efficiency model. A performance map is created for each selected heat exchanger sizing conditions of the sensitivity analysis. Heat exchangers with larger heat transfer area have a greater UA coefficient.

Heat pump and backup boiler

- **Control strategy:** The HP modulates its capacity and switches between SH and DHW production to maintain the tanks at their respective setpoint temperatures. In the case of a simultaneous demand, priority is given to DHW.
- **Sizing:**
  - **Heat pump and boiler:** In monovalent systems, the HP is sized to meet 100% of the heat demand in SH and DHW:
    - **SH:** The HP is designed to meet SH peak demand of the simulated retrofitting state within 18 hours, reserving the remaining 6 hours for DHW cycles, with production temperature of 55°C and an outdoor temperature of -4°C.
    - **DHW:** The HP is sized according to SIA 385/2 standard [45] assuming the same conditions used for DHW tank sizing, explained above, and a production temperature of 65°C at an outdoor temperature of -4°C.

    After following the above sizing procedure separately, the higher of the two capacities (SH/DHW) is finally selected.

    In hybrid systems, the HP is sized to meet 100% of the heat demand in SH and DHW (monovalent system) of the fully retrofitted building. In previous retrofitting steps, the backup boiler is therefore needed to meet the SH load when it exceeds the HP capacity. The backup boiler capacity is set to meet the design SH load (outdoor air temperature of -4°C) of the building for the current retrofitting step.
  - **Circulation pump:** The pump is sized to achieve a 5 K temperature difference between HP supply and return.
- **Energy performance:** HP COP and heating capacity are derived from manufacturer data for HP units available on the market [76,77], as a function of the outdoor air temperature and the condenser inlet temperature (Appendix 11.6). The available performance maps include both minimum and maximum capacity for the high-efficiency R290 HP, which is equipped with an inverter and therefore designed to operate efficiently at part load, but only maximum capacity for the "regular" R410A HP, which uses fixed-speed compressors and varies its output by activating one or more of them. Since this unit is not specifically designed for efficient part-load operation, its part-load efficiency is assumed equal to its full-load efficiency. In hybrid systems, the boiler efficiency is assumed equal to 90% relative to the higher heating value.

5 Integrated building and SH/DHW system simulations

5.1 Integrated building and SH/DHW system model

The building and SH/DHW system models presented in Chapters 3 and 4 are combined into a single TRNSYS model, as illustrated in Figure 19. This integrated model accounts, at each time step, for the interactions between the building's indoor temperature, the heat emitters, and the rest of the SH/DHW system, thereby providing more realistic system temperature levels than with uncoupled models would.

This integrated model is first used to simulate a baseline scenario: a non-renovated building supplied by an ASHP system. The identified retrofitting and optimization measures are then implemented into the model and combined into various scenarios, representing different levels of system optimizations and retrofitting depth (from partial to full), in order to explore their impact on energy and environmental performance indicators and identify the most favorable scenarios.

This chapter first presents the performance indicators used to compare the different scenarios and assess the impact of retrofitting/optimization measures on the system production and distribution temperatures, efficiency, renewable energy integration and decarbonization. It then details the simulation results for the baseline scenario: a non-renovated building supplied by an ASHP system. Finally, it presents the sensitivity analysis, along with the corresponding results, relative to the implementation of various building envelope retrofitting measures and SH/DHW system optimizations.

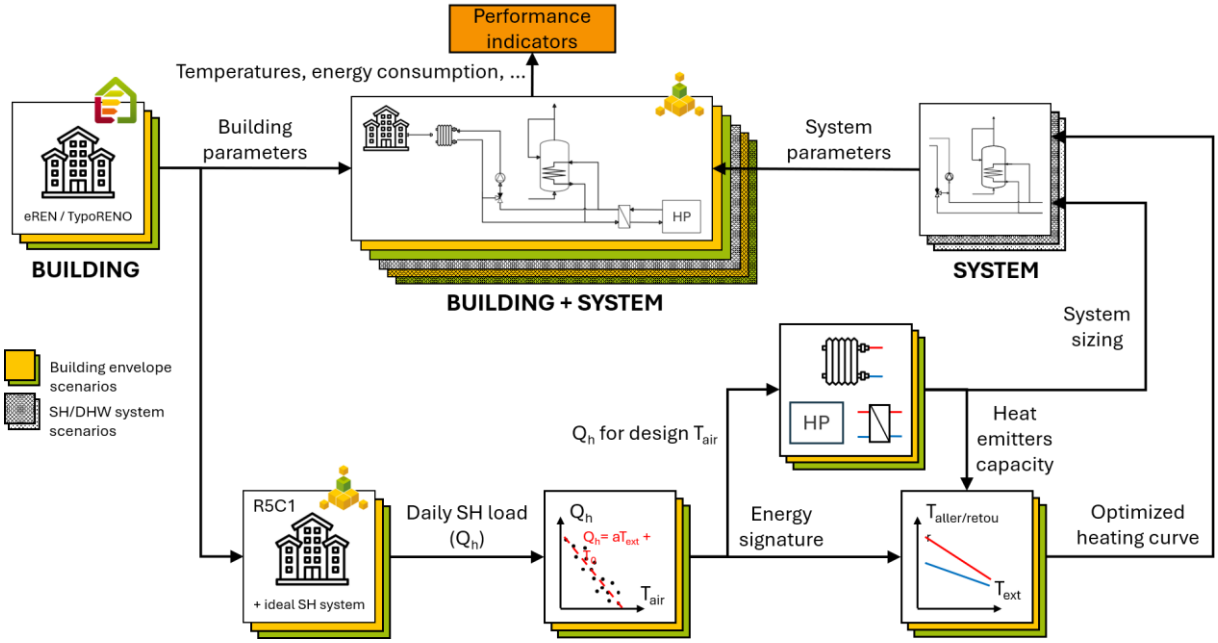


Figure 19: Methodology for the definition of sensitivity analysis scenarios for various building typologies and envelope retrofitting measures, as well as various SH/DHW system typologies and optimization measures

5.2 Performance indicators

Several performance indicators are identified to evaluate the impact of the retrofitting and optimization measures on the system.

5.2.1. Temperature levels

The first indicators are the annual heat-weighted average temperatures (supply/return/DT) at different locations in the system (Figure 20). The most important temperatures being the production temperatures (HP condenser supply/return temperatures) since the efficiency of the heat pump, and thus the integration of renewables in the system depend on them. Nonetheless, the other temperatures allow to identify the strengths and weaknesses in terms of temperature levels, which in turn allow to target the most promising optimization measures.

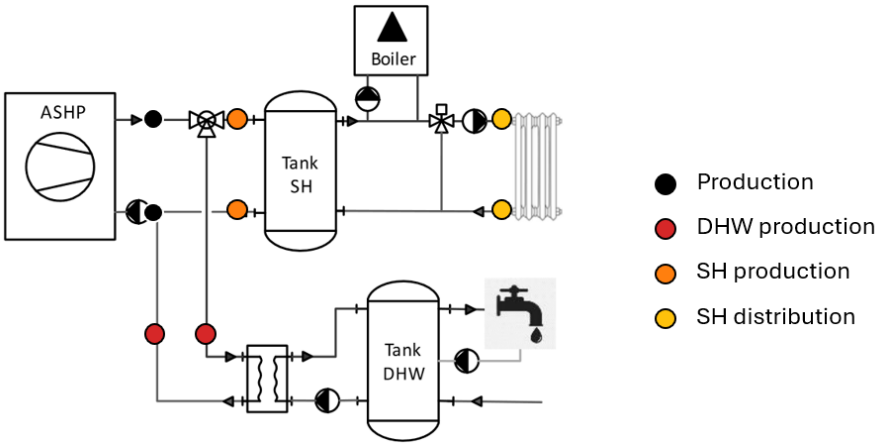


Figure 20: Locations in the system for the evaluation of annual average supply/return temperature levels

5.2.2. Energy performance

The energy performance of the system is first evaluated with the specific heat demand (SH and DHW, in kWh/m²). Then the impact of the lowered temperature levels on the heat production efficiency is assessed with the seasonal performance factor of the HP (SPF_{HP}), calculated according to Equation (4). It is defined as the ratio of annual heat production (Q_{HP}) to annual HP electricity consumption (E_{HP}).

$$SPF_{HP} = \frac{Q_{HP}}{E_{HP}} \quad (4)$$

To account for the heat production (Q_{backup}) and energy consumption (E_{backup}) of the backup boiler, we calculate the seasonal performance factor of the system (SPF_{system}) as per Equation (5), including the heat production and energy consumption of both the HP and the backup boiler.

$$SPF_{system} = \frac{Q_{HP} + Q_{backup}}{E_{HP} + E_{backup}} \quad (5)$$

These two SPF do not take into account the electricity consumption of the system auxiliaries (circulation pumps, controllers, etc.).

5.2.3. Environmental performance

The environmental performance of the system before and after implementation of retrofitting/optimization measures is evaluated in terms of decarbonization, using the CO_{2eq} emissions related to the operation of the heat generators (HP and backup boiler), as well as renewable energy integration, with the renewable energy fraction of the heat production.

Emissions related to the electricity consumption are calculated using Equation (6), where $E_{HP,h}$ correspond to the hourly HP electricity consumption. The hourly emission factor of the electricity ($f_{elec.h}$ in $kgCO_{2eq}/kWh_{elec}$) is based on the hourly CO_{2eq} content of the Swiss electricity mix from the work of Romano et al. [78], taking into account domestic generation as well as imports from neighboring countries. Since the system is modeled for a typical year rather than an actual year, we use the hourly

average of years 2017-2021. The annual average is equal to 96 gCO2eq/kWh$_{elec}$, but daily peak values reach up to 200-300 gCO2eq/kWh$_{elec}$ (see Appendix 11.3 for the whole profile).

$$C_{grid} = \sum_{h} E_{HP,h} \cdot f_{elec.h} \quad (6)$$

Emissions related to the backup heater production (gas-fired boiler) are calculated using Equation (7), with a constant emission factor (f_{gas}) equal to 230 CO_{2eq}/kWh$_{th}$ [79]. Finally, the total emissions of the system are evaluated using Equation (8).

$$C_{gas} = E_{backup} \cdot f_{gas} \quad (7)$$

$$C_{system} = C_{grid} + C_{gas} \quad (8)$$

Total emissions are then divided either by the building ERA, to provide an indicator of the carbon emissions intensity of the building (in kgCO_{2eq}/m² of ERA), or by the heat produced, to evaluate the efficiency of the system in terms of emissions (in gCO_{2eq}/kWh$_{th}$).

Note that we only consider emissions related to the energy consumption of the heating system. Embodied energy of the building retrofit and the system (e.g. heat pump, etc.) is not included.

As described in Equation (9), the annual renewable energy fraction ($\%Ren$) corresponds to sum of the energy extracted from the air by the HP (Q_{air}) and the renewable energy from the electricity mix ($E_{elec,ren}$), divided by the total amount of heat produced by the HP and the backup boiler. The renewable energy from the electricity consumption ($E_{elec,ren}$) is assessed with Equation (10), where $\%Ren_{elec,h}$ is the hourly Swiss electricity share produced by primary energy originating from renewable sources, according to the work of Romano et al. [78] (as hourly average for years 2017-2021).

$$\%Ren = \frac{Q_{air} + E_{elec,ren}}{Q_{HP} + Q_{backup}} \quad (9)$$

$$E_{elec,ren} = \sum_{h} E_{HP,h} \cdot \%Ren_{elec,h} \quad (10)$$

5.3 Baseline scenario

The first integrated building and SH/DHW system simulation is done for the non-renovated eREN4 building typology, supplied by an ASHP system. The main characteristics of the energy model (component sizing, control strategy, etc.) are described in section 3.4 for the building and section 4.4 for the system. This section presents the simulation results, including the performance indicators described in section 5.2.

5.3.1. System parameters

The main parameters of the baseline scenario are summarized in Table 11. This scenario is defined to reflect operating conditions frequently observed in existing non-renovated MFB in Switzerland, as highlighted by Khoury et al. [58], rather than following the SIA 380/1 standard [30]. This approach aims to represent the actual initial state of the building, prior to any retrofitting or optimization measures. Key deviations from the standard values include:

- Indoor temperature: 22°C, instead of the standard value of 20°C
- Ventilation flow rate: 1.0 m³/h.m², instead of the standard value of 0.7 m³/h.m²

Table 11: Summary of the main parameters of the baseline scenario

Type	Parameter	Value
Building	Building typology	eREN 4
	Envelope retrofitting stage	Non-renovated (E0)
	Energy reference area (ERA)	1'475 m²
	Indoor temperature setpoint	22°C
Ventilation	Ventilation flow rate	1.0 $m^3/h.m^2_{ERA}$
Heat generation	Heat pump system type	Monovalent system with regular R410A HP without inverter
	Heat pump capacity	104 kW (at A7/W35)
	Backup boiler capacity	None
Space heating	Annual SH demand	107 kWh/m².year (386 MJ/m².an)
	Peak SH demand (at -4°C outdoor air)	38.7 W/m²
	Volume of SH buffer tank	1.04 m³ (10 L/kW_{th} HP at A7/W35)
Heat emitters	Radiator capacity	53 W/m² at 62/52/22°C (76 W/m² at 75/65/20°C, EN442 standard)
	Radiator oversizing factor	100% (no oversizing compared to SH demand at -10°C without solar and internal gains)
	Heating curve type	Non-optimized (as per benchmark, see Figure 14)
	Heating curve temperatures	63/52°C (at -10°C outdoor air) 40/36°C (at +10°C outdoor air)
	Maximum total distribution flowrate	17.0 m³/h
DHW	Number of occupants	37 (40 m²/occ)
	Daily tapping volume	35 L/occ.day
	Volume of DHW tank	0.61 m³
	Heat exchanger area	medium

This results in an annual SH demand of 107 kWh/m². When including an annual DHW demand of 35 kWh/m², calculated in accordance with Geneva's heat demand index methodology ("Indice de dépense de chaleur", IDC) [80], it yields a total heat demand of 142 kWh/m² per year (511 MJ/m²). When compared against the distribution of Geneva's MFB building stock (Figure 21), the baseline building falls within a range representative of a large share of existing MFBs, specifically those legally required to undergo partial retrofitting and/or optimization measures as per [81].

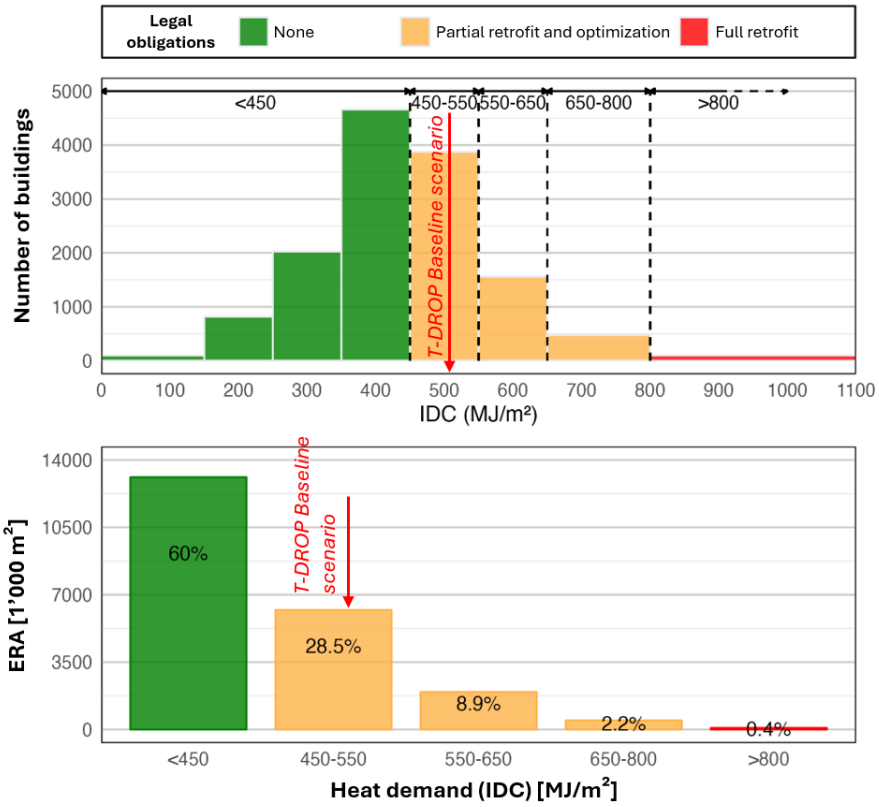


Figure 21: Heat demand index (“Indice de dépense de chaleur”, IDC) of the baseline building compared to the distribution of the MFB building stock in the canton of Geneva (translated from [56])

5.3.2. Temperature levels

Since the project focuses on the temperature levels, it is worth comparing the simulated temperatures to those observed in practice. Figure 22 shows the simulated supply and return temperatures of the heat emitters, alongside the median of the heating curves measured in existing buildings from [64] (Figure 14), which is used as model input and referred to as the non-optimized heating curve in the remainder of the report.

Except for a few rare cases, the supply temperature closely follows the heating curve set as input to the controller. However, the simulated return temperature is significantly lower than observed in the measurements. As described in section 4.5, the SH distribution pump in the model modulates its flow rate between a maximum value (set to match the temperature difference of the measured systems’ heating curve at the design outdoor temperature) and 20% of this value to meet the SH load. In addition, this minimum flow rate is always maintained through the emitters, even when the indoor temperature setpoint has been reached. In practice, thermostatic valves may close when no heat is required, and a bypass may allow circulation within the SH loop without flow through the emitters. As a result, little or no heat is transferred from the SH loop to the building under such conditions. Consequently, the model tends to produce lower flow rates, larger supply/return temperature differences, and lower return temperatures than those observed in practice.

This simplified modeling approach is not expected to significantly affect HP performance indicators, as the SH buffer tank and mixing valve decouple the SH distribution loop from the heat pump loop. Moreover, HP performance is influenced primarily by the supply temperature rather than the return temperature. The impact would, however, be more significant for DH substations, where return temperature is a key factor for DH performance and renewable energy integration.

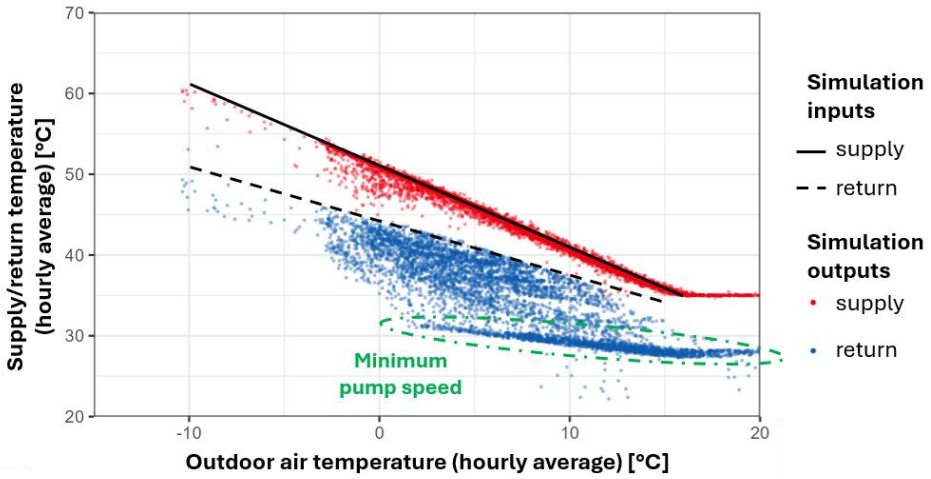


Figure 22: Hourly simulation results for the SH distribution supply/return temperature (inlet/outlet temperature of the heat emitters) of the non-retrofitted baseline scenario and median heating curve from [64] (Figure 14) used as input to the model and referred to as non-optimized heating curve.

The lowest return temperatures occur when the SH loop operates at its minimum flow rate while the indoor temperature is close to or above the setpoint (22°C in the baseline scenario). This situation occurs frequently in mid-season, when the SH demand is low (Figure 23). The pump controller then lowers the flow rate to limit the heat supplied and prevent overheating. Some overheating nevertheless occurs, because the SH pump fully stops only if the indoor temperature exceeds the setpoint by 1.5 K. Operation at minimum flow rate therefore sometimes still supplies more heat than required to meet the SH load. However, the resulting rise in indoor temperature remains reasonable, generally kept below 1.5 K above the setpoint (i.e. below 23.5°C) and only occasionally reaching up to 2 K above it (i.e. 24°C) near the summer season due to internal and solar gains adding up to the excess SH supply. In practice, such a rise might be compensated by occupants opening the windows, which is not accounted for in the model.

Conversely, in the heart of winter, the indoor temperature is often below the 22°C setpoint, as the system does not fully meet the SH load, but rarely by more than 1 K (i.e. below 21°C). For all cases simulated in this project, the indoor temperature is verified not to fall more than 1 K below the setpoint for more than 300 hours per year, as an indicator that the setpoint is met and kept within a reasonable range. This indicator is inspired by the definition of unmet load hours in ASHRAE Standard 90.1-2019 [72]. Although low indoor temperatures are observed in September in Figure 23, they are excluded from this indicator as they occur outside of the defined heating season (from October 1 to June 1, section 4.5).

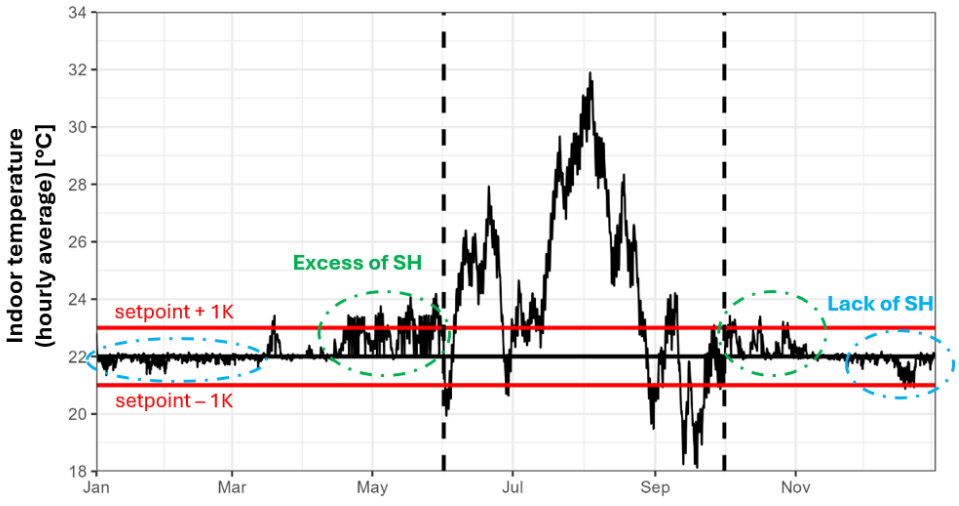


Figure 23: Hourly indoor temperature of the building for the non-retrofitted baseline scenario

On average (heat-weighted) over the entire year, these distribution-side SH supply/return temperatures are equal to 45.7/36.8°C, as shown in Figure 24. The production-side SH temperatures are slightly higher (47.3/42.7°C) because the HP maintains the SH buffer tank at the supply temperature setpoint given by the heating curve, with a hysteresis of +0 K to +5 K, as explained in section 4.5. Note that this range is conservative: in practice, the buffer tank could likely be kept within 0-1 K of the heating curve, provided the building and SH system have sufficient thermal inertia. Since the HP operates with a supply/return temperature difference of approximately 5 K, the average return temperature is about 5 K lower than the supply temperature. The average HP supply/return temperatures (49.0/44.3°C) are a few degrees higher than the SH production temperatures, due to the DHW production temperatures (56.0/50.6°C), which are high to prevent legionella proliferation. Since the DHW demand accounts for a relatively small portion of the total heat demand in this non-retrofitted building (20%, see Figure 25), the higher DHW temperatures have a limited impact on the average HP production temperatures. However, this influence would be more significant for buildings with lower SH demand.

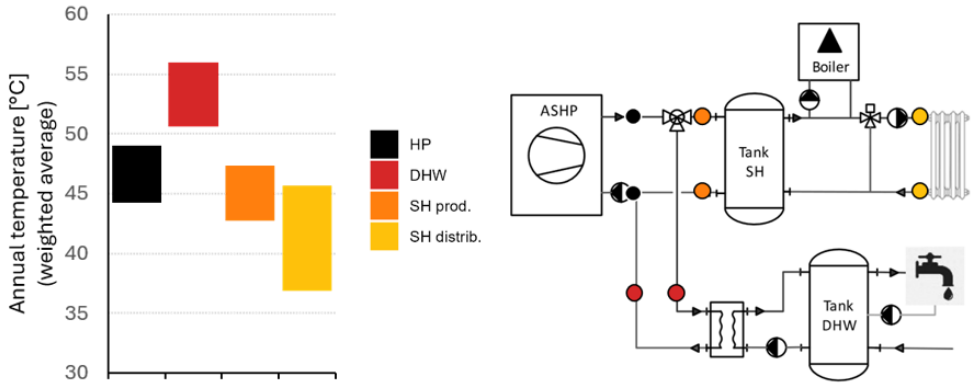


Figure 24: Annual average (heat-weighted) supply/return temperatures for the non-retrofitted baseline scenario. Each bar represents the average supply (top) and return temperature (bottom), and their difference (bar height).

5.3.3. Energy balance

The energy balance results for the baseline scenario are presented in Figure 25 (annual results) and Figure 26 (daily results).

The annual SPF of the HP is equal to 2.90, but the it fluctuates on a daily basis throughout the year. It drops to about 2.0 during the winter peak SH demand, when the HP operates at its lowest COP. In contrast, it rises to about 3.5 during summer, due to high outdoor air temperature which improve the HP COP, even with high DHW production temperatures. The daily SPF is highest in mid-season (up to 4.10) when the outdoor air temperature is relatively high, and the average HP production temperature is a mix of the high DHW temperature and relatively low SH temperature at that time of year. On an annual basis, the SPF for DHW and for SH production are very close, respectively 2.93 and 2.90. The higher SPF for DHW production than for SH reflects the high SPF during the summer months, as well as the non-optimized heating curve and relatively high SH production temperatures required for the non-renovated building.

The system generates 5.9 kgCO_{2eq}/m² annually due to its electricity consumption, with a renewable share of 80%. Emissions are lowest during summer (about 0.6 g/m².day) due to the low heat demand and low carbon content of the Swiss electricity mix (see Appendix 11.3). They are significantly higher during the winter (up to 75 g/m².day), reflecting the higher heat demand and smaller share of renewable energy in the electricity mix.

It is interesting to note that the system delivers a small excess of SH (2.9 kWh/m².year). It is attributed to mid-season operation explained in the previous section, during which the SH distribution pump continues operating at its minimum flow rate even after the indoor temperature has exceeded the 22°C setpoint. It isa compensated by the unmet SH load during the winter (1.3 kWh/m².year), resulting in net excess SH production of 1.6 kWh/m².year.

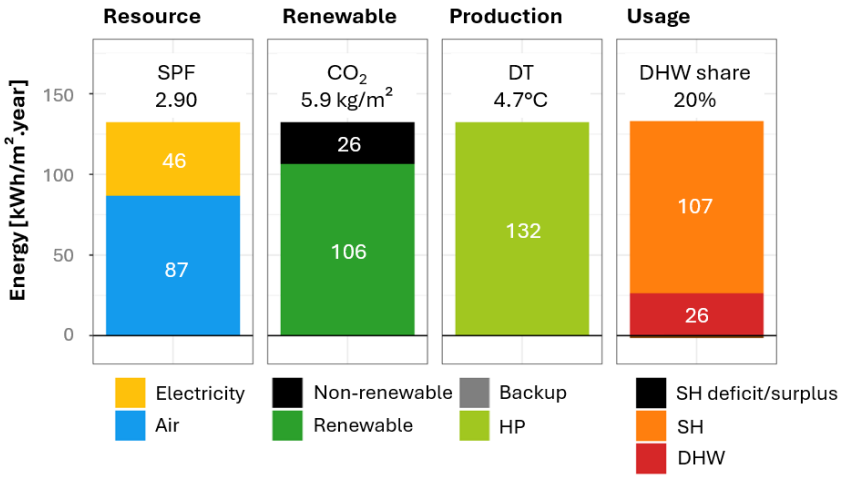


Figure 25: Annual energy balance results and performance indicators for the non-retrofitted baseline scenario

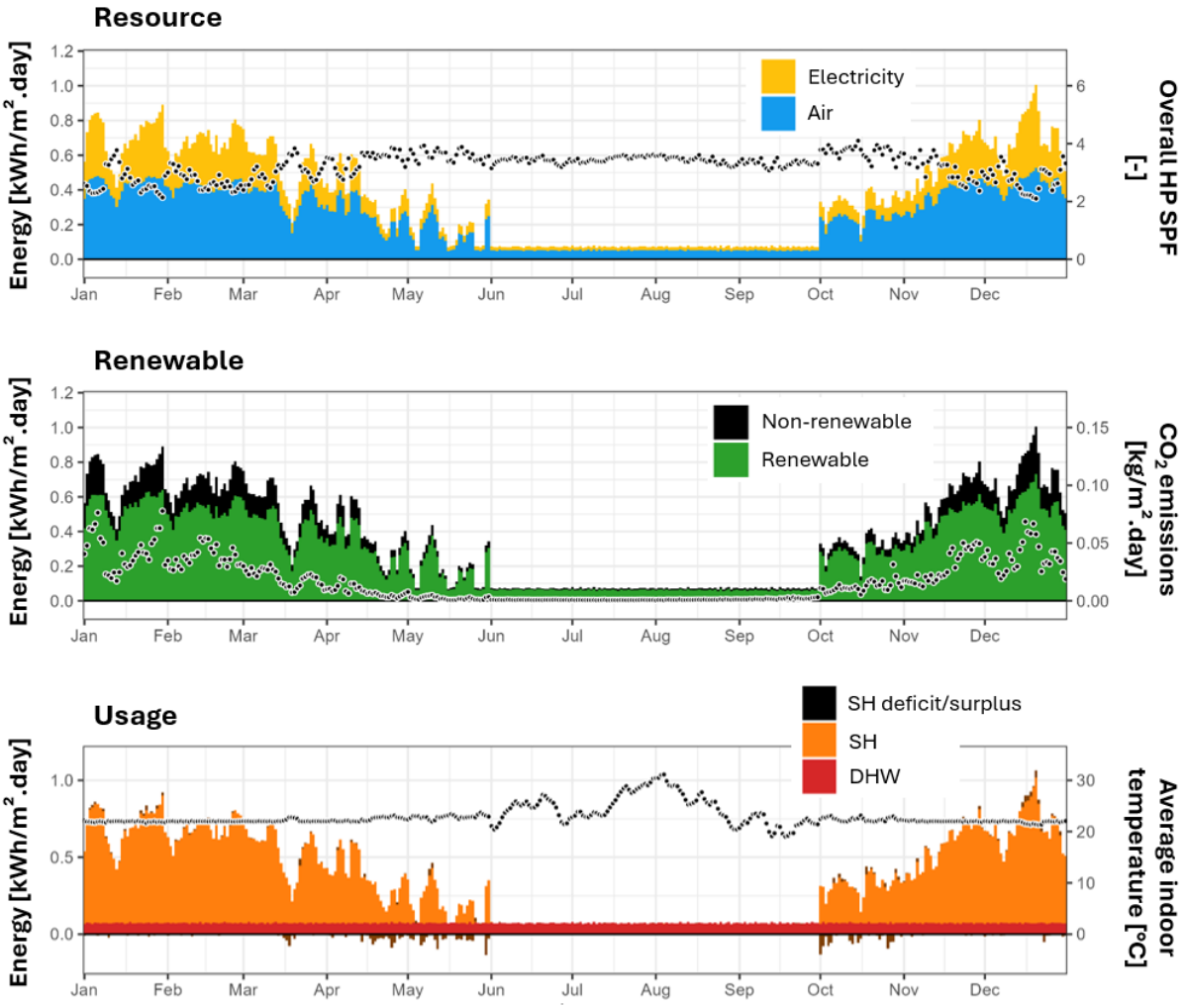


Figure 26: Daily energy balance results and performance indicators for the non-retrofitted baseline scenario

5.4 Sensitivity analysis

5.4.1. Scenarios

The sensitivity analysis combines targeted measures on the building side with measures on the SH/DHW system side, across different building and system typologies, as illustrated in Figure 27.

On the building side, the analysis covers, for each selected building typology, the envelope retrofitting measures presented in Chapter 3, as well as (for the reference building typology only) two further parameters influencing the SH demand: the indoor temperature setpoint and the ventilation fresh air flow rate.

On the system side, for each SH/DHW system typology, the analysis evaluates the impact of the system optimization and replacement measures presented in Chapter 4 (e.g. heating curve optimization, DHW heat exchanger sizing), as well as the sensitivity to the DHW demand, which can vary considerably from one building to another depending on occupant behavior [82].

Building-side and system-side measures are then combined into scenarios representing different typologies, system optimizations and retrofitting depths (from partial to full). These scenarios are simulated to assess the impact of the retrofitting and optimization measures on the performance indicators defined in section 5.2.

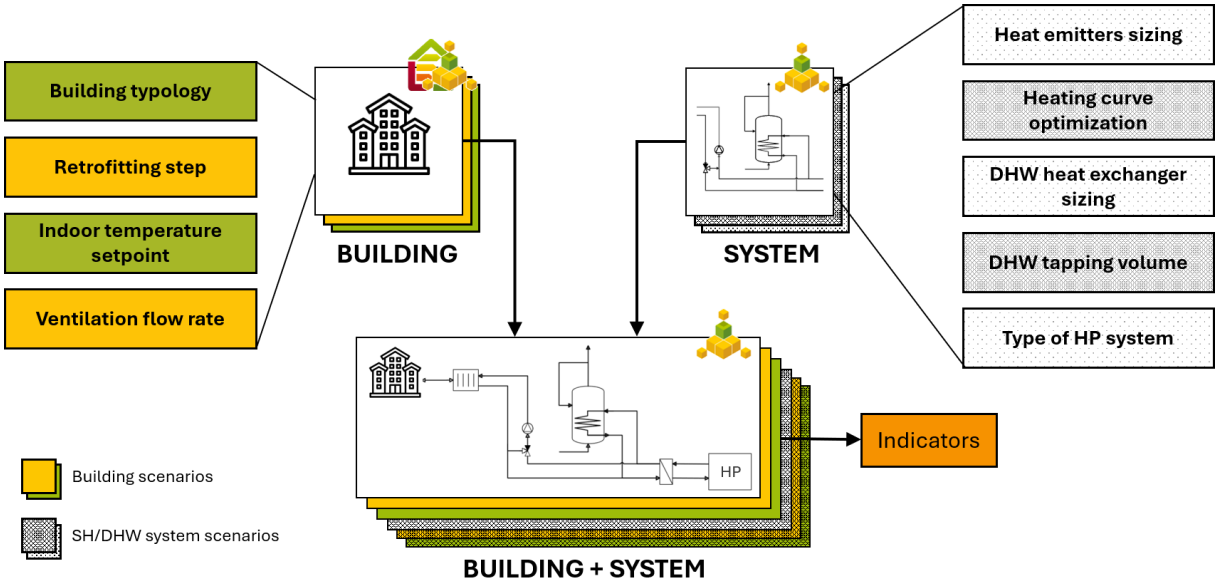


Figure 27: Illustration of the sensitivity analysis parameters and scenarios

The following parameters are varied for this analysis. Parameters corresponding to the baseline scenario are underlined.

Building:

- **Building typology:** **<u>eREN 4</u>** (small-scale building), eREN 7 (large-scale building) and TypoRENO I2 (very large-scale building), as defined in section 3.3
- **Building retrofitting step:** from **<u>non-retrofitted (E0)</u>** to fully retrofitted (E3 for typologies eREN 4 and eREN 7, E4 for typology TypoRENO I2)
- **Indoor air temperature setpoint:** 20°C (SIA 380/1 standard value [30]), 21°C, **<u>22°C</u>** and 23°C (last two values reflect operating conditions frequently observed in existing non-renovated MFB in Switzerland, as highlighted by Khoury et al. [58])

- **Ventilation flow rate:** 0.7 m³/h.m² (SIA 380/1 standard value [30]), **1.0 m³/h.m²** and 1.5 m³/h.m² (last two values both reflect operating conditions frequently observed in existing non-renovated MFB in Switzerland, as highlighted by Khoury et al. [58], with and without air change due to window opening)

SH/DHW system:

- **Initial heat emitters oversizing: no oversizing (+0%)**, +20% or +40% oversizing compared to the non-retrofitted building for operating conditions 62/52/22°C (supply/return/indoor), which are the operations conditions of the baseline scenario (estimated based on the SH demand at -10°C outdoor air temperature, without internal or solar gains)
- **Heating curve: Non-optimized** (as per benchmark results for radiators [64], see Figure 14) or optimized using the "high-flow" method for the current retrofitting step and installed heat emitters capacity (see section 4.4)
- **DHW heat exchanger heat transfer area:** small (0.4 times the medium area, UA/Q = 0.167 1/K at design conditions), **medium** (UA/Q = 0.226 1/K) and large (1.7 times the medium area, UA/Q = 0.328 1/K). See Appendix 11.5 for more details on the DHW heat exchanger sizing and modeling.
- **DHW tapping volume:** 17.5 L/occ. per day (corresponds to a case where Joulia heat recovery systems are implemented in the apartments, with an assumed heat recovery efficiency of 50% see section 4.3 for details), 25 L/occ. per day, **35 L/occ. per day** (SIA 385/2 standard value for MFB [56]) and 50 L/occ. per day
- **Heat production: Monovalent system with regular R410A HP without inverter**, monovalent system with high-efficiency R290 HP with inverter and hybrid system with R410A HP without inverter and a gas-fired boiler (see more details in section 4.3).

Each measure is simulated for the baseline building typology (eREN 4), for each retrofitting step, with and without heating curve optimization, so as to analyze each measure separately (see example in Table 12). For the sensitivity analysis on the building typology, the same principle is applied: each retrofitting step is simulated with and without heating curve optimization. This results in a total of 138 scenarios simulated for this sensitivity analysis. For each scenario, system sizing is carried out as described in section 4.5.

In addition, a fully optimized case is also analyzed to assess the performance indicators for the best case scenario (if we chose to implement all measures): all optimization measures are applied and simulated for each retrofitting step for the baseline building typology (eREN 4) heated by a monovalent ASHP system, with and without heating curve optimization. It includes the following modifications compared to the baseline:

- Lowered indoor temperature setpoint to the standard value (20°C)
- Optimized ventilation flow rate to match the standard value (0.7 m³/h.m²)
- High initial heat emitters oversizing (+40%)
- Large DHW heat exchanger transfer area
- Standard DHW tapping volume (35 L/occ. per day) with Joulia heat recovery systems, resulting in DHW tapping of 17.5 L/occ. per day
- High-efficiency R290 HP

Only the most relevant results of the sensitivity analysis are presented in the following sections.

Table 12: Sample of the sensitivity analysis scenarios

#	Building typology	Retrofitting step	Indoor temperature [°C]	Heat generation	Initial heat emitter oversizing factor	Heating curve	DHW heat exchanger transfer area	DHW tapping volume [L/occ.day]	Ventilation flow rate [m³/h.m²]
1	eRen4	E0	22	Monovalent system with regular R410A HP	100%	Non-optimized	Medium	35	1.0
2	eRen4	E1	22	Monovalent system with regular R410A HP	100%	Non-optimized	Medium	35	1.0
3	eRen4	E2	22	Monovalent system with regular R410A HP	100%	Non-optimized	Medium	35	1.0
4	eRen4	E3	22	Monovalent system with regular R410A HP	100%	Non-optimized	Medium	35	1.0
5	eRen4	E0	22	Monovalent system with regular R410A HP	100%	Optimized (high-flow)	Medium	35	1.0
6	eRen4	E1	22	Monovalent system with regular R410A HP	100%	Optimized (high-flow)	Medium	35	1.0
7	eRen4	E2	22	Monovalent system with regular R410A HP	100%	Optimized (high-flow)	Medium	35	1.0
8	eRen4	E3	22	Monovalent system with regular R410A HP	100%	Optimized (high-flow)	Medium	35	1.0
9	eRen4	E0	22	Monovalent system with regular R410A HP	120%	Non-optimized	Medium	35	1.0
10	eRen4	E1	22	Monovalent system with regular R410A HP	120%	Non-optimized	Medium	35	1.0
11	eRen4	E2	22	Monovalent system with regular R410A HP	120%	Non-optimized	Medium	35	1.0
12	eRen4	E3	22	Monovalent system with regular R410A HP	120%	Non-optimized	Medium	35	1.0
13	eRen4	E0	22	Monovalent system with regular R410A HP	120%	Optimized (high-flow)	Medium	35	1.0
14	eRen4	E1	22	Monovalent system with regular R410A HP	120%	Optimized (high-flow)	Medium	35	1.0
15	eRen4	E2	22	Monovalent system with regular R410A HP	120%	Optimized (high-flow)	Medium	35	1.0
16	eRen4	E3	22	Monovalent system with regular R410A HP	120%	Optimized (high-flow)	Medium	35	1.0
⋮									
25	eRen4	E0	22	Monovalent system with regular R410A HP	100%	Non-optimized	Medium	17.5	1.0
26	eRen4	E1	22	Monovalent system with regular R410A HP	100%	Non-optimized	Medium	17.5	1.0
27	eRen4	E2	22	Monovalent system with regular R410A HP	100%	Non-optimized	Medium	17.5	1.0
28	eRen4	E3	22	Monovalent system with regular R410A HP	100%	Non-optimized	Medium	17.5	1.0
29	eRen4	E0	22	Monovalent system with regular R410A HP	100%	Optimized (high-flow)	Medium	17.5	1.0
30	eRen4	E1	22	Monovalent system with regular R410A HP	100%	Optimized (high-flow)	Medium	17.5	1.0
31	eRen4	E2	22	Monovalent system with regular R410A HP	100%	Optimized (high-flow)	Medium	17.5	1.0
32	eRen4	E3	22	Monovalent system with regular R410A HP	100%	Optimized (high-flow)	Medium	17.5	1.0
⋮									
139	eRen4	E0	20	Monovalent system with high-efficiency HP	140%	Non-optimized	Large	17.5	0.7
140	eRen4	E1	20	Monovalent system with high-efficiency HP	140%	Non-optimized	Large	17.5	0.7
141	eRen4	E2	20	Monovalent system with high-efficiency HP	140%	Non-optimized	Large	17.5	0.7
142	eRen4	E3	20	Monovalent system with high-efficiency HP	140%	Non-optimized	Large	17.5	0.7
143	eRen4	E0	20	Monovalent system with high-efficiency HP	140%	Optimized (high-flow)	Large	17.5	0.7
144	eRen4	E1	20	Monovalent system with high-efficiency HP	140%	Optimized (high-flow)	Large	17.5	0.7
145	eRen4	E2	20	Monovalent system with high-efficiency HP	140%	Optimized (high-flow)	Large	17.5	0.7
146	eRen4	E3	20	Monovalent system with high-efficiency HP	140%	Optimized (high-flow)	Large	17.5	0.7

5.4.2. Impact of heating curve optimization

The first step consists in evaluating the impact of optimizing the heating curve relative to the non-optimized case. Figure 28 shows the annual average HP production temperature and HP SPF, with and without heating curve optimization, as a function of the total heat demand (SH and DHW) which varies with building retrofitting of the baseline case.

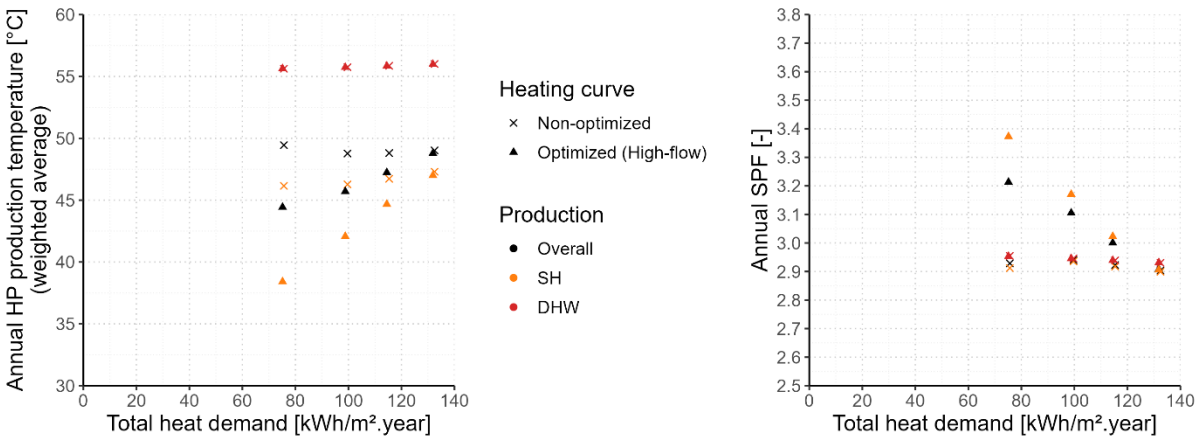


Figure 28: Annual average HP production temperature and HP SPF for each service, with and without heating curve optimization

Without heating curve optimization

The annual average HP production temperature for DHW remains unchanged in all cases (≈ 56°C), i.e. with/without heating curve optimization and with/without retrofit, since no modification is applied to the

DHW. For SH, it decreases slightly from 47°C (non-renovated building) to 46°C (fully retrofitted). The overall HP production temperature stays close to 49°C regardless of retrofitting status. These small variations observed are due to the increase in DHW fraction (the ratio of DHW demand to total heat demand) as the heat demand is reduced with retrofitting: the slightly lower average SH distribution temperature is offset by the higher DHW fraction and high DHW temperature.

The annual SPF for DHW likewise remains unchanged in all cases (≈ 2.94), since no modification is applied to the DHW. The three annual SPFs are very similar for all cases: 2.92 for SH and 2.94 for DHW, giving an overall SPF of about 2.92.

With heating curve optimization

Optimizing the heating curve significantly lowers the annual average HP supply temperature for SH, by up to 8 K (fully retrofitted building) compared to the non-optimized heating curve. This results in annual average supply temperature for SH of 47°C (non-retrofitted building) to 38.5°C (fully retrofitted). Reducing the SH demand by 10 kWh/m².year lowers the SH supply temperature by 1.51 K. This carries over to the overall HP supply temperature, which is reduced by up to 5 K compared to the non-optimized heating curves. It ranges from 49°C (non-retrofitted) to 44.5°C (fully retrofitted). Reducing the SH demand by 10 kWh/m².year lowers the overall supply temperature by 0.77 K, i.e. about half as fast as the SH temperature, since the high DHW supply temperatures drive the overall temperature upward.

Thanks to the optimization of the heating curve, and associated lowered SH supply temperature, the SH SPF increases by up to 0.46 compared to the case without optimization of the heating curve. It varies from 2.91 (non-retrofitted) to 3.37 (fully retrofitted), i.e. reducing the SH demand by 10 kWh/m².year increases the SH SPF by 0.08. The overall SPF follows the same trend but with smaller magnitude, ranging from 2.91 (non-retrofitted) to 3.21 (fully retrofitted, +0.28 compared to the non-optimized heating curve), i.e. reducing the SH demand by 10 kWh/m².year increases the overall SPF by 0.05. The SH SPF therefore increases about 1.6 times faster than the overall SPF with the reduction of the SH demand.

Figure 29 shows the corresponding results for CO_2 emissions of the heat production.

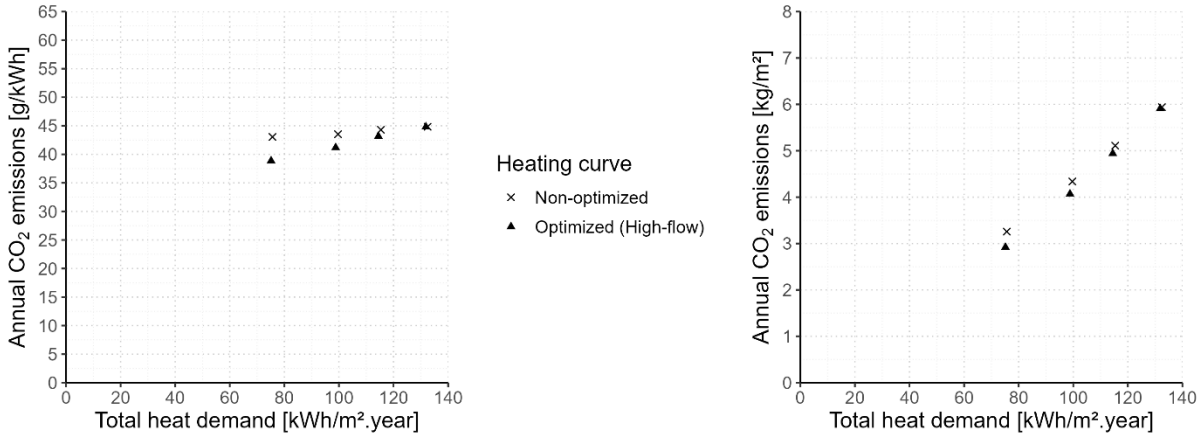


Figure 29: Annual CO_2 emissions for the heat production, in gCO_{2eq}/kWh and $kgCO_{2eq}$/m², with and without heating curve optimization

Without heating curve optimization

Due to the slight increase in overall SPF with retrofitting, the CO_2 emissions decrease slightly from 45 to 43 g/kWh, reflecting the improved efficiency of the heat production. It corresponds to a reduction of about 0.3 g/kWh per 10 kWh/m².year saved.

Per unit of floor area, there is a major reduction thanks to the envelope retrofit, with emissions decreasing from 5.9 kg/m² (non-retrofitted) to 3.3 kg/m² (fully retrofitted), reflecting the improved efficiency of the building. It corresponds to a reduction of about 0.47 kg/m² per 10 kWh/m².year saved.

With heating curve optimization

Thanks to the significant increase in SPF with the optimization of the heating curve, the emissions in g/kWh decrease three times faster than without optimization, at 1.0 g/kWh per 10 kWh/m².year saved.

The emissions in kg/m² are similar to the cases without heating curve optimization, indicating that the reduction in heat demand is the main driver of the building's carbon intensity. Optimizing the heating curve, and thereby improving the heat production efficiency, yields an additional reduction (beyond that from the envelope retrofit) of 3% (retrofitting step 1) to 10% (fully retrofitted) relative to the emissions without heating curve optimization. The reduction of the CO_2 emissions in this case corresponds to about 0.53 kg/m² per 10 kWh/m².year saved.

The renewable energy share for the HP production (see section 5.2.3), remains relatively constant across these cases, ranging from approximately 80% to 82%, regardless of building retrofitting status or heating curve optimization. This limited variation is primarily due to characteristics of the Swiss electricity mix, whose renewable share varies within a relatively narrow range throughout the year (see Appendix 11.8), typically between 40% and 60%, with higher values from May to October and a peak of around 70% in June. As a result, changes in the seasonal distribution of electricity consumption have only a modest influence on the annual renewable energy share of the system.

Building retrofitting and heating curve optimization nevertheless have a small positive effect on this indicator. Improving the heat pump SPF increases the amount of renewable heat extracted from the outdoor air relative to the electricity consumption. In addition, reducing the SH demand decreases the share of electricity consumed during the heating season, when the renewable share of the Swiss electricity mix is generally lower. Both effects therefore contribute to a slight increase in the overall renewable energy share.

When considering all simulated scenarios presented in section 5.4.1, including hybrid HP systems, the renewable energy share varies only between 75 and 84%. Given this relatively narrow range, the indicator provides limited discrimination between the scenarios studied and is therefore not discussed further in the remainder of the report. It may, however, be more relevant for DH substations, where building-level optimization and retrofitting measures can influence the heat production mix towards a better integration of renewable energy sources.

5.4.3. Impact of heat emitters sizing

One parameter has a major influence on the outcome of the heating curve optimization: the initial heat emitters sizing (heat emitters capacity that was installed when the building was built). The larger the heat emitters installed in the building, the lower the SH supply temperature can be set (i.e. the greater the achievable temperature reduction).

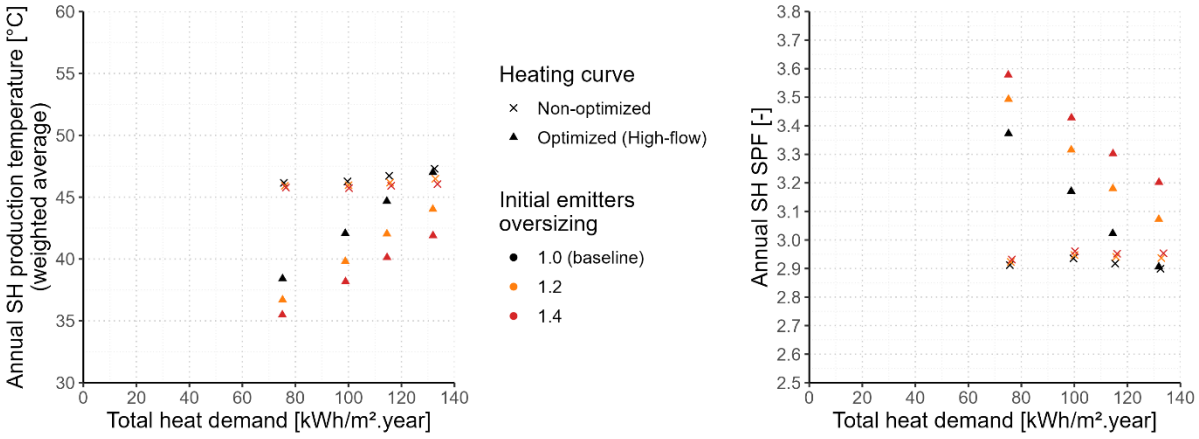


Figure 30: Annual average HP production temperature for SH and annual HP SPF in SH, with and without heating curve optimization, for various heat emitter sizing of the non-renovated building

Figure 30 illustrates the influence of the initial heat emitters sizing at the initial state (non-retrofitted building) on the average SH supply temperature and the HP SPF in SH. Even without retrofitting the building, the average SH supply temperature can be lowered by 3.0 K with emitters initially oversized by 20%, and by 5.1 K with 40% oversizing. When the building is fully retrofitted, the effect of initial oversizing is less pronounced: 1.7 K for 20% oversizing and 2.9 K for 40% oversizing. Relative to the non-optimized heating curve, the gap is very substantial, reaching up to 10.3 K (with 40% initial oversizing) for the fully retrofitted building. The SH supply temperature is then lowered from 45.8°C to 35.5°C. The resulting overall HP production temperature follows the same trend as when the emitters are not oversized in the initial state: it decreases roughly half as fast as the SH supply temperature as the SH demand decreases.

The SH supply temperature reduction is as follows:

- **No initial oversizing:** -0.77 K per 10 kWh/m².year saved
- **20% initial oversizing:** -0.54 K per 10 kWh/m².year saved
- **40% initial oversizing:** -0.38 K per 10 kWh/m².year saved

Given its significant impact on the temperature levels and performance indicators, optimizing the heating curve is clearly an essential measure. Scenarios without heating curve optimization are therefore excluded from the remainder of the results analysis presented in this chapter.

It is interesting to note that a partially retrofitted building (retrofitting step 2, total demand of 100 kWh/m².year) with no initial oversizing reaches the same average SH supply temperature (≈ 42°C) as a non-retrofitted building (total demand of 135 kWh/m².year) with emitters initially oversized by 40%. The impact of retrofitting and optimizations measures on the temperature levels and performance indicators therefore depends strongly on the initial heat emitters sizing.

Rather than the heat emitters sizing in the initial state, Figure 31 considers the influence of the effective heat emitter sizing, i.e. the ratio between the installed emitters capacity and the design SH load in the building's current state (including envelope retrofit and optimizations), across all simulated cases except those without an optimized heating curve. A clear trend emerges: the annual average SH supply temperature, SH SPF and CO_2 emissions are all directly linked to the effective emitters sizing. Lowering the SH temperature, increasing the SH SPF and reducing the CO_2 emissions all require increasing the effective emitters oversizing, so that these indicators move along the curves shown in Figure 31.

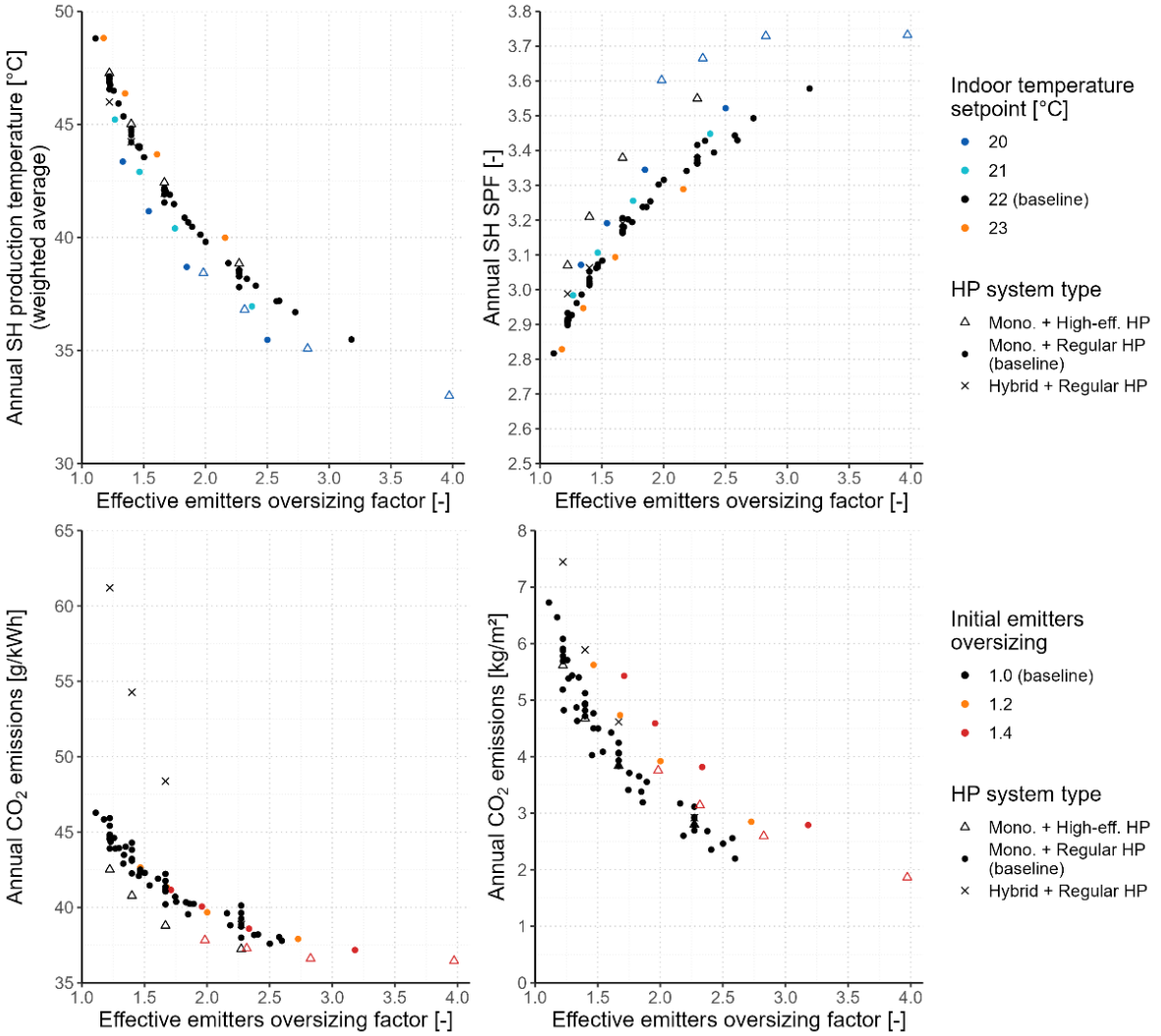


Figure 31: Annual average HP production temperature for SH, HP SPF in SH, and CO_2 emissions in g/kWh and kg/m². All results from the sensitivity are included, except for scenarios without heating curve optimization.

Figure 32 shows the effective emitter oversizing as a function of the SH demand for all cases (again excluding scenarios without heating curve optimization). There is a clear relationship between the SH demand, the initial emitters oversizing and the effective emitters oversizing. The effective oversizing can be increased in two ways: i) by increasing the installed emitters capacity through radiator replacement (i.e. raising the initial oversizing, which corresponds to moving upward on the graph), or ii) by reducing the SH demand (moving along the curve for a given initial sizing). Buildings with the same SH demand and the same initial emitters sizing share the same effective oversizing, and therefore the same temperature levels and performance indicators.

Note: An effective oversizing always exists, even for the non-retrofitted scenarios. As explained in Chapter 4, the heat emitters capacity is set equal to the SH load of the non-retrofitted building for an outdoor air temperature of -10°C (the former design temperature in use when the buildings studied here were built), without solar and internal gains. The peak SH load of each scenario, however, is determined for an outdoor air temperature of -4°C and accounts for internal and solar gains. It is therefore lower than the SH load used for heat emitters sizing. The ratio between the two is consequently always greater than 1.

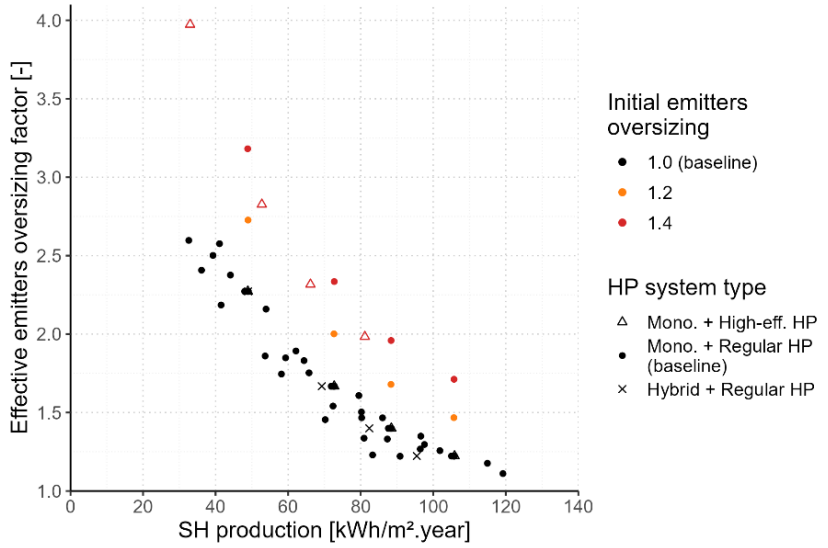


Figure 32: Relationship between effective heat emitters sizing and annual SH demand. All results from the sensitivity are included, except for scenarios without heating curve optimization.

5.4.4. SH optimization measures

Since the effective heat emitters oversizing is one of the main drivers of the SH supply temperature reduction, the SH SPF increase and CO_2 emissions reduction, it is worth examining optimization measures that reduce the SH demand. Among those studied, two affect the space heating demand (in addition to the envelope retrofit): the ventilation flow rate and the indoor temperature setpoint.

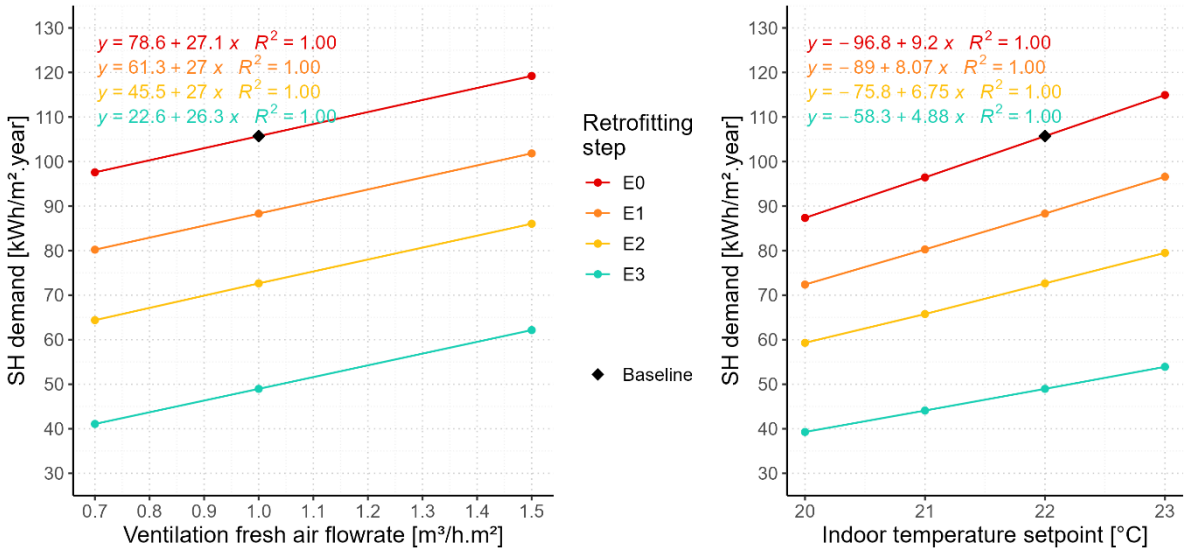


Figure 33: SH demand of the eREN 4 building typology (baseline) at each retrofitting step (Ei) for various ventilation flow rates (left; at the baseline indoor temperature setpoint of 22°C) and indoor temperature setpoints (right; at the baseline ventilation flow rate of 1.0 m³/h.m²). The equations of each curve is given.

Figure 33 shows the annual SH demand of the eREN 4 building (baseline typology) for various ventilation flow rates (at the baseline indoor temperature setpoint of 22°C) and indoor temperature setpoints (at the baseline ventilation flow rate of 1.0 m³/h.m²). Results are as follows:

- **Ventilation flow rate:** Reducing the flow rate by 0.1 m³/h.m² lowers the SH demand by 2.70 kWh/m².year (consistent with the value of 2.43 kWh/m².year from [36]), independently from

the retrofitting status. As a result, the fully retrofitted building (E3) with a high ventilation flow rate of 1.5 m³/h.m² has the same SH demand (90 kWh/m².year) as the partially retrofitted building E2 with the normative flow rate (0.7 m³/h.m²).

- **Indoor temperature setpoint:** Reducing the setpoint by 1 K reduces the SH demand by 5 to 9 kWh/m².year, depending on the retrofitting status. This corresponds to a 10-12% reduction relative to the case with an indoor temperature of 20°C, independently from the retrofitting status (consistent with the value of 10.7% ± 0.9% from [36]). As a result, the partially retrofitted building E2 with a high indoor temperature of 23°C has the same SH demand (80 kWh/m².year) as the partially retrofitted building E1 (one retrofitting step less) with a lower indoor temperature of 21°C.

By placing the building's SH demand and initial emitters sizing on Figure 32, the effective heat emitters sizing can be determined, and hence the temperature levels and performance indicators using Figure 31.

5.4.5. Impact of building typology

The building typology only has only a minor impact on the results presented above. Scenarios with typologies different from the baseline (eREN 4) are included in Figure 31 and Figure 32, and they follow the same trend as all the other cases.

The main influence of the building typology lies in the fact that the SH demand of the non-retrofitted building varies from one typology to another, so the typologies have different installed heat emitters capacities (even at the same oversizing factor). As a result, if buildings of different typologies reach the same SH demand after retrofitting or optimization, they will have different effective heat emitters oversizing, and therefore different temperature levels and performance indicators.

An example is given in Table 13:

- **Two non-retrofitted buildings (E0) have different SH demand** (106 kWh/m².year for eREN 4 and 83 kWh/m².year for TypoRENO I2) **but the same effective heat emitters sizing** (22-23%), in blue in Table 13. This results in a similar annual average HP production temperature (48.8°C), HP SPF (≈ 2.92) and CO_2 emissions relative to the heat production (≈ 44.6 g/kWh). The CO_2 emissions per unit of floor area differ, however (5.9 and 4.8 kg/m²), because their SH demands differ.
- **Two partially retrofitted buildings** (at different retrofitting steps) **have a similar SH demand** (70-73 kWh/m².year) **but different effective emitters oversizing** (67% and 45%), in red in Table 13. This affects both the HP production temperature and SPF: the TypoRENO I2 building, with the lower effective oversizing, has a higher annual average production temperature (47.1°C instead of 45.7°C for eREN 4) and a lower HP SPF (3.03 instead of 3.11), leading to higher CO_2 emissions relative to heat production (42.1 instead of 41.2 g/kWh). However, since their SH demand is the same and their HP SPFs are relatively close, their CO_2 emissions per unit of floor area are similar (4.0-4.1 kg/m²).

Table 13: Example of simulation results for the eREN 4 (baseline) and TypoRENO I2 building typologies at different envelope retrofitting steps (Ei), highlighting the influence of the effective heat emitter sizing.

Building typology	Retrofitting step	SH demand [kWh/m².year]	Effective emitters oversizing	Average HP production temperature [°C]	Annual HP SPF	CO_2 emissions	
						[g/kWh]	[kg/m²]
eRen4	E0	106	22%	48.8	2.91	44.8	5.9
	E2	73	67%	45.7	3.11	41.2	4.1
TypoReno I2	E0	83	23%	48.8	2.92	44.4	4.8
	E1	70	45%	47.1	3.03	42.1	4.0

5.4.6. DHW optimization measures

As shown in section 5.4.2, the high average DHW production temperature (≈ 56°C) drives the overall production temperature upward (44-49°C, depending on the retrofitting status), despite the relatively low SH supply temperatures in some cases (38.5°C for the fully retrofitted building). With retrofitting, the overall average HP production temperature therefore decreases only half as fast as the SH production temperature. The influence of the DHW temperature levels is all the greater because the DHW fraction is higher in the fully retrofitted building (35%, against only 20% in the non-retrofitted building).

Two aspects are analyzed: the sensitivity to the DHW demand (via the daily DHW tapping volume) and the DHW heat exchanger sizing. Figure 34 shows the resulting annual average HP production temperature and annual SPF for DHW production, across all simulated cases (with heating curve optimization).

DHW heat exchanger sizing

As expected, reducing the heat transfer area of the DHW heat exchanger raises the average DHW production temperature: from 55-56°C with the medium baseline heat exchanger to about 59°C with a smaller heat exchanger (i.e. about +3-4 K). Conversely, increasing the heat transfer area from a medium to a large heat exchanger lowers the temperature by about 1 K, down to 54.5°C. As shown in Figure 34 (right), this reduction of 1 K of the DHW production temperature raises the DHW SPF by about 0.05.

The overall HP production (not shown) is only slightly affected, since the DHW fraction is relatively small (20-35%): the higher the DHW fraction, the larger the effect. The change is negligible for the non-retrofitted building and, when fully retrofitted, reaches +1 K for the small heat exchanger and -0.4 K for the large one. For the fully retrofitted building, this translates into an overall SPF change about three times smaller than the DHW SPF change: -0.05 with the small heat exchanger, and +0.02 with the large one.

These results correspond to changing only the heat exchanger size, with no adjustment to the DHW pump flow rate, tank charging strategy, etc. In principle, a larger heat transfer area would allow the DHW pump flow rate to be reduced, increasing the temperature difference on the secondary side, improving tank stratification and thus lowering the average DHW production temperature further.

The effect on CO_2 emissions is negligible, for two reasons: i) the annual DHW production profile is the same regardless of the DHW tapping volume, so seasonal variations in the electricity mix affect the system identically, and ii) about a third of DHW production occurs in summer, when the carbon content of the electricity mix is low, so improving DHW production efficiency has little effect compared to the emissions from SH production. This effect would be more pronounced if the seasonal variation in DHW demand were taken into account, since demand is roughly twice as high in winter (when the electricity mix is more carbon-intensive) as in summer.

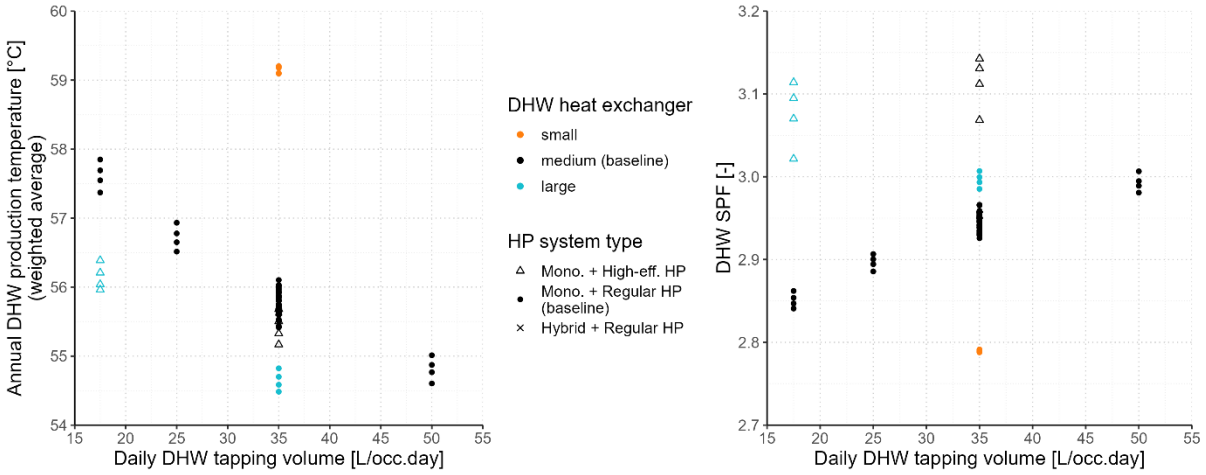


Figure 34: Annual average HP production temperature for DHW (left) and corresponding DHW SPF (right) with respect to the daily DHW tapping volume per occupant. All results from the sensitivity are included, except for scenarios without heating curve optimization.

Daily DHW tapping volume

As shown in Figure 34 (left), reducing the DHW demand (through a lower DHW tapping volume) leads to a slight, roughly linear increase in the average DHW production temperature: from about 55-56°C for 35 L/occ.day (baseline) to up to 57.5°C (+2 K) for 17.5 L/occ.day (Joulia system), and down to about 54.8°C (-1 K) with 50 L/occ.day. The DHW production temperature varies somewhat linearly with the daily DHW tapping volume: reducing the daily DHW tapping volume by 10 L/occ.day increases the DHW supply temperature by about 0.9 K.

This counter-intuitive effect (lower DHW demand raising the DHW production temperature) arises from tank stratification. With higher tapping volumes, more cold water enters the bottom of the tank, reducing the average tank temperature, improving stratification and lowering the average return temperature to the HP. Since the HP operates at a roughly constant condenser temperature difference (about 5 K), the average DHW production temperature decreases accordingly.

The DHW SPF (Figure 34, right) likewise varies almost linearly with the daily DHW tapping volume, between 2.85 and 3.00: increasing the daily DHW tapping volume by 10 L/occ.day raises the DHW SPF by about 0.04.

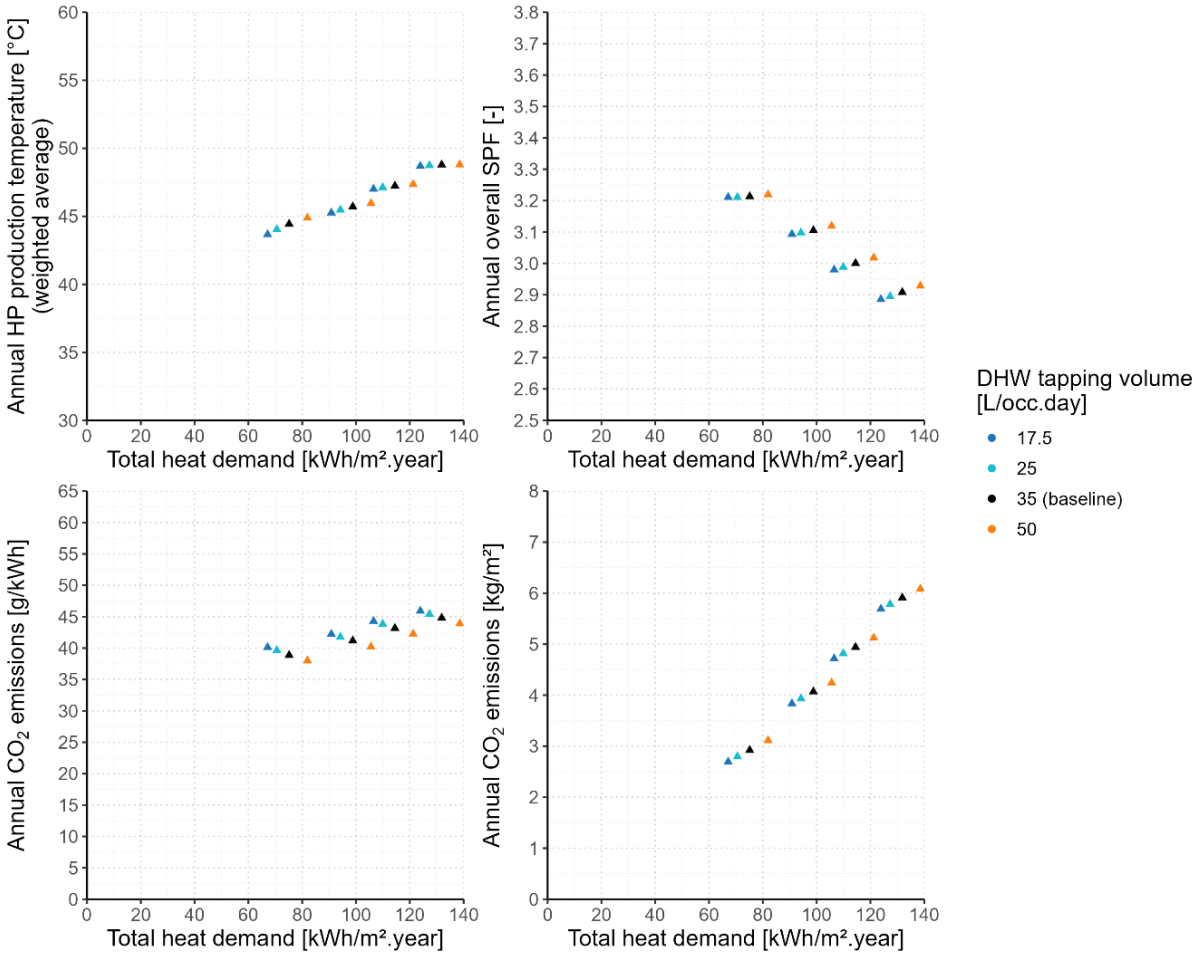


Figure 35: Annual average HP production temperature, HP SPF, and CO_2 emissions in g/kWh and kg/m², for various daily DHW tapping volume per occupant

The overall annual HP production temperature, however, is only slightly affected (Figure 35, top left): there is no impact for the non-retrofitted building, and the effect becomes visible only with retrofitting: -0.8 K for 17.5 L/occ.day and +0.5 K for 50 L/occ.day, relative to the baseline of 35 L/occ.day.

Despite a slight decrease in the DHW production temperature at high DHW tapping, the overall average production temperature increases due to the higher DHW fraction (which remains produced at a higher temperature than the SH). The reduction in DHW temperature is therefore outweighed by the increase in DHW demand.

The impact on the overall SPF (Figure 35, top right) is rather small: at most +0.05 between the minimum (17.5 L/occ.day) and maximum (50 L/occ.day) tapping volume, from 2.88 to 2.93, for the non-retrofitted building. The effect is negligeable for fully retrofitted buildings.

The effect on CO_2 emissions is limited, and goes in the opposite directions for the two indicators (g/kWh and kg/m²). Relative to the heat production (Figure 35, bottom left), it is small, about 5% difference between 17.5 and 50 L/occ.day, since the annual SPFs are very close. Emissions decrease slightly as the draw-off volume increases, owing to the higher SPF and to the larger DHW fraction, which raises the share of heat produced in summer (when the carbon content of the electricity mix is lower). Relative to the floor area (Figure 35, bottom right), emissions decrease as the DHW tapping volume decreases, reaching a 7-14% reduction between 50 and 17.5 L/occ.day, because the annual demand decreases (even when the annual SPF is very similar).

It is important to note that the average production temperature alone is not a sufficient performance indicator: the same average production temperature can correspond to different annual SPFs (depending on the DHW fraction), and conversely, different average production temperatures can yield the same annual SPF. For instance, in the non-retrofitted building, the average production temperature is unchanged across DHW tapping volumes, yet the annual SPF differs because both the DHW fraction and the DHW SPF change.

For a DHN substation, the impact of the DHW measures would, in principle, differ, since the network supply temperature must be high enough to meet the more demanding of the SH and DHW requirements (the DHW temperature in this study). In addition, the substation's return temperature to the DHN is a mix of the SH and DHW temperatures, whereas the HP alternates between SH and DHW production.

5.4.7. Impact of HP system type

Two alternative HP system types are analyzed. Neither affects the temperature levels compared to the baseline (monovalent system with "regular" R410A HP), but both affect the energy and environmental performance indicators (Figure 36).

Monovalent system (same as the baseline system) with a high-efficiency R290 HP

Switching to a high-efficiency HP does not affect the temperature levels, but it increases the HP SPF by about 0.18 on average. The SPF still rises with decreasing SH demand at the same rate as the baseline HP: reducing the SH demand by 10 kWh/m².year increases the overall SPF by about 0.05. In terms of CO_2 emissions, this corresponds to a 4 to 6% reduction compared to the baseline HP, both per unit of heat produced and per unit of floor area.

It is worth noting that some HP units on the market achieve higher COPs than the high-efficiency unit selected for this study (see Appendix 11.6). However, these units seems to be available mainly at lower capacities, typically around 20 kW, whereas the selected HP unit has a capacity in the 40-50 kW range, for which standard commercial products are still not widely available. This is an important consideration for large MFBs, since the simulated HP capacities range from approximately 25 to 75 W/m², therefore reaching up to 450 kW for the non-retrofitted very large-scale typology (8'000 m² of heated floor area). The selected HP unit therefore provides a more representative capacity for the larger and less-retrofitted buildings considered in this study. For buildings with lower SH requirements, in particular fully-retrofitted buildings, smaller HP units could be used, potentially allowing the selection of higher-efficiency models and resulting in higher SPF values.

Hybrid system (with the same HP as the baseline HP)

The HP SPF increases by up to 0.07 in the non-retrofitted scenario, because the HP then produces a smaller share of the heat at low outdoor air temperatures, where its COP is lowest. This gain diminishes as the building is retrofitted, since the HP covers an increasing share of the heat production (it is sized to operate without backup in the fully retrofitted scenario). However, the overall system efficiency (including the boiler) is reduced by up to 0.28 compared to the monovalent baseline system in the non-retrofitted scenario, because the boiler is far less efficient than the HP, even at low outdoor air temperatures.

This significantly increases the CO_2 emissions relative to the heat production, especially in the non-retrofitted scenario: 39-61 g/kWh (fully retrofitted to non-retrofitted) instead of 39-45 g/kWh for the baseline system, an increase of up to 37% (non-retrofitted scenario). Emissions per unit of floor area rise similarly: 2.9-7.4 kg/m² instead of 2.9-5.9 kg/m², an increase of up to 26%. Although the hybrid system therefore emits more than the monovalent systems, its emissions decrease faster with retrofitting (since the HP eventually covers the entire demand) by 4 g/kWh or 0.8 kg/m² per 10 kWh/m²·year saved, respectively 4 and 1.6 times faster than the baseline system (1 g/kWh and 0.5 kg/m²).

Overall, the impact of the boiler remains relatively limited in these scenarios, as it covers only 9% of the total heat demand even in the worst case (non-retrofitted building): the HP, sized to cover the full demand of the fully retrofitted building, still covers 91% of the heat demand of the non-retrofitted building.

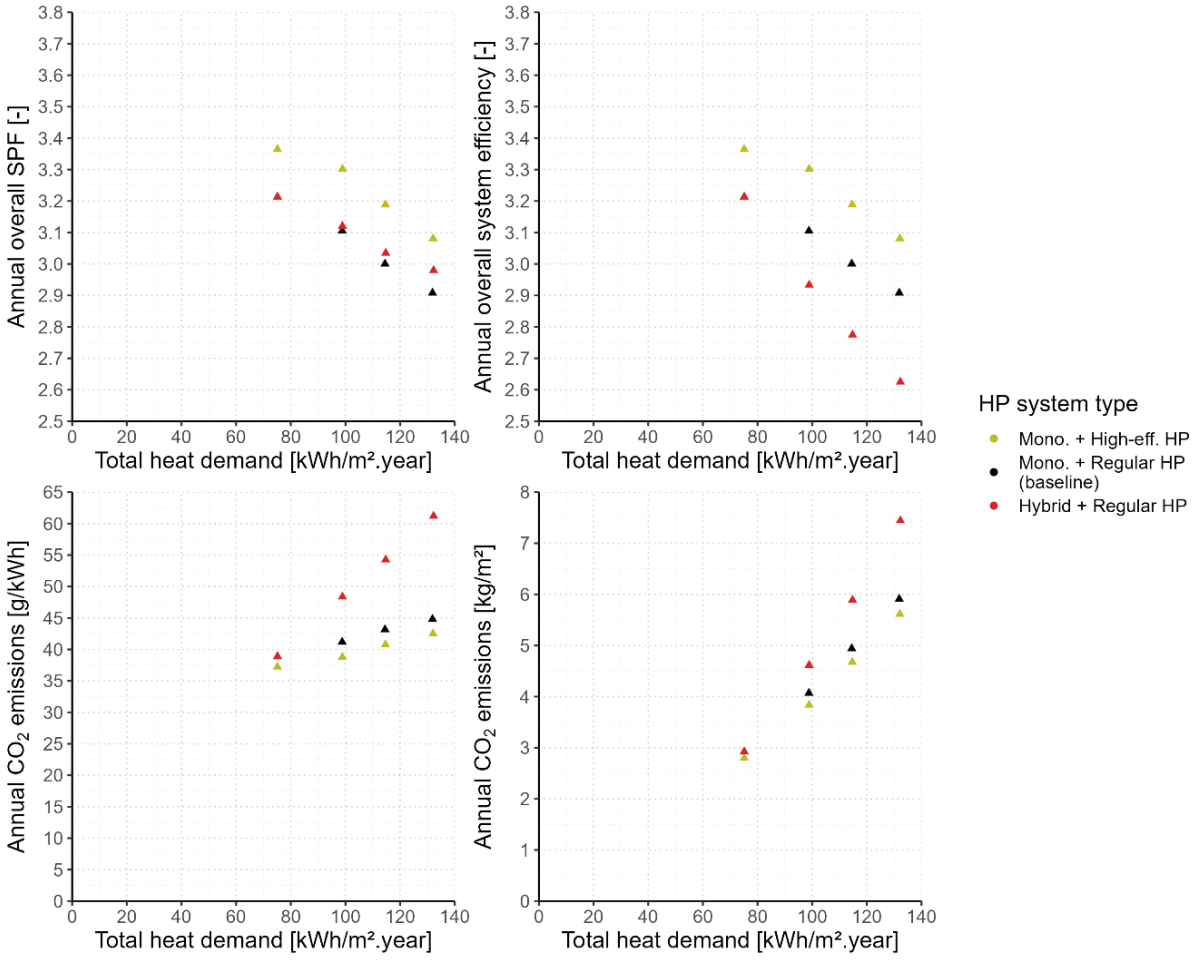


Figure 36: Annual average HP SPF, overall system energy efficiency (boiler + HP), and CO_2 emissions in g/kWh and kg/m², for various types of HP system

5.4.8. Best-case scenario

Figure 37 summarizes the results of all the eREN 4 building scenarios with monovalent HP systems and optimized heating curves, sorted by retrofitting step (from non-retrofitted to fully retrofitted), and compares them with the best-case scenario, in which all optimization measures are applied. For every indicator, the best-case scenario brings a substantial improvement relative to most cases (1st to 9th decile):

- **Average HP production temperature:** 40.5-41.7°C, instead of 43.4-49.8°C
- **Overall HP SPF:** 3.45-3.54, instead of 2.86-3.32
- **CO_2 emissions:**
    - 36.5-37.8 g/kWh, instead of 37.3-45.9 g/kWh
    - 1.9-3.8 kg/m², instead of 2.6-6.4 kg/m²

In the best-case scenario, the indicators depend little on the building's retrofitting status, with one exception: the CO_2 emissions per unit of floor area, which are strongly influenced by retrofitting (as highlighted in section 5.4.2).

The improvement achieved by the best-case scenario is more pronounced for the non-retrofitted building than for the fully retrofitted one. In the latter case, the improvement is relatively small, as some scenarios with only one optimization measure come close to the same performance. This indicates that: i) applying the full set of optimization measures to an already fully retrofitted building is unlikely to be worthwhile, particularly in terms of cost-effectiveness; and ii) with the appropriate optimization measures, a well-optimized building at a given retrofitting step can reach a performance comparable to that of the next step (a non-retrofitted building approaching a partially retrofitted one, and a partially retrofitted building approaching a fully retrofitted one).

This conclusion does not hold, however, for the CO_2 emissions per unit of floor area, which correspond to the emissions in absolute terms (those we ultimately aim to reduce in order to decarbonize the building stock), rather than relative to the amount of heat produced. Building retrofitting therefore remains essential to reduce the CO_2 emissions from heat supply, and optimization alone cannot compensate for it. In Figure 37, for example, the non-retrofitted building cases emit between 4.9 and 6.7 kg/m² (3.8 kg/m² in the best-case scenario), whereas the fully retrofitted building cases emit roughly half as much, between 2.5 and 3.6 kg/m² (1.9 kg/m² in the best-case scenario).

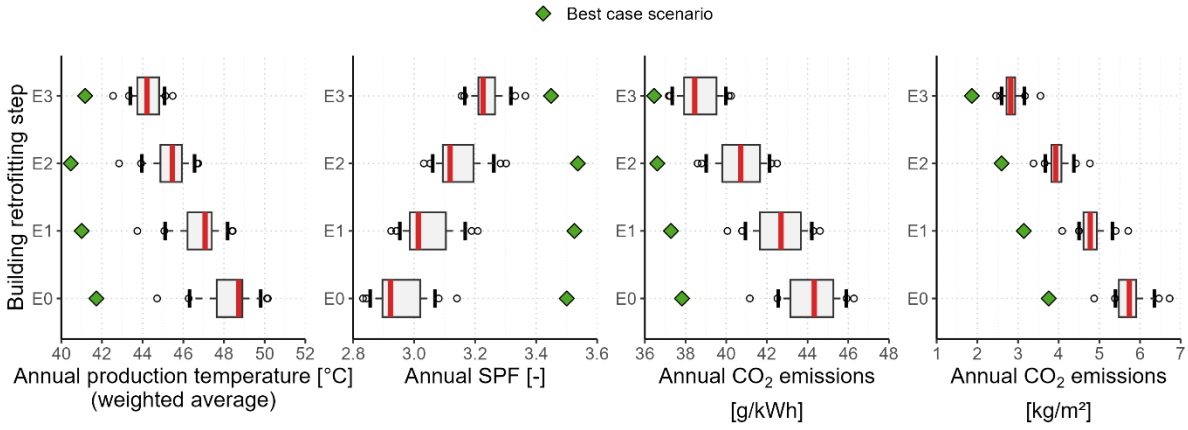


Figure 37: Comparison of the annual average HP production temperature and performance indicators at each building retrofitting step (Ei), between the best-case scenario and all other scenarios. Results are shown for the eREN 4 building typology (baseline) heated by a monovalent HP system. Scenarios with hybrid HP systems or without heating curve optimization are excluded. The whiskers represent the 1st and 9th deciles (10% and 90% of values), and the box the 1st and 3rd quartiles (25% and 75% of values).

The characteristics of the cases closest to the best-case scenario (i.e. the one or two outliers on the best-case side of Figure 37) vary depending on the performance indicator and the level of envelope retrofitting:

- **Average production temperature:** The lowest annual average production temperatures are achieved either with a high initial heat emitter oversizing (+40%) or by reducing the indoor temperature setpoint (20°C). For the fully retrofitted building, however, an initial heat emitter oversizing of +20% performs slightly better than lowering indoor temperature setpoint to 20°C.
- **Overall HP SPF:** The highest annual SPFs are obtained either with a high initial heat emitter oversizing (+40%) or with a high-efficiency HP. For non-retrofitted and partially retrofitted buildings (step E1), the initial oversizing of +40% yields a higher SPF than the high-efficiency HP, whereas it is the opposite for more deeply retrofitted buildings.
- **CO_2 emissions per unit of heat produced (g/kWh):** Consistently, these emissions follow the same trend as the HP SPF, since a higher SPF directly reduces the electricity required to produce one unit of heat. However, regardless of the retrofitting status, an initial emitter oversizing of +40% results in slightly lower emissions than the use of a high-efficiency HP, despite a slightly lower SPF, suggesting that a different seasonal distribution of electricity consumption influencing the resulting emissions.
- **CO_2 emissions per unit of floor area (kg/m²):** The lowest emissions per unit of floor area are obtained for the cases with the lowest SH demand, namely those with reduced indoor temperature setpoints (20-21°C) or an optimized ventilation flow rate (0.7 m³/h.m²). In the non-retrofitted cases, the lower setpoints give lower emissions than the optimized ventilation, but for partially and fully retrofitted buildings, the optimized ventilation outperforms the 21°C setpoint, as it results in a lower SH demand.

5.4.9. Results summary

Table 14 summarizes the results of the sensitivity analysis for the baseline scenarios (without heating curve optimization) and for each sensitivity parameter (with heating curve optimization). It quantifies the impact of each parameter on the energy and environmental performance indicators and highlights the key takeaways.

As a reminder, each optimization measure (or sensitivity parameter) is simulated for the baseline building typology (eREN 4), for each envelope retrofitting step, with and without heating curve optimization, so as to analyze each measure separately. For the sensitivity analysis on the building typology, the same principle is applied: each retrofitting step is simulated with and without heating curve optimization. To highlight the effect of the optimization measures, the table presents the results obtained with heating curve optimization for all sensitivity parameters, while the baseline scenario corresponds to the cases without heating curve optimization.

It is important to note that the results presented throughout this section correspond to optimization measures applied individually, in combination only with envelope retrofitting and heating curve optimization. Their impact may therefore differ when several measures are combined, as interactions between measures can either amplify or reduce their individual effects.

Table 14: Summary of the sensitivity analysis for the baseline scenarios and for each sensitivity parameter

Indicator (→) Parameter (↓)	Heat demand	Annual average supply temperatures	Energy efficiency	CO_2 emissions per kWh	CO_2 emissions per unit area	Key takeaway
Baseline (no optim.)	-	Per -10 kWh/m².year: → Small effect (SH) → Very small effect (overall)	Per -10 kWh/m².year: → Very small effect (SH SPF) → Very small effect (overall SPF)	Per -10 kWh/m².year: → -0.3 g/kWh	Per -10 kWh/m².year: → -0.47 kg/m²	Without heating curve optimization, retrofitting barely lowers temperatures or improves the SPF; only CO_2 per area decreases, driven by the lower demand.
Heating curve optimization	No effect	Per -10 kWh/m².year: → -1.51 K (SH) → -0.77 K (overall)	Per -10 kWh/m².year: → +0.08 (SH SPF) → +0.05 (overall SPF)	Per -10 kWh/m².year: → -1.0 g/kWh	Per -10 kWh/m².year: → -0.53 kg/m² (-3 to -10% on top of retrofit)	Key measure: strongly lowers supply temperatures and raises the SPF. Treated as a prerequisite for all other measures.
Initial heat emitters oversizing	No effect	Per -10 kWh/m².year: (SH / overall) → **0%:** -1.51 / -0.77 K → **+20%:** -1.29 / -0.54 K → **+40%:** -1.13 / -0.38 K See Figure 31	Per -10 kWh/m².year: (SH / overall) → **0%:** +0.082 / +0.054 → **+20%:** +0.074 / +0.043 → **+40%:** +0.066 / +0.034 See Figure 31	Per -10 kWh/m².year: → **0%:** -1.0 g/kWh → **+20%:** -0.8 g/kWh → **+40%:** -0.7 g/kWh See Figure 31	Per -10 kWh/m².year: → **0%:** -0.53 kg/m² → **+20%:** -0.49 kg/m² → **+40%:** -0.46 kg/m² See Figure 31	Larger initial emitters oversizing gives lower temperatures and higher SPF at a given SH demand. What ultimately matters is the effective oversizing (Figure 31), which can be raised either by replacing radiators or by reducing the SH demand.
Ventilation flow rate	Per -0.1 m³/h.m²: → -2.70 kWh/m².year (SH) *i.e. per -0.37 m³/h.m²:* *→ -10 kWh/m².year (SH)*	See Figure 31 and Figure 32	See Figure 31 and Figure 32	See Figure 31 and Figure 32	See Figure 31 and Figure 32	Influences the SH demand and then acts on all indicators through the effective emitters oversizing relationship (Figure 31 and Figure 32).
Indoor temperature setpoint	Per -1 K: → -10 to -12% (SH)	See Figure 31 and Figure 32	See Figure 31 and Figure 32	See Figure 31 and Figure 32	See Figure 31 and Figure 32	Same mechanism as ventilation; a strong SH demand lever (10–12% per K) that can bring a building close to the next retrofitting step.
Building typology	Initial SH demand (at E0) varies from one typology to another	See Figure 31 and Figure 32	See Figure 31 and Figure 32	See Figure 31 and Figure 32	See Figure 31 and Figure 32	No effect of its own; typologies differ only through their initial SH demand, which sets the installed capacity, the effective oversizing and hence the indicators.
DHW heat exchanger sizing	No effect	**Small area:** → +3 to 4 K (DHW) → No to small effect (overall) **Large area:** → -1 K (DHW) → No to very small effect (overall)	**Small area:** → -0.15 / -0.05 (DHW / overall SPF) **Large area:** → +0.05 / +0.02 (DHW / overall SPF) -1 K (DHW) → ≈ +0.05 (DHW SPF)	Almost no effect	Almost no effect	Affects mainly the DHW side and is modest overall: a small transfer area is detrimental, raising the DHW temperature and lowering the SPF, so a generous area is preferable. The overall SPF and CO_2 emissions are barely affected, due to the low DHW fraction and the low carbon content of the summer electricity mix.
DHW tapping volume	Sets the DHW demand (18-33 kWh/m².year) and DHW fraction (15-44%)	Per -10 L/occ.day: → +0.9 K (DHW) → No to small effect (overall)	Per -10 L/occ.day: → -0.04 (DHW SPF) → No to small effect (overall SPF)	Small effect (≈ 5% difference between 17.5 and 50 L/occ. per day)	Small effect (7-14% difference between 17.5 and 50 L/occ. per day)	Counter-intuitively, lower demand raises the DHW temperature (stratification) but reduce the total demand, so CO_2 emissions per unit area decrease while per-kWh emissions rise.
Type of HP system	No effect	No effect	**Monovalent + High-eff. HP:** → +0.18 on average (overall SPF) **Hybrid + Regular HP:** → +0 to +0.07 (overall SPF) → -0 to -0.28 (overall syst. eff.)	**Monovalent + High-eff. HP:** → -4 to -6% **Hybrid + Regular HP:** per -10 kWh/m².year → -4 g/kWh (up to +37% vs baseline)	**Monovalent + High-eff. HP:** → -4 to -6% **Hybrid + Regular HP:** per -10 kWh/m².year → -0.8 kg/m² (up to +26% vs baseline)	The high-efficiency HP improves the SPF and lowers emissions. The hybrid system's gas boiler, though it covers at most 9% of the demand, is enough to raise emissions noticeably when the building is not or only partially retrofitted.

6 Discussion

6.1 Insights from simulation results

Space heating

The results show that the reduction of SH supply temperatures is primarily governed by the building's effective emitter oversizing, defined as the ratio between the installed emitter capacity and the actual space heating load. Regardless of building typology, any measure that reduces the space heating demand increases this effective oversizing and enables lower distribution temperatures. Lower distribution temperatures, in turn, improve heat production efficiency and reduce CO_2 emissions associated with heat generation. Demand reduction therefore acts on both fronts: it improves the production efficiency (and hence the CO_2 emissions per unit of heat produced, in g/kWh) and simultaneously reduces the absolute emissions per unit of heated floor area (kg/m²).

Envelope retrofitting plays an essential role here, because it substantially reduces the space heating demand and therefore increases the effective emitter oversizing. In principle, beyond its impact on energy performance, retrofitting also improves thermal comfort by removing the sensation of cold radiated by poorly insulated surfaces. For a given indoor air temperature, occupants generally perceive a renovated building as more comfortable, making lower temperature setpoints possible (or more acceptable), which further reinforces the space demand reduction achieved by retrofitting.

Results also indicate that significant improvements can be achieved before major envelope retrofits are undertaken. Measures such as ventilation optimization (for example through humidity-controlled ventilation) or the reduction of indoor temperature setpoints can yield benefits comparable to those obtained through an additional step of envelope retrofitting, in terms of SH demand, system efficiency and emissions. Such measures are generally less expensive, easier to implement and can therefore provide an effective short-term strategy while more extensive renovations are being planned.

However, simulations demonstrate that these demand-side measures only reach their full potential when combined with heating curve optimization. When the heating curve is optimized, each reduction of the SH demand by 10 kWh/m².year lowers the average SH supply temperature by 1.5 K and raises the SH SPF by 0.08. As a result, the CO_2 emissions per unit of heat produced decrease about three times faster than with SH demand reduction alone (i.e. without heating curve optimization), and yield an additional reduction of 3-10% in CO_2 emissions per unit of floor area compared with retrofitting alone.

It should be noted that the achievable temperature reduction strongly depends on the pre-existing characteristics and condition of the heat distribution system. The simulations assume a properly balanced hydraulic network, free of faulty components, radiators all equipped with thermostatic valves, etc. A poorly balanced system cannot reach the performance reported here, as the hydraulically disadvantaged zones limit the temperature reduction. Likewise, undersized emitters in specific zones will limit the extent to which supply temperatures can be reduced, even in a well-balanced system. This can be addressed by selectively replacing certain radiators with larger or more efficient units, as proposed in [15,34].

DHW

The results clearly show that DHW production constitutes the main temperature constraint within the SH/DHW system. While SH supply temperatures can be substantially reduced through retrofitting and optimization measures, DHW production still requires significantly higher temperature levels to prevent legionella proliferation. Consequently, the average production temperature of the overall system decreases only about half as fast as the SH production temperature. This limitation becomes increasingly important as buildings are retrofitted, since the DHW share of the total heat demand rises as the SH demand decreases.

The DHW optimization measures investigated in this study have a relatively modest impact on the temperature levels and overall performance indicators. One of the reasons is that, unlike SH, reducing the DHW demand (through a lower DHW tapping volume) does not necessarily improve production efficiency. This counter-intuitive effect arises from tank stratification. With higher DHW tapping volumes, more cold water enters the bottom of the tank, reducing the average tank temperature, improving stratification and lowering the average return temperature to the HP. Since the HP operates at a roughly constant condenser temperature difference (about 5 K), the average DHW production temperature decreases accordingly. Lower DHW tapping volumes have the opposite effect, raising the average DHW production temperature and thus lowering the DHW SPF and increasing the CO_2 emissions per unit of heat produced. Reducing the DHW demand does, however, still lower the absolute CO_2 emissions per unit of floor area. These opposing effects limit the overall impact of DHW demand reduction on the annual performance indicators.

Another factor reducing the influence of DHW optimization is the seasonal distribution of DHW production. Unlike space heating, DHW is produced throughout the year, including summer periods (about one third of the heat produced for DHW) when the carbon intensity of the Swiss electricity mix is relatively low. As a result, improving DHW production efficiency has a smaller effect on annual CO_2 emissions and integration of renewable energy than improving space heating production. This conclusion may, however, be specific to decentralized air-source heat pump systems. For instance, district heating substations operation and constraints differ from those of air-source HPs and my respond differently to DHW optimization measures. Even so, DHW optimization can still lower the average DHW production temperature, and hence the return temperature to the HP, reducing the risk of HP faults and improving system reliability.

Although the DHW optimization measures investigated here provide only moderate benefits, many additional DHW optimization measures exist. These include, but are not limited to, DHW circulation control optimization, improved pipe insulation, optimized storage charging strategies and hydraulic connection points. Most of these measures primarily aim to reduce return temperatures rather than supply temperatures, since the DHW production temperature constraint would remain unchanged in many cases, owing to the risk of legionella proliferation. Further reductions in DHW production temperatures would require alternative concepts such as instantaneous DHW preparation (which removes potable water storage and therefore allows a lower production temperature) or non-thermal anti-legionella treatments [53,83].

Heat pump system type

The comparison between HP system typologies highlights the importance of distinguishing between long-term performance and transition strategies.

Using a high-efficiency R290 HP consistently improves energy and environmental performance without affecting system temperature levels. The observed increase in SPF and corresponding reduction in CO_2 emissions demonstrate the importance of technological progress in HP design, even when operating conditions remain unchanged.

A hybrid system (HP and gas boiler) presents a different perspective. Although the gas boiler covers only a small share of the annual heat demand (9% maximum), it significantly increases CO_2 emissions in non-retrofitted buildings compared with a monovalent HP system (+37% in g/kWh and +26% in kg/m²). This illustrates how even limited boiler operation can strongly affect environmental performance. Nevertheless, the implementation of monovalent HP systems is not always feasible in large existing MFBs because of space constraints, limited electrical grid capacity or high investment cost [84]. In such cases, a hybrid system represents a viable transitional solution, enabling an immediate fuel-switch in buildings where a fully monovalent system is not yet feasible. Even when the HP covers only 50–70% of the total heat demand, hybrid systems still reduce CO_2 emissions by around 60% compared with a gas boiler-only system.

Nevertheless, the results also suggest that hybrid systems may represent an interesting transitional solution. As the building SH demand decreases through retrofitting or operational optimization, the contribution of the boiler rapidly diminishes and the performance gap between hybrid and monovalent

systems narrows. In situations where immediate implementation of a monovalent system is not technically or economically feasible, a properly controlled hybrid system may therefore facilitate earlier deployment of HPs rather than delaying the transition until full envelope retrofits have been completed. This conclusion is consistent with findings from other projects such as AirBival [8,69] and FlexiRenove [28]. However, achieving the expected energy and environmental performance requires appropriate control strategies and hydraulic configuration, as boilers tend to take over in hybrid system and significantly reduce the contribution of the HP [8,69,85].

Combining the measures

Combining all the optimization measures studied (the best-case scenario of Section 5.4.8) brings out two complementary messages. For the temperature levels and the efficiency indicators, optimization and retrofitting are, to some extent, interchangeable: a well-optimized building can match the performance of a building one retrofitting step further. Optimization therefore offers a fast, low-cost way to improve poorly performing buildings without waiting for deep retrofit, which is particularly valuable given the slow pace of envelope renovation. However, as a building becomes more retrofitted, the additional gain from each further optimization measure diminishes, and applying the full set of measures may not prove cost-effective. The measures should thus be prioritized according to the state of the building rather than applied systematically.

For the absolute CO_2 emissions (per unit of floor area), the quantity that ultimately matters for decarbonizing the building stock, optimization and retrofitting are not interchangeable but complementary. Optimization improves the efficiency of heat production but cannot substantially reduce the heat demand, which governs the absolute emissions. Envelope retrofitting therefore remains fundamental: optimization can accelerate decarbonization, complement the retrofit and bridge the period before it is carried out, but it cannot replace it in the long-term.

6.2 Limitations and possible future work

6.2.1. Performance indicators

HP efficiency

The energy performance results are specific to the “regular” R410A HP model selected, for which a manufacturer's performance map was available, and may differ for other HPs, as illustrated by the simulation results obtained with the high-efficiency R290 HP. Some HP units available on the market achieve higher COPs than the high-efficiency HP unit selected for this study. However, these higher-efficiency models seems to be mainly available at smaller capacities, limiting their applicability to the large MFBs considered in this study, in particular before full retrofitting of their building envelope. Smaller buildings with lower SH loads could therefore potentially achieve higher SPF values through the use of higher-efficiency HP models. Conversely, the performance maps we used are obtained under laboratory conditions, which differ from (and tend to be more favorable than) the actual operating conditions in MFBs. The former limitation may therefore lead to an underestimation of the SPF that could be achieved with other available HP models, whereas the latter may lead to an overestimation of the SPF achievable in practice with the selected HPs. Consequently, the SPF values reported here should be interpreted primarily as comparative indicators between scenarios rather than as predictions of actual field performance.

Climate zone

The energy and environmental performance results presented here are dependent on the climate zone. In colder regions, SH would represent a larger share of the total heat demand, likely increasing the benefits of SH-related optimization measures relative to DHW measures. DHW optimization measures would therefore have less impact, except during summer, when systems in both cold and mild regions only operate for DHW production.

Electricity mix

Furthermore, the environmental performance results (CO_2 emissions and renewable share) depend on the electricity mix. The results presented here are representative of the Swiss context and of buildings exclusively supplied by electricity from the grid. A different electricity mix, local photovoltaic production or battery storage could substantially modify the environmental performance of the systems investigated.

Economic performance

In addition, the present analysis focuses on energy and environmental performance indicators. However, the practical relevance of the different measures also depends on their economic performance. While some of the measures presented have a smaller impact on the energy and environmental indicators than others, they may also require a much smaller investment, making them far more cost-effective and therefore more likely to be implemented on the short term. An economic analysis (including investment costs, operating costs, etc.) was initially planned for both envelope retrofitting and SH/DHW system measures. Such was done for building retrofitting measures, while the economic analysis of SH/DHW optimization measures will be investigated in future work within the partnership with Geneva's local utility (SIG). Combining energy, environmental and economic performance indicators will make it possible to identify not only the most effective measures, but also the most cost-effective pathways towards building decarbonization.

6.2.2. Space heating

SH distribution system / Hydraulic balancing

One of the key limitations of the modeling approach concerns the simplified SH distribution system: the building is represented as a single thermal zone supplied by an equivalent heat emitter. This simplification does not capture the variability found in actual MFBs, where different apartments and zones often exhibit different heat losses, emitter capacities and occupant behaviors. If the distribution system is not properly balanced, higher heating curves are needed to maintain the indoor temperature setpoint in some zones, while causing overheating in others (which in turn may lead occupants to open windows to regulate the indoor temperature), thereby increasing space heating consumption and lowering the heat production efficiency. The simulations therefore represent an idealized case with a perfectly balanced distribution network and homogeneous emitter performance.

Heat emitter flow rate

Furthermore, as discussed in section 5.3.2, a minimum flow rate is always maintained through the emitters, even when the indoor temperature setpoint has been reached. In practice, thermostatic valves may close when no heat is required, and a bypass may allow circulation within the SH loop without flow through the emitters. As a result, little or no heat is transferred from the SH loop to the building under such conditions. Consequently, the model tends to produce lower flow rates, larger supply/return temperature differences, and lower return temperatures than those observed in practice. This is not expected to significantly affect performance indicators of the HP system, for two reasons: i) the SH buffer tank and mixing valve decouple the SH distribution loop from the HP loop, ii) HP performance is primarily influenced by the supply temperature rather than the return temperature. The impact would, however, be more significant for DH substations, where return temperature is a key factor for DH performance and renewable energy integration.

Beyond the importance of heat emitters sizing discussed in section 5.4.3, another factor strongly influencing the minimum SH distribution temperature is the maximum allowable flow rate through the emitters. The higher the maximum flow rate, the lower the required supply temperature. The heating curves considered in this project therefore depend on the assumptions made in this respect (see the method in Appendix 11.3).

6.2.3. Domestic hot water

DHW demand

The DHW model also relies on simplified assumptions. Daily demand is assumed to be constant throughout the year, whereas actual DHW consumption exhibits significant seasonal variation due to occupancy patterns and variations in cold-water temperature, leading to a daily demand in winter about twice that in summer [38] (Appendix 3). As the results show, DHW optimization measures have a limited impact on the annual indicators, partly because about a third of the DHW is produced in summer, when the carbon content of the electricity mix is relatively low. In addition, the DHW demands simulated here are rather low (18.1-33.3 kWh/m².year) compared with measured MFBs in Geneva (21.7-56.8 kWh/m².year, average 35.7 kWh/m².year) [82]. Accounting for a higher DHW demand and for its seasonal variation (which would shift a larger share of the DHW production to winter) would give greater weight to DHW production in the annual balance, so that optimizing it would have a greater impact on the overall performance indicators (while, conversely, SH optimization measures would have a smaller one).

Finally, possible variations in occupant density between building typologies were not considered. Since occupant density directly influences DHW demand, accounting for this factor could have an impact on the performance indicators and outcomes regarding the influence of the building typology.

DHW optimization measures

The results identify DHW production as one of the main barriers to further reducing system temperature levels. Additional research should therefore focus on measures specifically targeting DHW generation. Such measures could include improved DHW pipes insulation, optimized DHW tank charging, instantaneous or semi-instantaneous DHW production, as presented in section 4.2. Some of these measures are, however, difficult or highly time-consuming to implement in TRNSYS, or require detailed Computational Fluid Dynamics (CFD) (for example improving DHW tank connections and hydraulic layout, as done in [60]).

Moreover, while some DHW optimization measures can be found in the literature and have been examined using dynamic energy models similar to those developed in this project, it lacks feedback from real operating systems to assess the actual benefits and drawbacks of their implementation. This is especially critical for DHW optimization measures, as they can affect not only comfort but can also have potential health implications through the risk of legionella proliferation. Such concerns tends to discourage stakeholders from trying innovative DHW systems. Monitoring campaigns and demonstration projects would therefore provide valuable insights into the real-world benefits and challenges associated with these measures, as well as encourage their implementation.

6.2.4. Building envelope

Initial state of the building envelope

The selected building typologies are derived from actual buildings, some of which may have already undergone retrofitting measures, unlike other buildings of the same typology. The initial state of the building (referred to as the non-retrofitted building throughout this report) may therefore differ from one building to another within the same typology, which in turn affects the impact and cost of the retrofitting measures.

Retrofit performance gap

In addition, this study assumes that the excepted energy savings from retrofitting are fully achieved. In practice, a significant energy performance gap is frequently observed between predicted and measured post-retrofit space heating consumption [36,86]. Various methods exist to reduce this gap, which have not been considered as retrofitting/optimization measures in this project but play an important role to

meet the expect SH demand after retrofitting. Among them, two specificities of the Canton of Geneva (SIG éco21) have shown good results in narrowing the performance gap [87]:

- « Assistant au Maître d'Ouvrage en Énergie » (AMOén) : A technical advisor on the building's energy performance, who helps developing the retrofitting strategy and monitors results before and after retrofitting, across all project phases (SIA 1 to 6).
- « Assistant au Maître d'Usage » (AMU): an external, neutral facilitator who handles social mediation between stakeholders (tenants, owners, contractors) to prevent conflicts during the renovation.

6.2.5. SH/DHW system

Initial state of the SH/DHW system

As stated in section 4.1, the reference building and SH/DHW system represents a properly functioning installation. It excludes faulty components, malfunctions and hydraulic configurations inherited from fossil-fuel boilers that would prevent integration of HPs. The reference system is assumed to have already received the minimum adaptations required to connect a HP (where necessary), and to follow current best practices in terms of control.

Data from the boiler room energy optimization contracts (Contrats d'Optimisation Énergétique, COE) implemented within the éco21 programme indicate that significant reductions in heat demand can be achieved through system optimization alone. The earliest COE projects, initiated in 2019, report reductions of around 20% in useful heat demand after three years, while more recent projects achieve similar savings over shorter periods [88]. These improvements are likely to include the correction of system deficiencies that are not represented in the present study.

A more detailed analysis of the COE database would allow to: i) position the reference system adopted in this project relative to the actual condition of buildings before and after COE optimization, and ii) identify the optimization measures implemented in practice, quantify their individual contribution, and compare their observed impact with the modeling results presented here. Such analysis is currently being carried out by the University of Geneva as part of the QueCalor project.

District heating substations

Future work should extend the analysis to other SH/DHW system typologies, and in particular to district heating substations. Unlike HPs, SSTs simultaneously provide SH and DHW and are subject to different supply and return temperature constraints. For instance, they can typically operate with larger temperature differences between supply and return temperatures. Lowering DHN supply and return temperatures has been identified as a key measure for decarbonizing the heat supply [17] and reducing DHN operating costs [18,19]. As DHNs are rapidly expanding in Switzerland and worldwide as a driver of the energy transition, understanding how building retrofitting and system optimization influence DHN temperatures becomes increasingly important. In particular, further work is needed to determine the most effective combinations of targeted envelope retrofitting and system optimization measures for reducing the temperature levels of existing buildings connected, or soon to be connected, to a DHN. Such analyses could also help identify the most suitable SST typologies for buildings that are not yet connected to a district heating network but may be connected in the future.

6.2.6. Sequencing of envelope retrofitting, system optimization and heat production replacement

Finally, the timing and sequencing of envelope retrofitting, system optimization and heat production replacement were not addressed in this project. Yet this issue is currently a major concern for the stakeholders involved, as it affects planning, system sizing, costs and the pace of decarbonization. In Switzerland, annual retrofit rates of the building stock currently remain quite low and ineffective (e.g. in the Canton of Geneva, an overall 1.7% per year, of which only 0.8% achieves an effective gain of at least one energy class [86]), while replacing a fossil-fuel boiler with a HP system in large multifamily buildings

often requires extensive planning, technical studies and administrative procedures. As a result, situations arise where an existing boiler reaches the end of its service life before the building has undergone significant envelope retrofitting. In such cases, installing a heat pump system may be technically feasible but difficult to implement within the timeframe imposed by the boiler replacement. This creates a challenging situation: in jurisdictions such as the Canton of Geneva where replacing a fossil-fuel boiler with another one is no longer permitted, a HP system may need to be installed under time pressure. In other jurisdictions, the boiler may instead be replaced by another fossil-fuel boiler, thereby postponing the transition to a renewable-based heat production by about twenty years. Coordinating building retrofitting and heating system replacement is therefore essential to avoid delays in the transition to renewable-based heating. This issue is investigated in the RENOWAVE project (SP 2.1, Task 4) [28].

7 Conclusions and outlook

The T-DROP project investigates how existing multifamily buildings (MFBs) can transition from high- to low-temperature heat distribution through combinations of targeted envelope retrofitting and technical optimization of heat distribution systems, and quantify the resulting benefits for renewable heat integration and decarbonization. To this end, building and space heating (SH) and domestic hot water (DHW) system models were developed, validated against case studies and combined into an integrated TRNSYS model, which was used to carry out a sensitivity analysis across building typologies, retrofitting depths and SH/DHW optimization measures.

The first objective was to establish how the SH/DHW distribution and production temperatures can be lowered. On the SH side, the achievable reduction in SH supply temperature is governed by the effective emitter oversizing, i.e. the ratio between the installed emitter capacity and the actual SH load. Any measure that reduces the SH demand (envelope retrofitting, but also lower indoor temperature setpoints or optimized ventilation fresh air flow rate) increases this ratio and enables lower temperatures, provided it is combined with heating curve optimization and the distribution system is properly balanced (a poorly balanced network or undersized emitters would otherwise limit the reduction). Without heating curve optimization, SH demand reduction alone barely lowers the production temperature. An analysis of several case studies further showed that emitters in existing MFBs are generally oversized (and even more so after retrofitting), leaving substantial room for SH temperature reduction. On the DHW side, however, the high production temperature required to limit the legionella risk remains the main constraint, pulling the overall production temperature upward and limiting the benefit of envelope retrofitting and SH optimization measures, increasingly so as retrofitting raises the DHW share of the total heat demand. The DHW optimization measures examined here bring only modest gains, and some of the other promising measures can be difficult and time-consuming to simulate, sometimes requiring detailed Computational Fluid Dynamics (CFD) modeling to be accurate. Most have already been studied in the literature, but with little feedback from real installations in MFBs, which, combined with the sensitivity of DHW to the legionella risk, leaves professionals reluctant to implement them.

The second objective was to quantify the benefits of these measures in terms of energy and environmental performance. These benefits are summarized in Table 14, which reports the effect of each selected optimization measure on the performance indicators. The temperature reduction translates directly into performance improvements: lower SH temperatures raise the heat pump SPF and reduce the CO_2 emissions per unit of heat produced, while the underlying demand reduction simultaneously lowers the absolute emissions per unit of floor area. A key conclusion is that, with respect to distribution/production temperatures and heat pump efficiency, optimization measures can partly compensate for the absence of deeper envelope retrofitting (a well-optimized building can match a building one retrofitting step further) so optimization offers a fast, low-cost way to improve poorly performing buildings while waiting for deeper envelope retrofit. For the absolute emissions that ultimately drive decarbonization, however, envelope retrofit and system optimization are complementary: optimization cannot substantially reduce the heat demand, so envelope retrofitting remains fundamental and optimization can accelerate and complement the effect of envelope retrofitting but cannot replace it. The choice of heat production unit is also important: a high-efficiency heat pump improves performance at unchanged temperatures, while a hybrid system, despite its boiler covering only a small share of the demand, can noticeably increase emissions in poorly retrofitted buildings. Hybrid heat pump systems yet remain an attractive transitional solution to accelerate decarbonization of MFBs, allowing heat pumps to be deployed early rather than after full retrofit, provided the control and hydraulics prevent the boiler from taking over.

Overall, the project shows that lowering distribution temperatures is best pursued not as an isolated objective but as a co-benefit of reducing the heat demand. The most effective decarbonization pathways combine targeted envelope retrofitting, heat distribution optimization and a well-chosen heat production system. The selection and implementation of these measures should be prioritized on a case-by-case basis according to the pre-existing characteristics and current state of each building, rather than applied uniformly across the building stock.

Several aspects deserve further investigation. DHW is confirmed as the main barrier to further temperature reduction, yet promising optimization measures (such as instantaneous DHW production, optimized storage charging strategies and improved hydraulic connections,…) are scarcely documented under real operating conditions for large MFBs. Pilot and demonstration projects are therefore needed to assess their feasibility, identify their benefits and limitations, and to build the confidence required for professionals to adopt them. The analysis should also be extended to district heating substations, whose constraints and operation differ from those of decentralized heat pumps. Reducing their supply and return temperature levels is essential to the coordinated expansion and decarbonization of district heating networks. Complementing the energy and environmental performance indicators with an economic analysis (already initiated for envelope retrofitting and to be extended to SH/DHW system measures) would make it possible to identify not only the most effective but also the most cost-effective decarbonization pathways. Finally, further work is needed on the coordination of envelope retrofitting, system optimization and heat production replacement. Such work would help define transition pathways that maximize the benefits of these measures while facilitating their implementation in practice.

8 National and international cooperation

The T-DROP project bears a strong link with current nation-wide projects in which both UNIGE and HEIG-VD are actively participating, namely:

- Renowave (Innosuisse Flagship project), in particular SP2.1 (FlexiRenove), which focuses on design and technical improvement of fuel-switch, i.e. from fossil to renewable energy via individual heat pumps in existing multifamily buildings.
- DeCarbCH (SFOE SWEET project), in particular WP7.1, which focuses on strategies and potentials of temperature reduction on existing district heating networks.

The T-DROP project results will directly contribute to the objectives of both projects.

In addition, HEIG-VD is also involved in the TypoRENO project [21], which aims at developing roadmaps for energy renovation of buildings with a patrimonial value. It is limited to the Canton of Vaud's building stock but encompasses a diverse range of multifamily typologies. The outputs of this project are used in T-DROP to establish building typologies and define realistic envelope retrofitting measures. Conversely, results from T-DROP will be complementary to this project as it will combine targeted envelope retrofitting measures to SH/DHW system retrofit, optimization and/or replacement measures.

At the international level, project members are also in contact with two research institutes whose projects address related questions:

- Fraunhofer IEE, regarding its "CoolDown" project [89], which focuses on the optimization of district heating supply in existing buildings and efficient integration of renewable heat sources into the DHN through secondary measures.
- Austrian Institute of Technology (AIT), regarding its "DeRiskDH" project [90], which aims to address the challenges associated with the integration of renewable-based heat sources. Challenges are in the optimization of the building stock with regard to return temperatures and flexibilities, in network hydraulics, bidirectional operation, the integration of seasonal storage and in the inclusion of consumers and business models.

Furthermore, the advisory board of the T-DROP project includes stakeholders active in the field, with diverse areas of expertise. It ensures the proposed measures are in line with actual challenges and compatible with technical, financial, and legal constraints. It is composed by the following partners:

- Loïc Quiquerez, Carolina Fraga, Gautier Falize, Hadia Khimda-Ouendi (SIG)
- Cédric Blondel (SIL)
- Jean-François Mino (MBG)
- François Baud (François Baud & Thomas Früh Atelier d'architecture SA)
- Anne-Valérie Narath, Charles Thoumyre (DGE-DIREN)
- Fabien Poumadère (Service des énergies de la ville d'Yverdon-les-Bains)
- Nadège Vetterli, Martin Ménard (SFOE)

All these partners are actively involved in the energy transition, namely with the DHN deployment and optimization for valorization of centralized renewable energy sources, setting up of fuel-switch program (from fossil fuel boilers to heat pumps) as well as building retrofit, in particular for multifamily buildings.

9 Publications and other communications

The work conducted by the partners as part of this project has resulted in the following publications and communications:

- Pitch presentation of the project during the 23rd Brenet Status-Seminar on August 27, 2024
- Olivier Paltenghi's Bachelor thesis on the case study of two MFB in Lausanne in collaboration with Services Industriels de Lausanne (SIL). The objective of this thesis was to study the impact of various optimization measures for space heating distribution and envelope renovation on the performance of an ASHP system (including bivalent solution with gas boiler).
- Romain Guinouet's internship report on the building typologies and retrofitting measures, as well as heat emitters sizing and hydraulic balancing method in existing MFBs.
- Participation to workshops with Geneva's local utility (SIG) on the challenges associated with DHW production for buildings equipped with HPs or connected to a DH. The aim to share experience and find solutions to optimize DHW systems, reduce their temperature levels, and increase integration of renewable heat production.

A conference or journal article is also planned, in order to share the project's results in a more concise form and for an international audience.

10 References

[1] OFEN (Office fédéral de l'énergie), Energy Research Masterplan 2021-2024, Berne, 2020.

[2] A. Kemmler, T. Spillmann, A. Piégsa, B. Notter, B. Cox, M. Jakob, G. Catenazzi, Analyse des schweizerischen Energieverbrauchs 2000 - 2019 nach Verwendungszwecken, Bundesamt für Energie, Bern, 2020. https://pubdb.bfe.admin.ch/de/publication/download/10260 (accessed April 4, 2022).

[3] OFEN (Office fédéral de l'énergie), Parc immobilier 2050 – Vision de l'OFEN, 2022.

[4] S. Schneider, J. Khoury, B.M. Lachal, P. Hollmuller, Geo-dependent heat demand model of the Swiss building stock: method, results and example of application, SCCER Future Energy Efficient Buildings & Districts, Genève, 2018. https://archive-ouverte.unige.ch/unige:103112.

[5] J. Khoury, Rénovation énergétique des bâtiments résidentiels collectifs: état des lieux, retours d'expérience et potentiels du parc genevois, Thèse de doctorat, Université de Genève, 2014. https://doi.org/10.13097/archive-ouverte/unige:48085.

[6] C. De Sousa Fraga, Heat pump systems for multifamily buildings: which resource for what demand?, Thèse de doctorat, Université de Genève, 2017. https://doi.org/10.13097/archive-ouverte/unige:94939.

[7] E. Romano, C. De Sousa Fraga, P. Hollmuller, CO2 emission savings of heat-pumps in the residential sector. Case study for multifamily buildings in Geneva, in: Proc. 13th IEA Heat Pump Conf. 2020, Jeju, Korea, 2020. https://archive-ouverte.unige.ch/unige:136512 (accessed June 27, 2022).

[8] O. Montero, P. Brischoux, S. Callegari, C. Fraga, M. Rüetschi, E. Vionnet, N. Calame, F. Rognon, M. Patel, P. Hollmuller, Large Air-to-Water Heat Pumps for Fuel-Boiler Substitution in Non-Retrofitted Multi-Family Buildings—Energy Performance, CO2 Savings, and Lessons Learned in Actual Conditions of Use, Energies 15 (2022) 5033. https://doi.org/10.3390/en15145033.

[9] S.A. Callegari, R. Pieroni, F. De Oliveira Filho, P.J. Naef, P. Hollmuller, La Fontenette – « Les Auréa » : Analyse technique et sociale d'un complexe d'immeubles HBM de haut standard énergétique, équipé d'une PAC centralisée sur eaux usées, (2021). https://archive-ouverte.unige.ch/unige:149374.

[10] J. Faessler, P. Hollmuller, F. Mermoud, L. Quiquerez, Réseaux thermiques multi-ressources efficients et renouvelables : Retour d'expérience sur la rénovation de la chaufferie de quartier de Laurana-Parc à Thônex (GE), Services Industriels de Genève (SIG), 2016. https://archive-ouverte.unige.ch/unige:93169.

[11] A. Heinz, R. Rieberer, Energetic and economic analysis of a PV-assisted air-to-water heat pump system for renovated residential buildings with high-temperature heat emission system, Appl. Energy 293 (2021) 116953. https://doi.org/10.1016/j.apenergy.2021.116953.

[12] M. Coenen, Accelerating the Dutch energy transition: Lowering operating temperatures of heat distribution systems in the built environment, Thesis (Design Project), University of Groningen, 2019. https://fse.studenttheses.ub.rug.nl/20606/ (accessed May 17, 2022).

[13] Services Industriels de Genève, Solutions éco21 : optimisation des installations, (2022). https://ww2.sig-ge.ch/immobilier/optimisation-energetique-et-environnementale/eco21-immobilier/optimisation-installations (accessed June 27, 2022).

[14] A. Primas, Y. Stettler, B. Sonderegger, Wärmepumpen für die Instandsetzung, Systemevaluation für die Instandsetzung, Fachstelle Energie- und Gebaüdetechnik, Amt für Hochbauten Stadt Zürich., 2014. https://www.stadt-zuerich.ch/hbd/de/index/hochbau/bauen-fuer-2000-watt/grundlagen-studienergebnisse/archiv-studien/2014/2014-08-egt-wp-bei-instandsetzungen.html.

[15] M. Lämmle, C. Bongs, J. Wapler, D. Günther, S. Hess, M. Kropp, S. Herkel, Performance of air and ground source heat pumps retrofitted to radiator heating systems and measures to reduce space heating temperatures in existing buildings, Energy 242 (2022) 122952. https://doi.org/10.1016/j.energy.2021.122952.

[16] S. Frederiksen, S. Werner, District heating and cooling, Studentlitteratur AB, Lund, 2013.

[17] N. Bertelsen, B.V. Mathiesen, S.R. Djørup, N.C.A. Schneider, S. Paardekooper, L. Sánchez García, J.Z. Thellufsen, J. Kapetanakis, L. Angelino, J. Kiruja, Integrating low-temperature renewables in district energy systems: Guidelines for policy makers, International Renewable Energy Agency, Abu Dhabi, Copenhagen, 2021.

[18] T. Nussbaumer, S. Thalmann, Influence of system design on heat distribution costs in district heating, Energy 101 (2016) 496–505. https://doi.org/10.1016/j.energy.2016.02.062.

[19] H. Averfalk, S. Werner, Novel low temperature heat distribution technology, Energy 145 (2018) 526–539. https://doi.org/10.1016/j.energy.2017.12.157.

[20] S. Schwab, J.-L. Rime, G. Jaquerod, L. Rinquet, G. Rey, R. Camponovo, P. Gallinelli, S. Citherlet, D. Favre, B. Périsset, G.-A. Morand, S. Dervey, Rénovation énergétique - Approche globale pour l'enveloppe du bâtiment, Institut d'architecture TRANSFORM et Institut du Paysage, d'Architecture, de la Construction et du Territoire, inPACT, Fribourg, 2017. https://www.smartlivinglab.ch/fr/projects/eren-energie-et-renovation/ (accessed October 6, 2022).

[21] HES-SO, HEIA-FR, TRANSFORM, HEIG-VD, IGT, Les fiches TypoRENO-VD, État Vaud (2023). https://www.vd.ch/themes/territoire-et-construction/monuments-et-sites/assurer-la-conservation-des-monuments-lors-de-travaux/conseils-et-principes-dintervention-sur-un-batiment/les-fiches-typoreno-vd (accessed December 15, 2023).

[22] HEPIA, Fiches typologiques des bâtiments - propositions de solutions pour une rénovation énergétique, ge.ch (2019). https://www.ge.ch/node/26003 (accessed October 6, 2022).

[23] RENOWAVE - Massive Decarbonization of the Swiss building stock, 2021.

[24] L. Rinquet, A. Geiger, S. Delmenico, L. Cardinale, Solution Rénovation (2018 - 2022), Solut. Rénovation HEPIA (n.d.). https://www.hesge.ch/hepia/recherche-developpement/projets-recherche/solution-renovation (accessed December 6, 2024).

[25] A. Leconte, Identification de caractéristiques réduites pour l'évaluation des performances des systèmes solaires combinés, Thèse de doctorat, Université de Grenoble, 2011. https://theses.hal.science/tel-00661209.

[26] ISO 13790:2008 : Energy Performance of Buildings - Calculation of Energy Use for Space Heating and Cooling, (2008). https://www.iso.org/standard/41974.html.

[27] S.A. Klein et al., TRNSYS 18: A Transient System Simulation Program, (2017). http://sel.me.wisc.edu/trnsys.

[28] P. El Hage, F. De Oliveira, P. Hollmuller, Renowave SP 2.1 Task 4: FlexiRenove - Stratégie flexible combinant rénovation thermique et le remplacement des chaudières fossiles, Université de Genève, Genève, 2025.

[29] SIA, Norme 380/1:2009 - L'énergie thermique dans le bâtiment, (2009).

[30] SIA, Norme 380/1:2016 - Besoins de chaleur pour le chauffage, (2016).

[31] Office fédéral de la statistique (OFS), Indice suisse des prix de la construction - Evolution des prix de la construction (multibases) Valeurs de l'indice par grande région et par type d'objet, Indice Suisse Prix Constr. - Evol. Prix Constr. Multibases Valeur Indice Par Gd. Région Par Type Obj. (2024). www.bfs.admin.ch/bfs/fr/home/statistiken/preise/baupreise.assetdetail.31967488.html.

[32] G. Giebeler, F. Musso, R. Fisch, K.-H. Petzinka, H. Krause, A. Rudolphi, Rénover le bâti - Maintenance, reconversion, extension, Presses polytechniques et universitaires romandes, 2012.

https://www.epflpress.org/produit/552/9782880749309/renover-le-bati (accessed December 9, 2024).

[33] S. Lasvaux, M. Giorgi, J. Lesage, G. Wagner, D. Favre, P. Padey, B. Périsset, K. Goulouti, M. Farsi, B. Volland, A. Galimshina, A. Hollberg, G. Habert, DUREE Project: Analysis of lifetimes of building elements in the literature and in renovation practices and sensitivity analyses on building LCA & LCC, Communauté de Recherche HEIG-VD & AIT-CETT, Université de Neuchâtel (UniNE), ETH Zürich, Yverdon-les-Bains, 2019. https://www.aramis.admin.ch/Texte/?ProjectID=38626 (accessed March 12, 2025).

[34] M. Roost, T. Schwery, F. Guyer, M. Mühlebach-Burkart, A. Witzig, J. Bruderer, F. Schranz, EffiWag: Effizienzpotenzial eines Ersatzes des Wärmeabgabesystems, Lemon Consult AG, ICP ZHAW, Zürich, Switzerland, 2025. https://www.aramis.admin.ch/Default?DocumentID=73608&Load=true (accessed October 20, 2025).

[35] F. Mermoud, J. Khoury, B.M. Lachal, Suivi énergétique du bâtiment 40-42 de l'avenue du Gros-Chêne à Onex (GE), rénové selon le standard MINERGIE® Aspects techniques et économiques, (2012). https://archive-ouverte.unige.ch/unige:23005.

[36] J. Khoury, Z. Alameddine, P. Hollmuller, Understanding and bridging the energy performance gap in building retrofit, CISBAT 2017 Int. Conf. Build. Dist. – Energy Effic. Nano Urban Scale 122 (2017) 217. https://doi.org/10.1016/j.egypro.2017.07.348.

[37] D. Majcen, Predicting energy consumption and savings in the housing stock: A performance gap analysis in the Netherlands, ABE Archit. Built Environ. (2016) 1–224. https://doi.org/10.7480/abe.2016.4.1154.

[38] S.A. Callegari, R. Novoa-Herzog, S. Schneider, P. Brischoux, A. Duret, X. Jobard, P. Hollmuller, Strategies and potentials of temperature reduction on existing district heating substations: two case studies, Université de Genève, 2023. https://archive-ouverte.unige.ch/unige:172333.

[39] S. Schneider, P. Brischoux, P. Hollmuller, Retour d'expérience énergétique sur le quartier des Vergers à Meyrin (Genève), Université de Genève, Genève, 2022. https://archive-ouverte.unige.ch/unige:164877.

[40] T. Cholewa, A. Siuta-Olcha, A.A. Argiriou, C.A. Balaras, Actual energy savings from the use of thermostatic radiator valves in residential buildings – Long term field evaluation, Energy Build. 151 (2017) 487–493. https://doi.org/10.1016/j.enbuild.2017.06.070.

[41] T. Benakopoulos, R. Salenbien, D. Vanhoudt, Dirk Vanhoudt, S. Svendsen, Improved Control of Radiator Heating Systems with Thermostatic Radiator Valves without Pre-Setting Function, Energies 12 (2019) 3215. https://doi.org/10.3390/en12173215.

[42] J.P. Fine, M.F. Touchie, A grouped control strategy for the retrofit of post-war multi-unit residential building hydronic space heating systems, Energy Build. 208 (2020) 109604. https://doi.org/10.1016/j.enbuild.2019.109604.

[43] D.S. Østergaard, S. Svendsen, Replacing critical radiators to increase the potential to use low-temperature district heating – A case study of 4 Danish single-family houses from the 1930s, Energy 110 (2016) 75–84. https://doi.org/10.1016/j.energy.2016.03.140.

[44] M. Tunzi, M. Tunzi, D.S. Østergaard, S. Svendsen, R. Boukhanouf, E. Cooper, Method to investigate and plan the application of low temperature district heating to existing hydraulic radiator systems in existing buildings, Energy 113 (2016) 413–421. https://doi.org/10.1016/j.energy.2016.07.033.

[45] SIA, Norme 385/1:2020 - Installations d'eau chaude sanitaire dans les bâtiments - Bases générales et exigences, (2020).

[46] M. Kropp, M. Lämmle, S. Herkel, H.-M. Henning, A. Velte-Schäfer, Enhancing heat pump performance for domestic hot water preparation: A comparative analysis in existing multi-family houses, Energy Build. 328 (2025) 115155. https://doi.org/10.1016/j.enbuild.2024.115155.

[47] M. Brand, J.E. Thorsen, S. Svendsen, Numerical modelling and experimental measurements for a low-temperature district heating substation for instantaneous preparation of DHW with respect to service pipes, Energy 41 (2012) 392–400. https://doi.org/10.1016/j.energy.2012.02.061.

[48] H. Averfalk, T. Benakopoulos, I. Best, et al, Low-Temperature District Heating Implementation Guidebook, 2021. http://publica.fraunhofer.de/dokumente/N-640204.html.

[49] X. Yang, H. Li, S. Svendsen, Decentralized substations for low-temperature district heating with no Legionella risk, and low return temperatures, Energy 110 (2016) 65–74. https://doi.org/10.1016/j.energy.2015.12.073.

[50] A. Tahiri, K.M. Smith, J.E. Thorsen, C.A. Hviid, S. Svendsen, Staged control of domestic hot water storage tanks to support district heating efficiency, Energy 263 (2023) 125493. https://doi.org/10.1016/j.energy.2022.125493.

[51] T. Huang, X. Yang, S. Svendsen, Multi-mode control method for the existing domestic hot water storage tanks with district heating supply, Energy 191 (2020) 116517. https://doi.org/10.1016/j.energy.2019.116517.

[52] R. Haberl, O. Türk, A. Bohren, M.Y. Haller, DHWStrat: Methode zur Bestimmung der Schichtungseffizienz von Warmwasserspeichern, SPF Institut für Solartechnik, Rapperswil, 2021. https://www.ost.ch/fileadmin/dateiliste/3_forschung_dienstleistung/institute/spf/forschung/projekte/dhwstrat_schlussbericht.pdf (accessed March 31, 2023).

[53] T. Benakopoulos, M. Tunzi, R. Salenbien, D. Vanhoudt, S. Svendsen, Low return temperature from domestic hot-water system based on instantaneous heat exchanger with chemical-based disinfection solution, Energy 215 (2021) 119211. https://doi.org/10.1016/j.energy.2020.119211.

[54] X. Yang, H. Li, S. Svendsen, Alternative solutions for inhibiting Legionella in domestic hot water systems based on low-temperature district heating, Build. Serv. Eng. Res. Technol. 37 (2016) 468–478. https://doi.org/10.1177/0143624415613945.

[55] A. Müller, L. Kranzl, F. Schipfer, R. Büchele, J. Binder, H. Schrammel, R.-R. Schmidt, R. Geyer, L. Paolo, R. Heimrath, T. Mach, M. Kuh, W. Baumgartner, M. Waser, A. Bernhofer, F. Schnappinger, H. Berger, T. Eisenhut, M. Buryy, N. Untermoser, J. Schröttner, S. Raudaschl, T2LowEx: Transformation von konventionellen Wärmenetzen in Richtung Niedertemperaturnetze durch sekundärseitige Maßnahmen, 2021. https://energieforschung.at/wp-content/uploads/sites/11/2021/12/Endbericht_final.pdf (accessed October 6, 2022).

[56] SIA, Norme 385/2:2025 - Installations d'eau chaude sanitaire dans les bâtiments - Besoins en eau chaude, exigences globales et dimensionnement, (2025).

[57] Société Suisse de l'Industrie du Gaz et des Eaux (SSIGE / SVGW, Directive pour l'hygiène dans les installations d'eau potable, (n.d.).

[58] J. Khoury, P. Hollmuller, B.M. Lachal, S. Schneider, U. Lehmann, COMPARE RENOVE : du catalogue de solutions à la performance réelle des rénovations énergétiques (écarts de performance, bonnes pratiques et enseignements tirés), (2018). https://archive-ouverte.unige.ch/unige:101940 (accessed October 16, 2019).

[59] K.-F. Hülser, Ventilation simple flux hygroréglable : Bilan de 4 ans de projets SIG-éco21, (2023). https://www.cuepe.ch/html/enseigne/pdf/trp-22-23-12.pdf.

[60] M. Haller, I. Mojic, M. Kaufmann, A. Huggenberger, J. Podhradsky, E. Frank, L. Lötscher, S. Boller, B. Meier, Disturbance of Stratification Caused by Direct Horizontal Inlets into a Water Storage Tank, in: Proc. EuroSun 2014 Conf., International Solar Energy Society, Aix-les-Bains, France, 2015: pp. 1–9. https://doi.org/10.18086/eurosun.2014.10.13.

[61] D.S. Østergaard, S. Svendsen, Are typical radiators over-dimensioned? An analysis of radiator dimensions in 1645 Danish houses, Energy Build. 178 (2018) 206–215. https://doi.org/10.1016/j.enbuild.2018.08.035.

[62] D.S. Østergaard, S. Svendsen, Costs and benefits of preparing existing Danish buildings for low-temperature district heating, Energy 176 (2019) 718–727. https://doi.org/10.1016/j.energy.2019.03.186.

[63] A. Reguis, B. Vand, J. Currie, Challenges for the Transition to Low-Temperature Heat in the UK: A Review, Energies 14 (2021) 7181. https://doi.org/10.3390/en14217181.

[64] L. Quiquerez, J.D. Cabrera Santelices, P. Hollmuller, B.M. Lachal, Températures de distribution de chauffage du parc immobilier genevois, Université de Genève, 2013. https://archive-ouverte.unige.ch/unige:27989.

[65] S. Holst, TRNSYS Type 362: Dynamic radiator model with pipes, (1996).

[66] P. Ljunggren, J. Wollerstrand, Optimum Performance of Radiator Space Heating Systems Connected to achieve lowest possible district heating return temperature, in: Proc. 10th Int. Symp. Dist. Heat. Cool., 2006.

[67] T. Van Oevelen, D. Vanhoudt, R. Salenbien, Evaluation of the return temperature reduction potential of optimized substation control, in: Energy Procedia, Hamburg, Germany, 2018: pp. 206–215. https://doi.org/10.1016/j.egypro.2018.08.185.

[68] P. Lauenburg, Improved supply of district heat to hydronic space heating systems, Doctoral Thesis, Lund University, 2009. https://www.energy.lth.se/fileadmin/energivetenskaper/Avhandlingar/Avhandling_-_Patrick_Lauenburg.pdf.

[69] N. Calame, G. Cuvillier, F. Rognon, O. Montero Dominguez, P. Brischoux, S.A. Callegari, P. Hollmuller, C. Fraga, M. Rüetschi, AirBiVal : Développement et optimisation de concepts hybrides de pompes à chaleur sur l'air pour des immeubles résidentiels collectifs, CSD, Université de Genève et Services Industriels de Genève, 2021. https://archive-ouverte.unige.ch/unige:156969.

[70] O. Montero D., P. Brischoux, C. Fraga, M. Rüetschi, N. Calame, F. Rognon, P. Hollmuller, Monovalent and Hybrid Air-source Heat Pump Concepts for Existing Multifamily Buildings – Energy Performance and CO_2 Savings, in: Proc. 14th IEA Heat Pump Conf., Chicago, Illinois, 2023. https://archive-ouverte.unige.ch/unige:169365 (accessed May 29, 2024).

[71] MeteoSchweiz, Bundesamt für Umwelt (BAFU), Baudirektion Kanton Zürich, Hochschule Luzern (HSLU), Schweizerischen Ingenieur- und Architektenverein (SIA), Anwendungsempfehlung zu den stündlichen Klimadatensätzen für die Zukunft in Ergänzung zu SIA 2028, 2022. https://cms.sia.ch/fr/api/getMedia/951 (accessed December 11, 2024).

[72] S. Goel, M. Rosenberg, E. Mets, C. Eley, ANSI/ASHRAE/IES Standard 90.1-2019 Performance Rating Method Reference Manual, Pacific Northwest National Laboratory, Richland, Washington, USA, 2023. https://www.energycodes.gov/sites/default/files/2023-12/90_1_2019_Appendix_G_PRM_2023.11.pdf.

[73] J.D. Cabrera Santelices, J.-L. Bertholet, P. Hollmuller, T.A.R. Legendre, H. Pehle, S. Schneider, J.A. Strobel, Suivi et quantification des économies d'énergie relatives aux mesures préconisées par la Task Force Energie du Canton de Genève - Hiver 2023 - 2024, Université de Genève, 2024. https://archive-ouverte.unige.ch/unige:182165 (accessed November 11, 2025).

[74] SIA, Norme 385/2:2015 - Installations d'eau chaude sanitaire dans les bâtiments - Besoins en eau chaude, exigences globales et dimensionnement, (2015).

[75] OFS (Office fédéral de la statistique), Construction et logement 2020, Office fédéral de la statistique (BFS), Neuchâtel, 2022. https://dam-api.bfs.admin.ch/hub/api/dam/assets/22304474/master.

[76] AERMEC, Reversible heat pumps high efficency - Technical manual: NRK 0200-0700, n.d.

[77] Hoval, Documentation technique Hoval Belaria Pro (40, 50) - Pompe à chaleur air/eau, (2025).

[78] E. Romano, M.K. Patel, P. Hollmuller, Applying trade mechanisms to quantify dynamic GHG emissions of electricity consumption in an open economy - the case of Switzerland, Energy (2024) 133398. https://doi.org/10.1016/j.energy.2024.133398.

[79] KBOB, eco-bau, IPB, Données des écobilans dans la construction 2009/1:2022, 2022. https://www.kbob.admin.ch/kbob/fr/home/themen-leistungen/nachhaltiges-bauen/oekobilanzdaten_baubereich.html (accessed August 10, 2022).

[80] OCEN (Office cantonal de l'énergie), Directive relative au calcul de l'indice de dépense de chaleur, (2022). https://www.ge.ch/document/directive-relative-au-calcul-indice-depense-chaleur.

[81] OCEN (Office cantonal de l'énergie), Guide d'application du règlement sur l'énergie relatif à l'efficience énergétique des bâtiments et à l'optimisation de leurs installations de production de chaleur, 2023. https://www.ge.ch/actualite/guide-accompagner-nouvelle-reglementation-bati-30-06-2023.

[82] L. Quiquerez, Analyse comparative des consommations de chaleur pour la production d'eau chaude sanitaire estimées à partir de relevés mensuels: Etude sur un échantillon de bâtiments résidentiels collectifs alimentés par un réseau de chaleur à Genève, 2017. https://archive-ouverte.unige.ch/unige:91218 (accessed November 12, 2019).

[83] X. Yang, Supply of domestic hot water at comfortable temperatures by low-temperature district heating without risk of legionella, PhD thesis, DTU Civil Engineering, Technical University of Denmark, 2016.

[84] O. Montero, P. Brischoux, C. Fraga, E. Vionnet, M. Ruëtschi, N. Calame, F. Rognon, M.K. Patel, P. Hollmuller, Accelerated Decarbonization of Non-retrofitted Multifamily Buildings, by Integrating Air-Source Heat Pumps in Existing Gas Boiler systems: Techno-Economic and Environmental Analysis, Submitted (2026).

[85] O. Montero D., P. Brischoux, P. Hollmuller, Gestion en cascade de pompes à chaleur air/eau pour immeubles résidentiels collectifs existants : Retours d'expérience sur sites pilotes et étude de sensibilité par simulation numérique, Université de Genève, 2023. https://archive-ouverte.unige.ch/unige:169458 (accessed September 15, 2023).

[86] B. Grandjean, S. Schneider, P. Hollmuller, Actual energy savings of more than 1000 renovated buildings in Geneva, J. Phys. Conf. Ser. 2042 (2021) 012145. https://doi.org/10.1088/1742-6596/2042/1/012145.

[87] L. Rinquet, G. Fowler, S. Delmenico, D. Iglesias, C. Cacheiro, Geneva's solution to bridge the performance gap in energy retrofit, J. Phys. Conf. Ser. 3140 (2025) 062030. https://doi.org/10.1088/1742-6596/3140/6/062030.

[88] J. Strobel, R. Novoa-Herzog, F. De Oliveira Filho, P. Hollmuller, Perspectives 2030 : Evolution du système énergétique du canton à l'horizon 2030, Etude réalisée sous mandat de l'Etat de Genève dans le cadre de la plateforme DYNAMO (OCEN - SIG/éco21 – UNIGE), Genève, 2026.

[89] Fraunhofer IEE, CoolDown – Optimization of piped heat supply in existing buildings, Fraunhofer Inst. Energy Econ. Energy Syst. Technol. (2025). https://www.iee.fraunhofer.de/en/research_projects/search/2024/cooldown.html (accessed January 7, 2025).

[90] AIT Austrian Institute Of Technology, DeRiskDH, ait.ac.at (n.d.). https://www.ait.ac.at/en/research-topics/flexibility-business-models/projects/deriskdh (accessed June 10, 2026).

[91] J.F. Belmonte, J.A. Almendros-Ibáñez, Integration of dynamic radiator models in building performance simulation tools: Effects of radiator thermal capacitance on buildings' heating system efficiency, in: Proc. 18th IBPSA Conf., Shangai, China, 2023. https://doi.org/https://doi.org/10.26868/25222708.2023.1144.

[92] Joulia SA, Technische Dokumentation Joulia-Twinline (Konkrete Massnahme gegen die Klimaerwärmung: Warm Duschen mit Joulia-Twinline), (2023). https://joulia.com/wp-content/uploads/2026/02/Joulia-Twinline_BROCHURE.pdf (accessed June 11, 2026).

[93] M.A. Baillifard, Equilibrage hydraulique, (2022).

[94] T. Cholewa, I. Balen, A. Siuta-Olcha, On the influence of local and zonal hydraulic balancing of heating system on energy savings in existing buildings – Long term experimental research, Energy Build. 179 (2018) 156–164. https://doi.org/10.1016/j.enbuild.2018.09.009.

[95] H.-I. Cho, D. Cabrera, M.K. Patel, Estimation of energy savings potential through hydraulic balancing of heating systems in buildings, J. Build. Eng. 28 (2020) 101030. https://doi.org/10.1016/j.jobe.2019.101030.

[96] L. Zhang, O. Gudmundsson, J.E. Thorsen, H. Li, X. Li, S. Svendsen, Method for reducing excess heat supply experienced in typical Chinese district heating systems by achieving hydraulic balance and improving indoor air temperature control at the building level, Energy 107 (2016) 431–442. https://doi.org/10.1016/j.energy.2016.03.138.

11 Appendix

11.1 Application of the methodology to eREN No5 building typology

The methodology for adapting the building retrofitting scenarios described in section 3.2.1 is applied here to the eREN No5 building typology.

This building typology corresponds to adjoining multifamily building built in 1960-1975. This building typology has 6-storey or more, and is located in peri urban zone. Its architecture is characterized by in-situ concrete facade, flat roof and sloping balconies and concrete floor with continuous slab. The case study selected to represent this typology is shown in Figure 38.



Figure 38: Picture of the building representing eREN No5 building typology. This building is located in Onex (GE).

For this building typology, the following retrofitting measures (as defined in the eREN project) were selected in order to reduce the SH needs below the specific SH needs limit defined by the SIA 380/1:2009 standard:

- Façade external insulation including thermal bridge insulation: U-value is reduced from 1.53 to 0.17 W/m².K after insulation
- Basement slab insulation: insulation with 10 cm mineral wool (U-value from 2.14 to 0.18 W/m².K after insulation)
- Replacement of double-glazed windows with triple-glazed windows with the following characteristics: Ug ~ 0.4 W/m².K, Uf ~ 1.2 W/m².K and g-value ~ 0.37

In the eREN project, those retrofitting measures were cumulated in order to reduce the building SH needs below the specific SH needs limit as defined by SIA 380/1:2009 standard. In the T-DROP project, the normalized thermal balance of the building according to SIA380/1:2016 standard was determined for the possible combination of these retrofitting measures. For each retrofitting scenario, the specific SH demand and the specific thermal power were defined using the LESOSAI software. The retrofitting

costs were also evaluated using the methodology described above. The CECB building thermal efficiency class was also determined for all scenarios. Table 15 shows the results for each retrofitting scenario.

Table 15: Characteristics of each retrofitting scenario defined for the eREN No5 building typology

No	Retrofitting scenario	SH demand (Qh) [kWh/m²ERA]	CECB energy class	Specific power [W/m² ERA]	Total retrofit cost [CHF]	Specific cost [CHF/m²ERA]
0	Initial condition	111.6	G	49.6		
0'	Current condition (roof renovated according to case study building)	110.5	G	49.3		
1	Slab (ground floor)	98.1	G	45.1	151 794	54
2	Windows	80.9	G	36.4	635 286	226
3	Façade	69.1	F	35.3	1 307 115	465
4	Slab + Windows	68.5	F	32.3	787 080	280
5	Façade + Windows	39.1	D	21.4	1 942 401	691
6	Façade + Slab	57.3	E	31.2	1 456 09	518
7	Façade + Slab + Windows	27.6	C	17.4	2 094 195	745

For each building typology selected for the T-DROP project, a synthetic fact sheet was compiled with the following information:

- Short description of the building typology
- Definition of retrofitting scenarios combining one or more retrofitting measures
- Characteristics and specific costs for each retrofitting scenario
- Specific SH demand, energy class and specific power for SH for each scenario

All updated fact sheets are available in Appendix 11.1.

11.2 Updated building retrofit sheets for predominant eREN typologies

Sheet for eREN No4 building typology

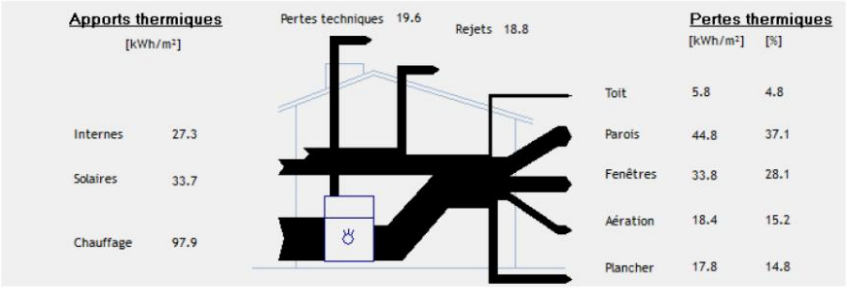
eRen 4 – Levant 137



Modification par rapport à eRen :
i. Méthode de calculs
ii. Station météorologique
iii. Adaptations mineures du bilan thermique existant

Mode de calculs	SIA 380/1 :2016
Station météorologique	Genève - Cointrin
Année de construction	1960
SRE [m²]	1475
Facteur de forme [-]	1.1
Besoin de chaleur limite [kWh/m²]	44.3
Coûts actualisé oct.2024	eRen adapté IDC (base 100, oct.2015)

Diagramme de Sankey – Etat existant



Scénario de rénovation	Description	QH [kWh/m²]	Classe env. th	Puissance [W/m²]	Coûts unitaire* [CHF/m²SRE]
Etat existant	Sans vannes thermostatiques Plancher des combles mis d'origine (non isolé) Fenêtres d'origine (Ug=3, Uf=1.9, psi=0.07)	116.3	G	45,7	
Etat existant	Avec vannes thermostatiques	94.7	G	42.2	
Fenêtres	Selon eRen + psi 0.04	79.1	F	35.7	206
Combles	Selon eRen	75.6	F	35.7	87
Façade, stores+Blacons	Selon eRen	68.5	E	32.4	569
Fenêtres+ combles		60.2	E	28.2	293
Fenêtres+combles +Façades	eRen, sc1	33.9	C	19.6	862

**Coûts eRen par mesure incluant les coûts de la mesure unitaire et les frais généraux au prorata du coût de la mesure.*

Sheet for eREN No5 building typology

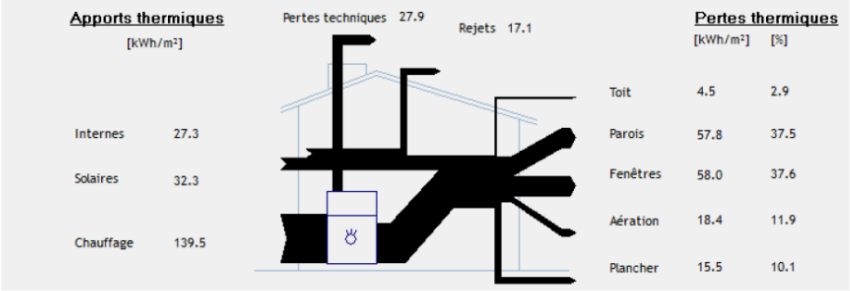
eRen 5 – Bois Chapelle 57 (BC57)



Modification par rapport à eRen :
i. Méthode de calculs
ii. Station météorologique
iii. Adaptations mineures du bilan thermique existant

Méthode de calculs	SIA 380/1 :2016
Station météorologique	Genève - Cointrin
Année de construction	1970
SRE [m²]	2 811
Facteur de forme [-]	0.796
Besoin de chaleur limite[kWh/m²]	34.6
Coûts actualisé oct.2024	eRen adapté IDC (base 100, oct.2015)

Diagramme de Sankey – Etat existant



Scénario de rénovation	Description	QH [kWh/m²]	Classe env. th	Puissance [W/m²]	Coûts unitaire* [CHF/m² SRE]
Etat existant	-	111.6	G	49,6	-
i. Plancher RDC		98,1	G	45,1	54.-
ii. Fenêtres		80,9	G	36,4	226.-
iii. Façades	Étages + attique+ caisson de store	69,1	F	35,3	465.-
iv. Plancher + Fenêtres		68,5	F	32,3	280.-
v. Façades + Fenêtres		39,1	D	21,4	691.-
vi. Façade + Plancher	Sc 1 eRen	57,3	E	31,2	518.-
vii. Façade + Plancher + Fenêtres	Sc2 eRen	27,6	C	17,4	745.-

**Coûts eRen par mesure incluant les coûts de la mesure unitaire et les frais généraux au prorata du coût de la mesure.*

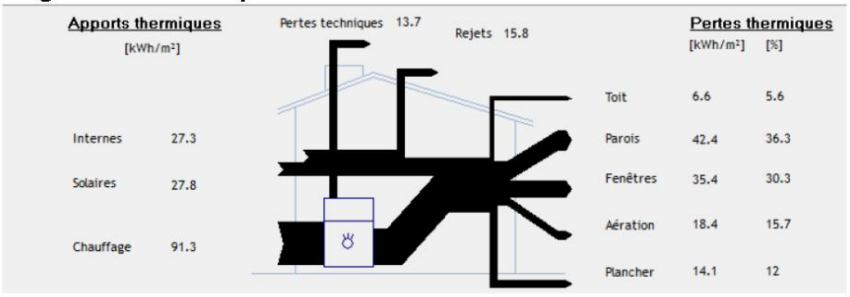
Sheet for eREN No7 building typology

eRen 7 – Fôret 20



Modification par rapport à eRen : i. Méthode de calculs ii. Station météorologique iii. Adaptations mineures du bilan thermique existant	
Mode de calculs	SIA 380/1 :2016
Station météorologique	Genève - Cointrin
Année de construction	1975
SRE [m²]	5 065
Facteur de forme [-]	0.752
Besoin de chaleur limite [kWh/m²]	33.7
Coûts actualisé oct.2024	eRen adapté IDC (base 100, oct.2015)

Diagramme de Sankey – Etat existant



Scénario de rénovation	Description	QH [kWh/m²]	Classe env. th	Puissance [W/m²]	Coûts unitaire* [CHF/m² SRE]
Etat existant	-	77.6	G	39	
Fenêtres	Selon eRen + psi 0.04	55.7	E	29.6	186
Plancher	Selon eRen	66.9	F	35.2	35
Toiture	Selon eRen	72.7	G	37.3	81
Stores+murs ss-sol	Selon eRen	66.6	F	35.1	70
Fen. + plancher		45.4	E	26	221
Fen.+ plancher + Toiture		40.8	D	24.3	302
Fen.+Plan.+Toit.+Stores+Mur Mss-sol	Sc.1 eRen	30.4	C	20.5	372

**Coûts eRen par mesure incluant les coûts de la mesure unitaire et les frais généraux au prorata du coût de la mesure.*

Sheet for eREN No8 building typology

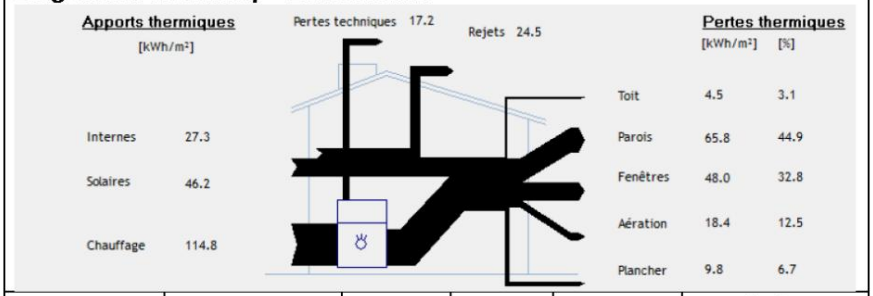
eRen 8 – BC89



Modification par rapport à eRen :
i. Méthode de calculs
ii. Station météorologique
iii. Adaptations mineures du bilan thermique existant

Mode de calculs	SIA 380/1 :2016
Station météorologique	Genève - Cointrin
Année de construction	1971
SRE [m²]	3 539
Facteur de forme [-]	0.656
Besoin de chaleur limite [kWh/m²]	31.7
Coûts actualisé oct.2024	eRen adapté IDC (base 100, oct.2015)

Diagramme de Sankey – Etat existant



Scénario de rénovation	Description	QH [kWh/m²]	Classe env. th	Puissance [W/m²]	Coûts unitaire* [CHF/m² SRE]
Etat origine	-	97.6	G	47.2	-
a. Fenêtres	Selon eRen avec psi 0.04	60.9	F	33.8	345
b. Façades	Selon eRen	49.8	E	30.5	494
c. Fenêtres/ Attique/ Plancher		59.5	F	33.2	522
d. Fenêtres/ Façades		24.8	C	19.6	839
e. Fenêtres/ Façades/ Plancher/ Attique	eRen SC1 (=SC2 dans BLD)	23.5	C	19.1	1016

**Coûts eRen par mesure incluant les coûts de la mesure unitaire et les frais généraux au prorata du coût de la mesure.*

Sheet for eREN No10 building typology

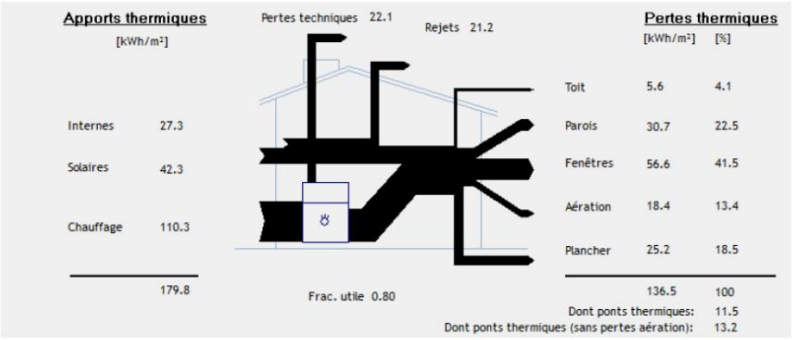
eRen 10 – La Roseraie



Modification par rapport à eRen :
i. Méthode de calculs
ii. Station météorologique
iii. Adaptations mineures du bilan thermique existant

Mode de calculs	SIA 380/1 :2016
Station météorologique	Genève - Cointrin
Année de construction	1988
SRE [m²]	5 215
Facteur de forme [-]	0.89
Besoin de chaleur limite [kWh/m²]	36.6
Coûts actualisé oct.2024	eRen adapté IDC (base 100, oct.2015)

Diagramme de Sankey – Etat existant



Scénario de rénovation	Description	QH [kWh/m²]	Classe env. th	Puissance [W/m²]	Coûts unitaire* [CHF/m²SRE]
Etat existant	-	88.2	G	44	-
a. Plafond sous-sol + murs contre non-chauffé selon eRen	Plafond: - EPS 20cm - λ = 0.036 W/(mk) Murs : - EPS 10cm - λ = 0.036 W/(mk)	66.4	F	33.8	86
b. Fenêtres façades selon eRen	- Uv : 0.6 W/(m²K) - Uf : 1.1 W/(m²K) - gp=0.45 [-] - PSI: 0.04 W/mK	62	F	31	287
c. Fenêtres, plafond sous-sol et murs contre non chauffé	Cf. a et b	37,2	D	22.5	373

**Coûts eRen par mesure incluant les coûts de la mesure unitaire et les frais généraux au prorata du coût de la mesure.*

11.3 Parameters and inputs of heat emitter model (TRNSYS Type 5897)

Table 16 and Table 17 show the parameters and the inputs for TRNSYS Type 5897 used to model heat emitters. Inputs differ from parameters as they can be changed at every type step of the simulation.

Table 16: Type 5897 parameters

Parameter	Description	Unit
Cm	Internal heat capacity of the building or building zone	J/K
Am	Effective mass area	m²
Af	Conditioned floor area of Energy Reference Area (ERA)	m²
Htr_w	Thermal transmission coefficients of glazed walls and windows	W/K
his	Thermal transmission coefficient between internal air and the wall surface (by default: 3.45)	W/(m².K)
hms	Heat transfer coefficient between nodes m and s (by default : 9.1)	W/(m².K)
xat	Ratio between the internal surfaces area and the floor area (by default : 4.5)	-
Nsurf	Number of surfaces to deal with for passive solar gains	-
Tair_set_H	Set point temperature for heating the building	°C
Tair_set_C	Set point temperature for cooling the building	°C

Table 17: Type 5897 inputs

Inputs	Description	Unit
Text	Ambient temperature	C
Tsup	Temperature of the air supplied in the ventilation system	C
Pint	Internal passive gains	kJ/h
Hve	Thermal transmission coefficient due to ventilation	W/K
Htr_op	Thermal transmission coefficient of opaque (inertial) building elements	W/K
Isol,i	Solar irradiation on surface i	kJ/(h.m²)
Fshob,i	Shading reduction factor from external obstacles for the solar effective collecting area of surface i	-
Asol,i	Effective solar collecting area of surface i	m²
Ploss_GLO,i	Heat flow due to thermal radiation to the sky from building element i	kJ/h

11.4 Installed heat emitters capacity and optimized heating curves

Installer heat emitters capacity

To determine the installed heat emitters capacity for each building typology presented in Chapter 3, the non-renovated building is simulated on an hourly basis in TRNSYS (RC model described in section 3.4), without solar and internal gains, supplied by an ideal SH system which maintains the indoor temperature equal to the chosen setpoint temperature (e.g. 22°C), thereby obtaining the hourly building SH demand.

Using the energy signature of the building based on daily SH values, we determine the SH load for an outdoor temperature of -10°C (Figure 39). The outdoor air temperature of -10°C corresponds to the design temperature globally used for the Swiss Plateau during the considered building construction period. As described in Equation (11), the installed heat emitters capacity $Q_{rad,design}$ is equal to that SH load ($Q_{SH,design}$), multiplied by the initial oversizing factor ($f_{rad,init}$). This oversizing factor is used to account for the fact that calculations of the SH load might have included some oversizing.

$$Q_{rad,design} = Q_{SH,design} \cdot f_{rad,init} = Q_{SH}(T_{outdoor} = -10°C) \cdot f_{rad,init} \quad (11)$$

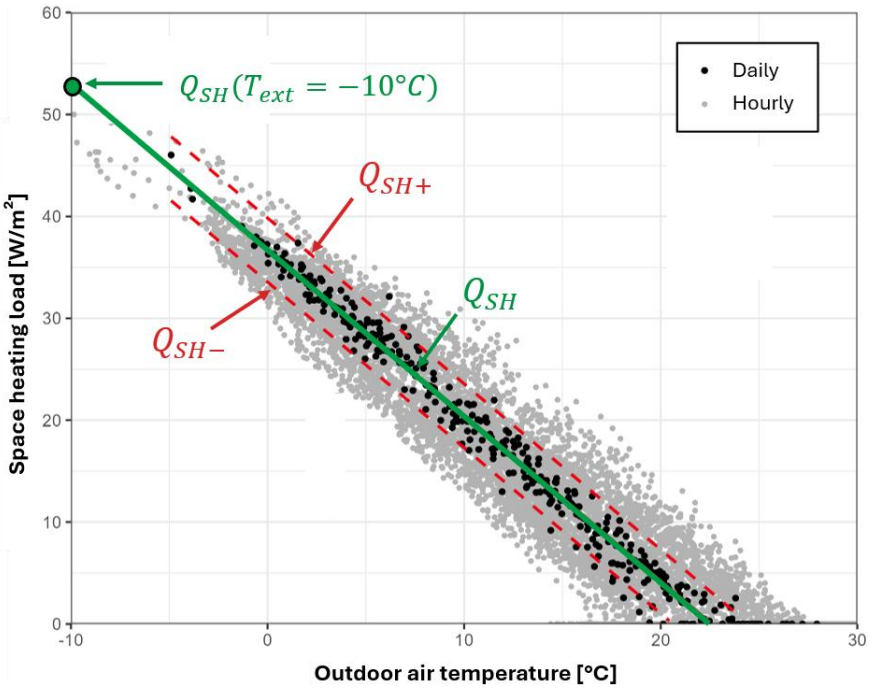


Figure 39: Building energy signature (green) produced from hourly simulation of the non-renovated eREN 4 building with an ideal SH system, an indoor temperature setpoint of 22°C and a ventilation flow rate of 1.0 m³/h.m². The red lines represent the 95% prediction interval (Q_{SH+} upper bound, Q_{SH-} lower bound) around the energy signature.

The heat emission capacity of the radiators depends on the type of radiators (cast-iron, aluminum,…) and the involved temperatures. It is defined for a specific set of supply/return/indoor temperatures. At design conditions, these temperatures are considered equal to 62/52/22°C (based on the temperatures typically observed in existing buildings [64], see section 4.4 and section 5.3.1). Therefore, the installed heat emitters capacity at 62/52/22°C is the building SH load for an outdoor temperature of -10°C ($Q_{rad,design}$) multiplied by the initial oversizing factor, as defined in Equation (11). The radiator constant K is then determined using Equation (12). This value is constant for a given heat emitter and does not depend on the operating conditions.

$$Q_{rad,design} = \mathrm{K} \cdot \Delta \mathrm{T}_{log}{}^{n} \Rightarrow K = \frac{Q_{rad,design}}{\Delta \mathrm{T}_{log}{}^{n}} \quad (12)$$

Where n is the radiator exponent, equal to 1.3 as typical value for radiators, and $\Delta \mathrm{T}_{log} = \frac{T_{supply} - T_{return}}{\ln(\frac{T_{supply} - T_{indoor}}{T_{return} - T_{indoor}})}$.

For example, as illustrated in Figure 39, the SH load $Q_{SH,design}$ for an outdoor temperature of -10°C is 53 W/m² (78 kW) for building typology eREN 4. Assuming an initial oversizing factor of 20%, it results in a heat emitter capacity $Q_{rad,design}$ of 64 W/m² (94 kW) at design conditions (62/52/22°C) and a radiator constant K of 0.93. When converted to EN442 standard conditions (75/65/20°C) using Equation (13), it corresponds to 91 W/m² (134 kW).

$$Q_{rad,EN442} = Q_{rad,design} \cdot \left(\frac{\Delta T_{log,EN442}}{\Delta T_{log,design}} \right)^{n} \quad (13)$$

The radiator thermal capacitance is set to 0.005 (kJ/K)/(kJ/h), as per manufacturers data reported in [91] for aluminum radiators.

Optimized heating curves

To obtain the "low-flow" and "high-flow" heating curves (see section 4.4), we calculate, for each building typology and envelope retrofitting step, the lowest supply temperature ("high-flow") or return temperature (low-flow") required to meet the SH load across various outdoor temperatures. This process is illustrated in Figure 40 and involves the following steps:

- **Calculate the SH load Q_{SH}^{+}:** For a given outdoor temperature $T_{outdoor}$, determine the SH load using the building energy signature. To ensure the supply temperature is sufficient to meet the SH demand, we base the optimized temperature on the daily SH energy signature $Q_{SH}{}^{+}$, which covers 95% of the daily SH values (upper red dashed line on Figure 39).
- **Determine the average heat emitter temperature ($\Delta \mathrm{T}_{log}$):** Using Equation (14), calculate the average temperature difference across the heat emitters required to satisfy the SH load at a given outdoor temperature.

$$\Delta \mathrm{T}_{log}(T_{outdoor}) = \sqrt[n]{\frac{Q_{SH}^{+}(T_{outdoor})}{K}} \quad (14)$$

- **Compute the supply/return temperatures:** Determine the supply and return temperatures that correspond to the calculated $\Delta \mathrm{T}_{log}$, which either minimize the supply temperature ("high-flow") or minimize the return temperature ("low-flow"), while meeting a set of constraints. These constraints include the maximum admissible flow rate (flow rate at design conditions for heat emitter sizing described above), the minimum flow rate (20% of the maximum flow rate) the minimum temperature difference between the fluid and the indoor temperature (2 K), and the maximum supply temperature (70°C).

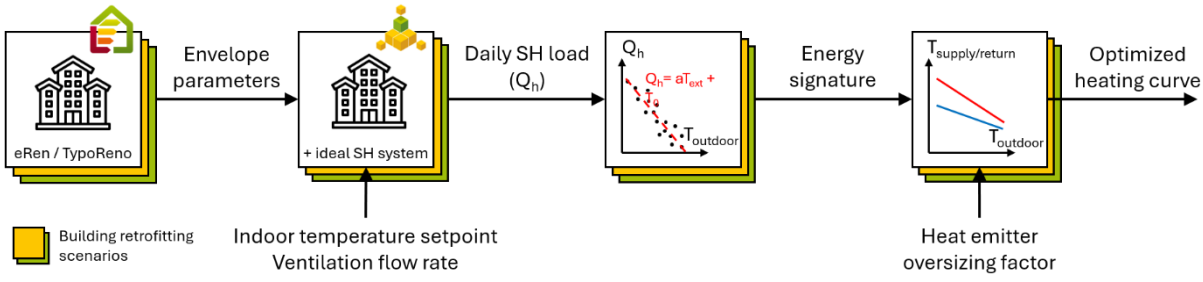


Figure 40: Process to determine the optimized SH distribution temperatures (heating curves) for each building typology and envelope retrofitting scenario

11.5 Modeling of DHW optimization measures

DHW heat exchanger sizing

DHW heat exchanger characteristics are determined using the SWEP International AB software “SSP G8”, based on the design conditions presented in Figure 41 for a heat load of 60 kW. This load corresponds to the DHW design load according to SIA standard 385/2 standard [74] for a medium-scale MFB with 4’000 m² heated floor area, 40 m² per occupant, 45 L/occ per day and 6 daily DHW cycles of 1 hour).

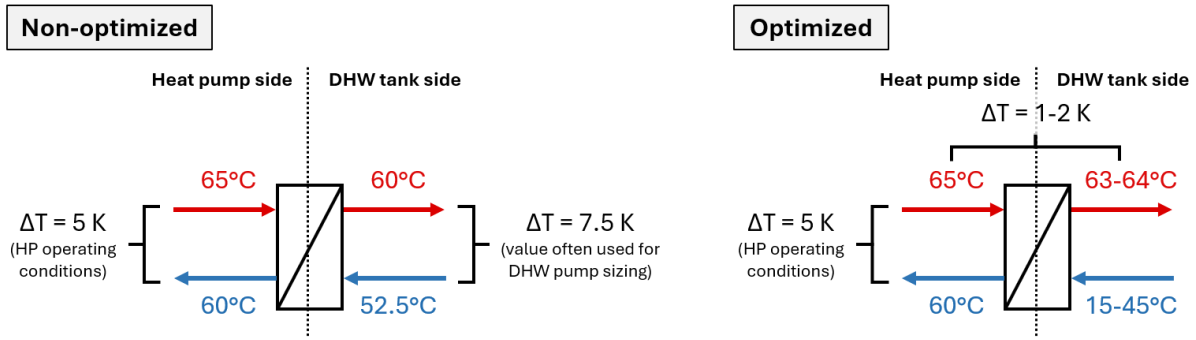


Figure 41: Illustration of non-optimized (left) and optimized (right) heat exchanger design conditions

Using these design conditions, the software proposes several heat exchanger models, with different heat transfer area. The characteristics of the final selection are summarized in Table 18.

Table 18: Characteristics of the DHW heat exchangers selected with the SWEP SSP G8 software for different design conditions

Model	Number of plates	Heat transfer area [m²]	Design temperatures [°C]				NTU	UA [kW/K]	Normalized UA (= UA/Q) [1/K]
			Prim. inlet (input)	Sec. inlet (input)	Sec. outlet (input)	Prim. outlet (result)			
B12MT	60	1.68	65.0	52.5	60.0	59.6	1.25	10.0	0.167
B16	100	3.92	65.0	45.0	64.0	57.0	4.30	13.6	0.226
B28	110	6.48	65.0	45.0	64.0	51.9	6.23	19.7	0.328

The same software is then used to the heat exchanger’s outlet temperatures for different inlet temperatures and flow rates, in order to assess its performance under various operating conditions. This analysis shows that the overall heat transfer coefficient (UA) is mainly governed by the primary and secondary flow rates, rather than by the temperature levels. Based on this simplification, a performance map of the average UA values is built as a function of the expected range of primary and secondary flow rates. Figure 42 shows the resulting performance maps created for the selected DHW heat exchangers, before normalization by the design heat transfer capacity (60 kW).

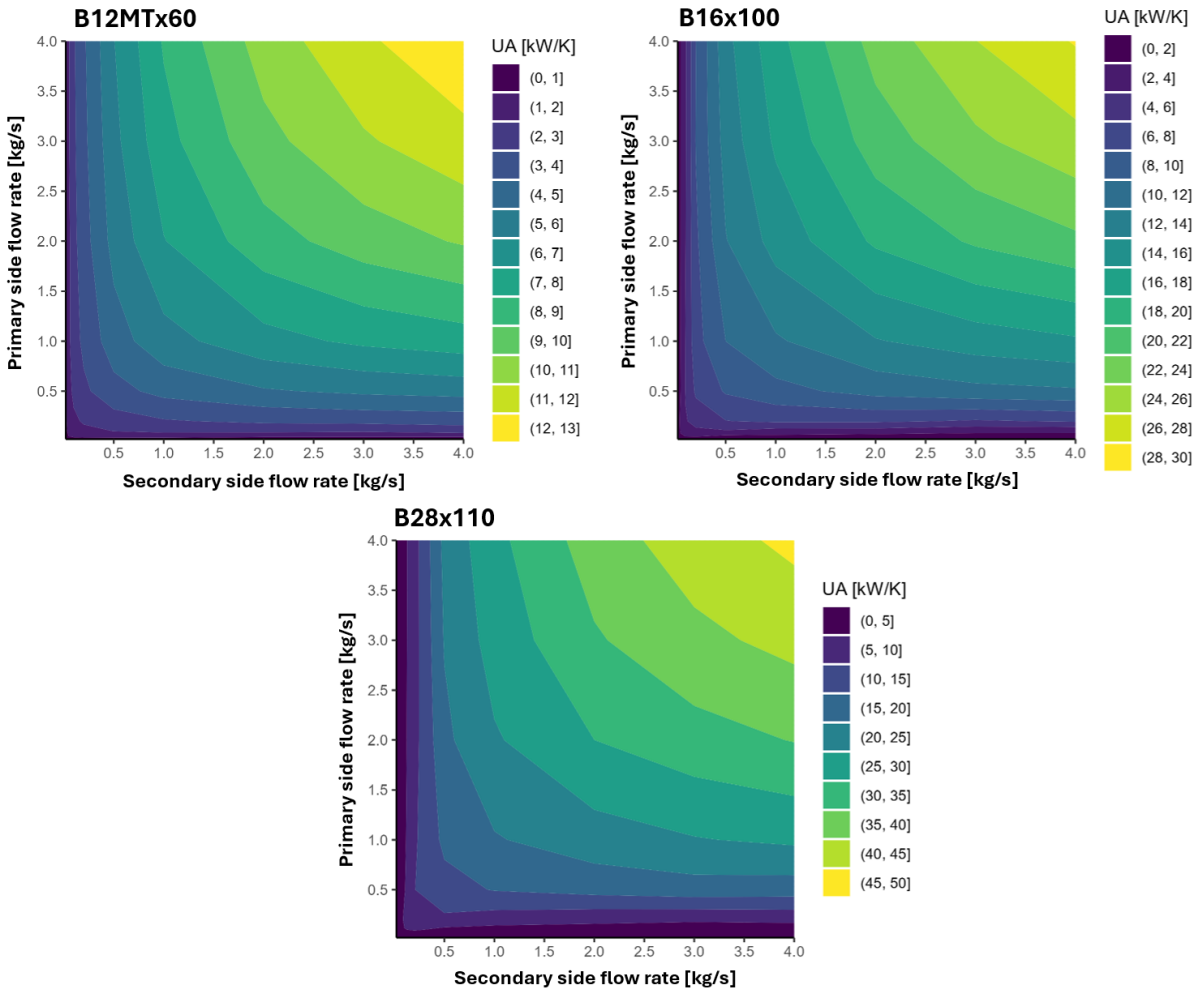


Figure 42: DHW heat exchanger performance maps for the small (top left), medium (top right) and large heat transfer areas

These performance maps are then used in the TRNSYS model of the system to calculate the heat exchanger's outlet temperatures from the inlet temperatures and flow rates, as described in Figure 43.

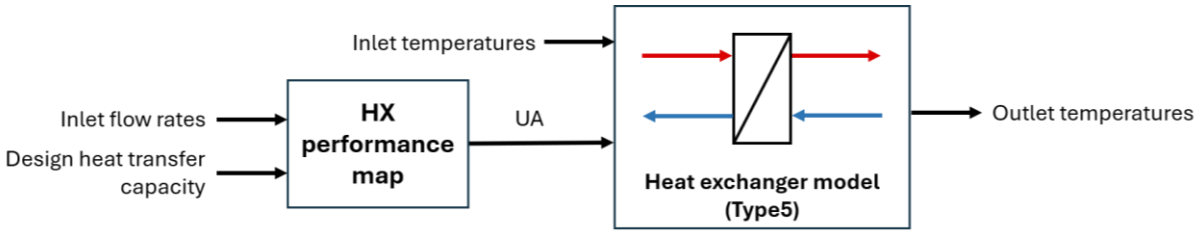


Figure 43: Description of the DHW heat exchanger modeling in TRNSYS

DHW heat recovery system “Joulia”

Figure 44 shows the heat recovery efficiency and power of Joulia heat recovery system provided by the manufacturer (Twinline model [92]). The efficiency ranges from 15% and 60%, depending on the model and size.

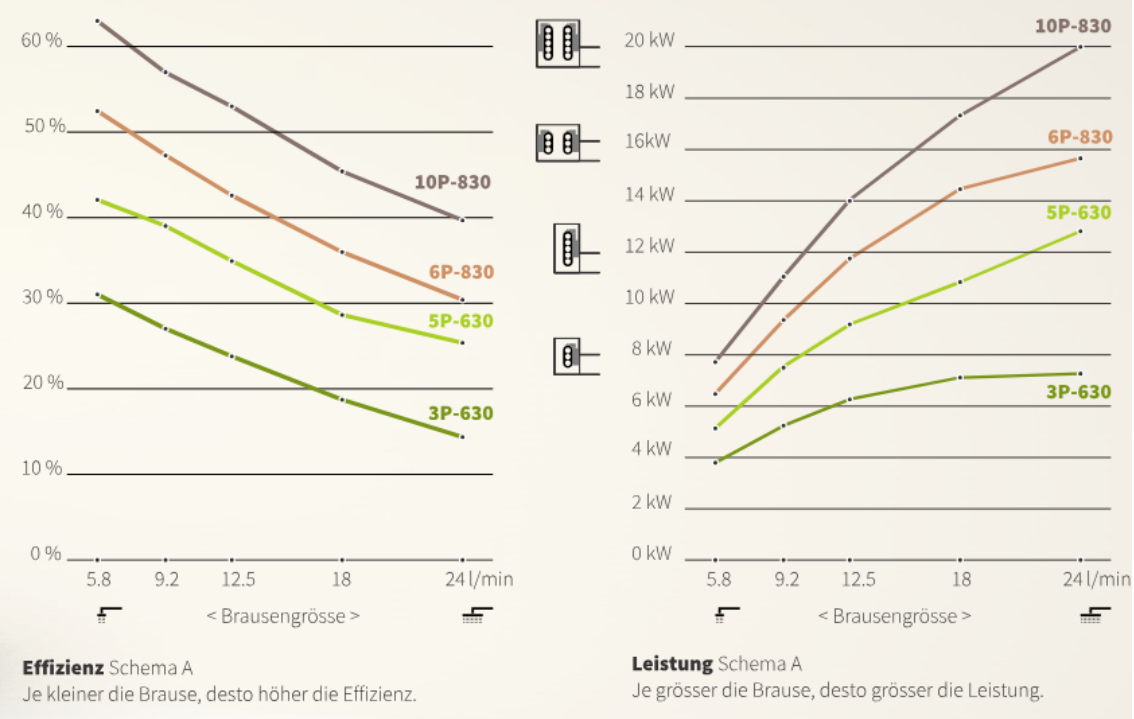
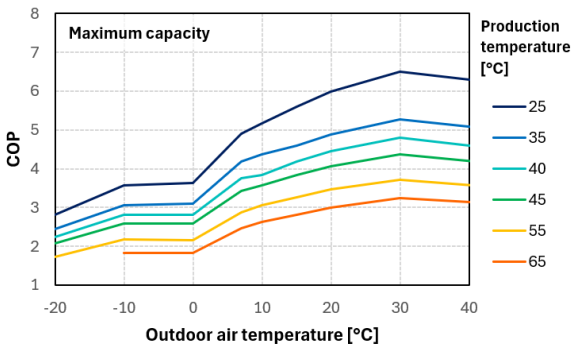


Figure 44: Heat recovery efficiency and power of Joulia heat recovery system (Twinline model [92])

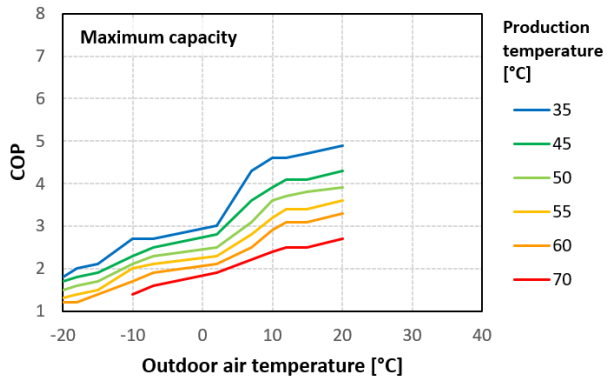
11.6 Heat pump performance maps

Regular R410A HP without inverter



COP at minimum capacity is assumed identical to COP at maximum capacity (no inverter)

High-efficiency R290 HP with inverter



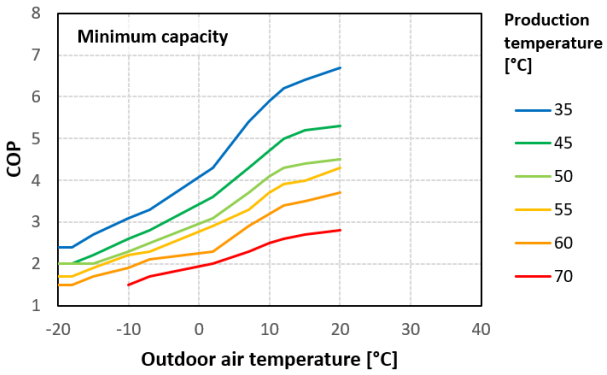


Figure 45: Performance maps of the HPs considered in this study, produced from manufacturers data [76,77]

11.7 Hydraulic balancing

Beyond improvements to the building's thermal envelope or the replacement of the heat-generation system—both of which are costly measures—it is worth considering hydraulic balancing of the existing distribution system in order to improve occupants' thermal comfort and reduce heating demand at a potentially attractive cost. Hydraulic balancing can, in some cases, provide an interesting and relatively accessible solution for achieving energy savings, although the resulting gains are generally more modest than those obtained through renovation works. However, this is not universally applicable: the theoretically attainable savings vary significantly from one building to another. Hydraulic imbalance occurs when certain branches of the network are more disadvantaged than others due to higher pressure losses, resulting in reduced water flow. This imbalance may stem from inadequate hydraulic adjustment during design or commissioning, from sizing errors, or from alterations made to the system over time. Poor hydraulic balancing leads to energy overconsumption, driven by a non-optimized heating curve and excessive electricity use by the circulation pump. It also results in thermal discomfort for occupants in overheated apartments or rooms, thereby degrading living conditions.

Heating demand and heating curve

In an unbalanced system, the most disadvantaged apartments force the heating control to increase the supply temperature. Because these branches experience higher pressure losses, they receive less water flow. To compensate, the heating curve is adjusted upward, increasing supply temperatures. This directly causes energy overconsumption: overheated rooms receive excess heat, which increases transmission and ventilation heat losses. Moreover, this can influence occupant behavior, such as frequent window opening during the heating season.

Equipment sizing

An unbalanced network affects both system components and any connected heating networks.

If the building is connected to a district heating network (DHN), this imbalance leads to an increase in return temperature and also to a higher heat consumption. Elevated return temperatures create several issues: they reduce the efficiency of heat distribution and heat production and limit the integration of renewable energy sources such as heat pumps, solar thermal systems, and low-temperature geothermal, all of which operate at lower temperatures. Higher return temperatures also increase thermal losses within the thermal grid.

For buildings equipped with a heat pump, higher supply and return temperatures have a negative impact on the COP, reducing the system's efficiency. In addition, they lead to higher investment costs, often requiring a larger-capacity heat pump. This can also result in frequent start-stop cycles at partial loads, shortening the lifespan of components such as compressors and expansion valves.

As for hydraulic pumps, a network imbalance forces the circulator to provide higher pressure to maintain flow, resulting in electrical overconsumption and operation outside the optimal efficiency point. These conditions may also generate hydraulic noise or cavitation, negatively affecting pump longevity.

Hydraulic Balancing implementation

Hydraulic balancing can be carried out using either static or dynamic methods.

Static balancing: Static balancing aims to equalize pressure losses between the different branches so that the target flow rates in each branch are achieved. This requires adding singular pressure losses in favorable branches so that they match those of the most disadvantaged branch. Static balancing can be implemented using static balancing valves or directly at terminal units using thermostatic radiator valves (TRV) with preset Kv values.

Static balancing ensures the nominal flow rates under nominal conditions. However, in most cases, consumers do not require nominal flow. When thermostatic valves close, overall flow decreases, and

flow in other branches tends to increase due to the pump curve. To maintain proper operation under partial load, dynamic balancing can be introduced.

Dynamic balancing: Dynamic balancing aims to maintain target flow rates in each loop or circuit, regardless of pressure variations caused by valve openings or closings elsewhere in the network. Several types of equipment can be used:

- Differential Pressure Control Valves (DPCV) maintain a constant differential pressure between two points. They are installed at the base of risers or on secondary branches, with a set ΔP.
- Pressure Independent Balancing and Regulating Valves (PIBRV) ensure constant flow over a given pressure range. They are installed at each terminal and set using a target flow rate. Their implementation requires the presence of thermostatic radiator valves (TRV).
- Pressure Independent Control Valves (PICV) regulate flow based on a control signal (temperature, etc.) while maintaining constant pressure. They are installed upstream of each hydraulic terminal.

All principle diagrams are shown in Figure 19, sourced from the course “Équilibrage hydraulique” taught at HEIG-VD [93].

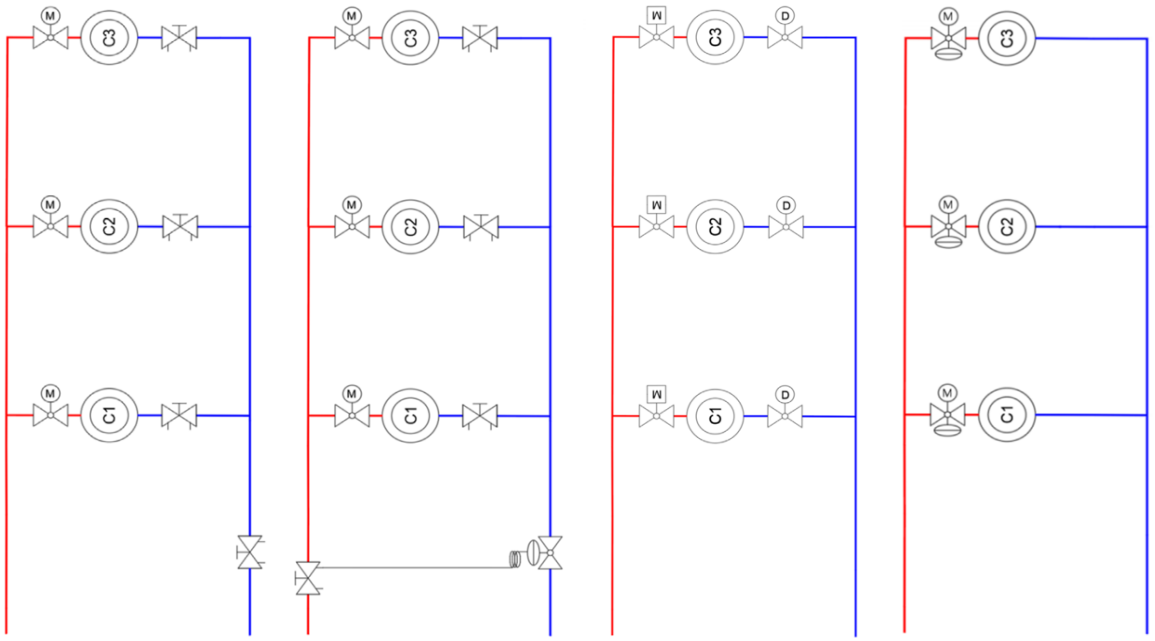


Figure 18: Existing solutions for implementing static or dynamic hydraulic balancing

Examples and results

To illustrate the importance of hydraulic balancing, we rely on a series of articles published in Switzerland and abroad that address this issue. Quantifying the savings achievable through hydraulic balancing is not straightforward: the operating conditions must remain constant before and after the intervention. This means that the building’s thermal envelope must remain unchanged, as well as user behavior. Only under these conditions, and with case studies equipped with appropriate measurement tools, can savings be accurately evaluated.

These publications report potential energy savings from hydraulic balancing ranging from 4% to 24% [94,95] depending on the measures implemented and the initial conditions of the system and building.

To carry out hydraulic balancing, several types of configurations and variants exist. Starting from the initial state of the network with its existing equipment, the study [94] analyzed four scenarios using different equipment, allowing a comparison of the resulting gains:

- Installation of TRV with Kv presetting at the valve head
- Installation of DPCV at riser base when preset TRV already exist
- Simultaneous installation of DPCV at riser base and preset TRV
- Installation of PIBRV directly at the terminal

The results of the study are shown in Table 10.

Table 19: Energy savings with different hydraulic balancing measures

Measure	Energy savings	Type	Implementation complexity
TRV with presetting	17,5 %	Static	Low
DPCV (with existing TRV)	18,1 %	Dynamic	Medium
TRV + DPCV (combined)	20,4 %	Dynamic	High
PIBRV	17,1 %	Dynamic	Medium

Thus, a static balancing approach—using preset TRV—already enables significant energy savings in the case studies. Dynamic balancing offers slightly higher gains, but at the cost of substantially higher investment.

A study on TRV use in multi-apartment buildings in China [96] reports a 17% reduction in heat consumption and a 42.8% reduction in pump electricity consumption. These savings result from reduced pressure losses in the network. It is important to note that such electricity savings are only possible with variable-speed pumps. For fixed-speed pumps—common before the 2000s—hydraulic balancing can homogenize flow distribution and improve thermal comfort but does not reduce pump electricity consumption.

In Switzerland, most buildings are already equipped with thermostatic valves due to renovation works or heat-generation system replacements. However, these valves are not necessarily preset, and static balancing is not systematically performed.

Summary and Nuances

In the context of the T-DROP project, hydraulic balancing could, in some cases, constitute an accessible measure leading to energy savings. It is advisable to consider this intervention as a complement to other actions, such as renovation of the thermal envelope or replacement of the heating system. Given the investment required for renovation works, neglecting hydraulic balancing would limit the potential energy savings. Additionally, improved occupant comfort and the possible reduction of noise related to system operation are further advantages.

Hydraulic balancing may also be relevant for domestic hot water (DHW) distribution networks. In buildings with multiple DHW branches, flow distribution between recirculation loops can be unbalanced for the same reasons as in heating networks: unequal pipe lengths, variable pressure losses, and lack of local regulation. The DHW circulation pump is generally a single unit located at the building's base. This configuration favors short loops with lower pressure losses, to the detriment of longer loops, resulting in insufficient return temperatures, slow heating at distant tapping points, or water stagnation in dead legs. To mitigate Legionella risks, temperatures in the DHW circulation loops are increased, which leads to higher thermal losses.

Before implementing hydraulic balancing, it is useful to rely on field experience and common practice, which may temper conclusions from the literature. A recurring difficulty is that, before the intervention, it is often very hard to predict the actual gains. Thus, as a first step, it may be advisable to install

temperature sensors to establish a baseline, identify the most disadvantaged rooms or apartments, and assess the extent of the imbalance.

One of the major obstacles to implementing hydraulic balancing lies in logistical constraints. It requires simultaneous and repeated access to multiple apartments, necessitating careful coordination with owners and tenants—an issue frequently noted by practitioners. Moreover, in the current renovation context, if radiators are replaced (modifying hydraulic characteristics) or if envelope interventions alter the building's thermal behavior, the gains from hydraulic balancing may be significantly reduced. As a result, professionals often consider that optimizing the heating curve is a more appropriate first step before undertaking full hydraulic balancing.

11.8 Carbon emissions and renewable energy fraction of the Swiss electricity mix

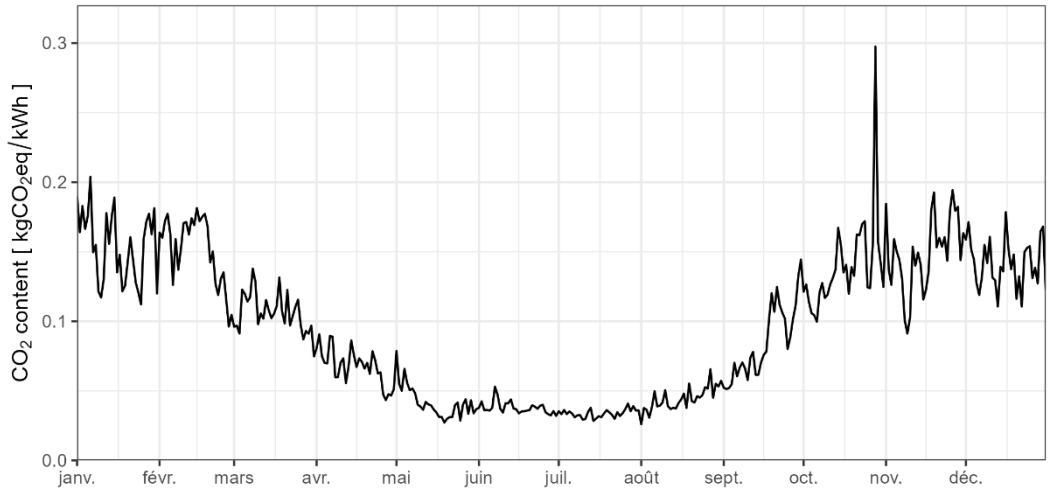


Figure 46: Daily CO_{2eq} content of Swiss electricity consumer mix, 2017-2021 average. Source: Romano et al. [78]



Figure 47: Daily renewable energy fraction of Swiss electricity consumer mix, 2017-2021 average. Source: Romano et al. [78]